

UCLA

UCLA Electronic Theses and Dissertations

Title

Trait-mediated coexistence in a hyperdiverse tropical forest or Why are there so many kinds of trees in the Central Amazon?

Permalink

<https://escholarship.org/uc/item/6mt4524k>

Author

Carita Vaz, Marcel Carita

Publication Date

2021

Peer reviewed|Thesis/dissertation

UNIVERSITY OF CALIFORNIA

Los Angeles

Trait-mediated coexistence in a hyperdiverse tropical forest
or
Why are there so many kinds of trees in the Central Amazon?

A dissertation submitted in partial satisfaction of the
requirements for the degree Doctor of Philosophy
in Biology

by

Marcel Caritá Vaz

2021

©Copyright 2021

by

Marcel Caritá Vaz

ABSTRACT OF THE DISSERTATION

Trait-mediated coexistence in a hyperdiverse tropical forest

or

Why are there so many kinds of trees in the Central Amazon?

by

Marcel Caritá Vaz

Doctor of Philosophy in Biology

University of California, Los Angeles, 2021

Professor Nathan Jared Boardman Kraft, Chair

Elucidating the mechanism that maintains tree diversity in tropical rainforests is one of the compelling ecological challenges of our time. The longevity and inherent rarity of tropical tree species, combined with species losses due to anthropogenic change, provide additional stumbling blocks to resolving this issue. However, conceptual theory combined with sophis-

ticated statistical techniques provide a way to overcome these issues. Despite differences in ecological dynamics and evolutionary trajectories, tree species are subject to a common set of ecophysiological constraints. These constraints provide a common denominator for elucidating the mechanisms by which large numbers of seemingly different species coexist within a forest. Plant ecophysiology provides the advantage of common metrics, such as plant functional traits, which in turn provide reliable proxies for characterizing the set of ecophysiological strategies adopted for rainforest tree species. Such trait-based approaches have proved essential in advancing our understanding of species coexistence in many different types of plant communities. Here I work to elucidate the coexistence mechanisms underlying the rich diversity of tree species in the Amazon rainforest. I develop a framework centered on an ecophysiological constraint — allocation trade-offs, which I argue, is foundational to tree species coexistence. The argument is as follows. Individuals are ultimately limited by the energy they extract from essential limiting resources. Resource limitation means unequal energy allocation to traits underlying survival, growth and reproduction: higher survival comes at the cost of reduced growth or lower reproduction. Within a given environment, species-specific differences in allocation trade-offs can generate only fitness differences and competitive exclusion (the R^* rule). However, in variable environments inter-specific differences in allocation trade-offs can lead to species-specific responses to environmental variation. Commonly termed performance trade-offs, these species-specific differences can allow species to limit themselves more than they do others, leading to niche differences and stable, long-term coexistence. I use this conceptual framework in my dissertation to eluci-

date tree species coexistence mechanisms in one of the most complex biological systems on the planet: the hyperdiverse forests of the Central Amazon. My work shows how allocation trade-offs that occur at the individual level can explain phenotypic trait diversity at different organizational levels, including nutrients within leaves (Ch.1), leaves within crowns (Ch.2), whole-plant allometries (Ch.3), and tree life-history (Ch.4). I use statistical models based on the Hierarchical Bayesian approach to connect species' trait data with their spatial distributions for over a thousand different species. I make the following key findings: 1) leaf nutrient allocation trade-offs arising from interactions with root symbionts can lead to diverging habitat specialization among tree species (Ch.1); 2) an imperfect leaf size-number trade-off can explain interspecific variation in shade tolerance in saplings (Ch.2); 3) a relaxed trade-off between height-gain and crown expansion in saplings allows for a decoupling between sapling and adult niches (Ch.3); and 4) the growth-reproduction trade-off underlies vertical niche segregation in adult trees (Ch.4). These four core results reinforce the importance of allocation trade-offs as the fundamental driver of niche divergence and coexistence of forest tree species. Furthermore, because the four allocation trade-offs studied here are only a small sample of the multitude of trade-offs that limit plant performance, combining only a handful of trade-offs could potentially explain a great deal of the hyperdiversity of trees seen in these Amazonian forests.

The dissertation of Marcel Caritá Vaz is approved.

Stephen P. Hubbell

Lawren Sack

Felipe Zapata

Nathan Jared Boardman Kraft, Chair

University of California, Los Angeles

2021

To...

The hundreds of millions of ancestors

From whom I have inherited

The perseverance to keep struggling.



Contents

| | |
|---|--------------|
| Abstract | ii |
| List of Figures | x |
| List of Tables | xiii |
| Acknowledgements | xiv |
| Curriculum vitae | xxiii |
| Introduction | 1 |
| 1 Leaf nutrients and habitat selection | 21 |
| 1.1 Introduction | 21 |
| 1.2 Conceptual framework | 23 |
| 1.3 Methods | 29 |
| 1.4 Results | 37 |
| 1.5 Discussion | 45 |
| 2 Leaf size-number trade-off | 59 |
| 2.1 Introduction | 59 |
| 2.2 Methods | 66 |
| 2.3 Results | 75 |
| 2.4 Discussion | 83 |
| 3 Decoupling of adult and sapling niches | 95 |
| 3.1 Introduction | 95 |
| 3.2 Conceptual framework | 99 |
| 3.3 Methods | 103 |
| 3.4 Results | 110 |
| 3.5 Discussion | 116 |

| | |
|---|------------|
| 4 Growth-reproduction trade-offs | 127 |
| 4.1 Introduction | 127 |
| 4.2 Methods | 131 |
| 4.3 Results | 135 |
| 4.4 Discussion | 141 |
| Concluding remarks | 147 |
| A Supplement for chapter 1 | 152 |
| B Supplement for chapter 2 | 162 |
| C Supplement for chapter 3 | 171 |
| D Supplement for chapter 4 | 181 |
| Bibliography | 188 |

List of Figures

| | | |
|-----|---|------|
| 0.1 | Just another day in the field. | xxii |
| 0.2 | ZF-3, the road that links the reserves of the Biological Dynamics of Forest Fragments Project to the Manaus-Caracas highway. | 7 |
| 0.3 | Canopy trees are especially susceptible to climate change. | 12 |
| 0.4 | <i>Cecropia sciadophylla</i> : the most successful pioneer species in the study site. . . | 20 |
| 1.1 | Conceptual figure depicting the three main hypotheses tested in this study. . . . | 28 |
| 1.2 | The contrast between plateau and gully forests. | 31 |
| 1.3 | Principal component analysis of leaf content of six macronutrients for 1,182 plants from 978 different species sampled in two contrasting soil habitats. | 39 |
| 1.4 | Differences in foliar content of six macronutrients between the gully and the plateau and between nitrogen-fixing legumes and non-fixing species. | 42 |
| 1.5 | Habitat association analyses show the partitioning and sharing of soil habitats among 359 tree species. | 43 |
| 1.6 | Relative abundance and basal area of nitrogen-fixing species across the three main habitats found in the forest plot. | 45 |
| 1.7 | Mean leaf nutrient content weighted by species's abundance in each quadrat of each major habitat type. | 46 |
| 1.8 | Common anti-herbivory defenses seen across tree species points to the importance of herbivory pressure in this forest. | 52 |
| 1.9 | Example of soil erosion at the Km 41 camp. | 58 |
| 2.1 | Conceptual figure depicting expected results under two alternative hypotheses: 1) size-number trade-offs serve as fitness equalizing mechanisms; and 2) size-number trade-offs promote niche differentiation. | 67 |
| 2.2 | A sample of the leaves sampled in this study shows the wide variance in leaf size among the single-leafed species found in the study site. | 70 |
| 2.3 | Distribution of leaf traits across the 490 saplings sampled in this study. | 77 |
| 2.4 | Interspecific trade-off between leaf size and number and its effects in total leaf area. | 79 |
| 2.5 | Individual and species level growth models. | 80 |
| 2.6 | Total leaf area and relative growth rate as a function of leaf dry mass and specific leaf area. | 82 |

| | | |
|-----|--|-----|
| 2.7 | Leaf size effects on plant architecture. | 85 |
| 2.8 | Bipinnate leaves of a canopy legume tree. | 94 |
| 3.1 | Two alternative hypotheses of within-strata species coexistence: 1) adult and sapling niche coupling associated with limiting similarity; and 2) ontogenetic niche shifting under light habitat filtering. | 103 |
| 3.2 | Interspecific similarities in adult size and dissimilarities in sapling growth strategies are negatively correlated. | 114 |
| 3.3 | Both sapling architecture and adult size were spatially aggregated at the local scale. | 115 |
| 3.4 | Sapling architecture can be decoupled from plant maximum height and even phylogeny. | 121 |
| 3.5 | The many evolutionary contingencies in plant development and the solutions plants have found. | 125 |
| 3.6 | Light beams trespassing the forest canopy close to dusk. | 126 |
| 4.1 | Predicted probability of reproduction as a function of trees' diameter at breast height for each of eight common species in the studied forest. | 136 |
| 4.2 | Predicted probability of reproduction as a function of tree's diameter at breast height for the average species and for the most common species. | 137 |
| 4.3 | Trade-off between critical size and the maximum probability of reproduction. | 139 |
| 4.4 | Reproductive potential of the whole forest stand depends on the distribution of tree size and the probability of reproducing of each size class. | 140 |
| 4.5 | Contrasting reproductive strategies between pioneer and shade-tolerant trees. | 145 |
| 4.6 | Epiphytes and lianas are functional groups that make up for a great deal of plant diversity in this forest. | 151 |
| A.1 | Topo-edaphic maps of the Km37 permanent plot. | 155 |
| A.2 | Intraspecific variation in leaf nutrients for the best sampled species. | 156 |
| A.3 | Differences in tree size between fixers and non-fixers in the plateau and in the gully. | 157 |
| A.4 | Richness, abundance, and basal area of N-fixing legumes, non-fixing legumes, and non-legumes across the three main habitats in the plot. | 157 |
| A.5 | Differences in leaf nutrient content between two habitats and between nitrogen-fixing legumes and non-fixing species. | 158 |
| A.6 | Differences in foliar content of six macronutrients between the gully and the plateau and between nitrogen-fixing legumes and non-fixing species. | 159 |
| A.7 | Differences in foliar nitrogen to phosphorus ratio between two habitats and between nitrogen-fixing legumes and non-fixing species. | 159 |
| A.8 | Differences in tree size between fixers and non-fixers in the plateau and in the gully. | 160 |
| A.9 | Mean leaf nutrient content weighted by trees' basal area in each quadrat of each major habitat type. | 160 |

| | | |
|------|---|-----|
| A.10 | Mean leaf nutrient content weighted by species' abundance in each major habitat type. | 161 |
| A.11 | Mean leaf nutrient content weighted by trees' basal area in each major habitat type. | 161 |
| B.1 | Relationship among leaf area, leaf dry mass and two forms of calculating specific leaf area. | 167 |
| B.2 | Across-species distribution of the point estimates of the species-specific parameters η_0 , η_D , η_L , η_M , and η_S | 168 |
| B.3 | Goodness of fit of the model describing total leaf number per sapling. | 168 |
| B.4 | General tradeoff model contrasted against observed sapling data. | 169 |
| B.5 | Across-species distribution of the point estimates of the species-specific parameters. | 169 |
| B.6 | Goodness of fit of the model describing relative growth rate. | 170 |
| B.7 | General relative growth rate (<i>RGR</i>) model contrasted against observed sapling total leaf area and predicted <i>RGR</i> by the individual model. | 170 |
| C.1 | Correlation between several H_{herb} metrics and H_{lit} | 175 |
| C.2 | Correlation between several D_{max} metrics and H_{herb} and H_{lit} | 176 |
| C.3 | Sapling architectural traits: height, crown projected area, crown relative thickness, stem diameter at breast height, and crown illumination index. | 177 |
| C.4 | Effects of sample size on the correlation between sapling optimism index and adult size | 178 |
| C.5 | Spatial autocorrelation of species-specific traits for the subplot with the highest sampling coverages. | 180 |
| D.1 | Effect of species' adult maximum size on each of the species-specific parameters: β , α , and κ | 187 |
| D.2 | Predicted P_R for hypothetical species with contrasting D_{max} | 187 |

List of Tables

| | | |
|-----|---|-----|
| 1.1 | Correlations among the six leaf nutrients quantified in this study. | 38 |
| 1.2 | Effects of habitat, N-fixation, and their interaction on the leaf content of six macronutrients. | 40 |
| 1.3 | Correlations between leaf nutrient content and habitat association. | 44 |
| 2.1 | Best-fit parameters for the models fitted in this study. | 78 |
| 3.1 | Distribution of species' maximum adult height indicates high vertical niche overlap in the studied forest. | 110 |
| 3.2 | Effects of adult size (H_{max}) on sapling architecture | 112 |
| 3.3 | Intra- and interspecific variances and correlations among the three architectural traits measured. | 112 |
| B.1 | Summary of the species-specific parameters fitted in this study when modeling total leaf number and relative growth rate as a function of sapling size, illumination, leaf dry mass and specific leaf area. | 166 |
| C.1 | Number of species, abundance, and sample size for each stratum using three different H_{max} estimates. | 173 |
| C.2 | Well-sampled and outlier species, their families, architectural models, maximum adult size, and sample size. | 174 |
| C.3 | Sapling trait combinations that maximize the correlation between $D_{H_{max}}$ and $D_{sapling}$ | 175 |
| C.4 | Spatial autocorrelation of sapling traits in each of 25 1-ha subplots. | 179 |
| D.1 | Summary of the species-specific parameters for all the 233 species used in this study. | 186 |
| D.2 | D_{max} effects on species-specific parameters. | 186 |

Acknowledgments

I must start by acknowledging that this work was done on unceded lands made into a natural reserve. Although the study site per se was unlikely ever inhabited [1], as the soil seems too poor to sustain crops and the closest river is miles away, it was still part of native people's territory. It is difficult to know with precision who this area would have belonged to, as it is situated at the intersection of three large nations: the Karibs, Aruaks, and Tukanos. These people were forced to abandon their lands in the aftermath of conflicts with Portuguese settlers.

I am thankful for my former advisor, Alexandre A. de Oliveira (Universidade de São Paulo - USP), who pioneered the study of tree hyperdiversity in the area [2], and for Alberto Vicentini (National Institute of Research of the Amazon, INPA), who continues the efforts to describe the immense diversity of plants in the area. They are both the principal investigators responsible for setting the largest permanent plot in the region, aka the Km37 plot. I am equally thankful to João Batista da Silva and the multiple field and taxonomy crews, who made the herculean work to map and identify the more than 150,000 trees present in the plot. Without the convenience of having all this data doing the work presented at chapters 3, 2, and 1 would be impossible.

Chapter 4, in turn, was only possible due to the very generous sharing of tree phenological data arduously collected by my friend, Nívia Bianca Lopes, for her masters thesis. Her work was part of a much larger experiment (Amazon Fertilization Experiment or AFEX), which

was done in an adjacent area, the Km41 reserve (4 km to the east of the Km37 plot). Again, this project was only possible due to countless hours of hard work in the field and in the collection, for which I must acknowledge the greatest taxonomist in the region, Paulo Apóstolo Assunção, who we lost to COVID19 earlier this year. His loss and the loss of his immense knowledge on the Amazon flora are irreparable.

In reality, none of these two massive projects (Km37 plot and AFEX) would exist if it was not for the titanic Biological Dynamics of Forest Fragments Project (BDFFP). This is likely the largest and longest-lived project ever done in a tropical forest and one that has contributed tremendously to further our understanding of the ecology and conservation of the Amazon forest. Long live the project! Projects of course are carried out by real people, and there is no one I am more thankful to than Rosely Hipólito, Ary Ferreira, Luís de Queiroz and many other heroes who run the project on a daily basis. I am thankful for José Luis Camargo too as the director of the project and as a friend, but I will get back to him again when I thank my intellectual mentors. I definitely also owe a lot to Manoel Fróes (Fig.0.1), my brother by choice, who had helped me back in 2009 during my masters, and saved me again during my Ph.D., from 2016 to 2019. Finally, I am thankful for Thomas Lovejoy's lifelong effort with the project, especially in securing the funding for the project to keep running for so many decades.

I thank Kyle Harms for generously shared the Km37 plot soil data that I used to characterize the plot habitats in chapter 1 and for all his help with the project design. Benjamin Turner and Santiago Trueba also provided invaluable contributions to improve the successful

proposal. Chapter 1, however, was only possible because of all the hard work of the lab technicians at the Plant Mineral Nutrition Laboratory at the Superior School of Agronomy Luiz Queirós. Additionally, if it was not for José Otávio Vaz, who patiently grinded hundreds of dry leaf samples, and for Talita Laurie Lustosa, who generously agreed to take custody of these samples for four long years, this project would have not been possible.

This dissertation was supported by numerous funding sources. Starting with Brazil's NSF, CAPES, which awarded me with a four-year fellowship (Science without Borders program, 2014, BEX:10079-13-0), without which I would not even consider applying for a Ph.D. program. CAPES also funded part of my travel expenses to the field. Then the Biology Department at the University of Maryland, College Park (UMD), funded a summer fellowship and a pilot field trip that ended up not happening because I had to undergo an appendectomy only one week before my flight was scheduled. In the following year, I was awarded with the Thomas Lovejoy grant, which allowed me to do the many field trips my project demanded (chapters 3 and 2). UCLA's Ecology and Evolutionary Biology department greatly supported my research with many significant grants (chapters 3 and 2) and fellowships. UCLA's graduate division also helped with travel expenses. The data collected by Nívia was jointly funded by the BDFFP and the Natural Environment Research Council (NERC, UK). Finally, the ForestGeo network funded most of the project described in chapter 1. All remaining expenses of my project, including material and measurement instruments were covered by the Kraft Lab.

I am deeply thankful to all my undergraduate students, who were one of my main moti-

vations to pursue this work, but in particular to Kiumars Edalati and Jiayu Li, whose help with leaf area measurements made chapter 2 possible. Kiumars also helped me to write that chapter and has been a wonderful collaborator. Chapter 3 was also only possible because of the immense work of compilation done by Celina Nishioka and Magdalene Lo. Grace Kumaishi, Sarah Williams, Jiahui Li, and Carly Pomeroy helped in projects that for lack of my time did not make it into this dissertation. Their projects are going to be great manuscripts in their own right.

I was extremely lucky to have only the best mentors that there can be. I am of course the most grateful for Nathan's brilliant mentorship. His unconditional support and enormous generosity for the past seven years, his profound ecological knowledge and past experience in the Amazon, and more important of all, his nurturing of my intellectual independence, have paved the way for my becoming a true doctor of philosophy. Next, I thank Priyanga Amarasekare, who has helped me tremendously to develop an ecological intuition of nature. Due to her theoretical expertise and incredible ability of synthesis and abstraction, I could visualize the line connecting all the different chapters of this dissertation. I owe her, therefore, the organization of the general conceptual framework used throughout this dissertation. I am also tremendously grateful for my committee, who have steered my projects into more promising directions. Steve Hubbell will always be a great reference and has helped me to think critically and rigorously about ecological ideas, especially those in chapter 3. Lawren Sack has helped me avoid pitfalls in my original project and gave me the idea for chapter 2. He has also helped me to acquire a much deeper understanding of plant physiology. If

today my ecological thinking is permeated by evolutionary principles, it was only due to the invaluable help of Felipe Zapata, who constantly pushed me to the evolutionary side. Not less important was the role of José Luis Camargo. Without his amazing mentorship and knowledge about the Amazonian ecosystem none of this project would have worked. It was only through his extremely generous offer that chapter 4 exists. I am also thankful for Ned Fetcher, for inviting me to join a fantastic project in Costa Rica, for his continuing support, and for always be willing to share his great energy and his knowledge about plant ecophysiology. Finally, I thank Robert Weiss for his amazing course on applied Bayesian analysis, which introduced me to a whole new way of doing and thinking statistics.

From my past life at USP, I am forever grateful for the early mentorship provided by Cristiane Jurinitz, who introduced me to the Modern Coexistence Theory, Sérgio Tadeu, for teaching me the basics on plant ecophysiology, and especially to Glauco Machado, who taught me Science as a philosophy of life and who convinced me that I should pursue a Ph.D. in the United States.

My dissertation greatly reflects the contribution, and patience, of several PIs and their labs. First of all, naturally, the Kraft lab has seen me talking for hours about my ideas and issues and reviewing manuscripts and proposals. In particular I want to thank Mary van Dyke, Kenji Hayashi, and Andy Kleinhesselink for invaluable and insightful comments throughout my stay at UCLA. I am profoundly thankful for all the help Ian McFadden has provided, especially with the spatial analyses of chapter 1. Lastly, I have no words to describe how much Gaurav Kandlikar has helped me with always very fruitful discussions about the

essence of species coexistence mechanisms, the role of functional traits in these mechanisms, the role of nature in life, of scientists in society and so much more. My Science greatly benefited from interactions on other labs too, especially the Sack Lab, where I could learn plant physiology more profoundly, the Zapata Lab, who helped me with the evolutionary aspect of my ideas, Rasoul Sharifi, who taught me so much about plant-soil interactions, and of course the Amarasekare Lab, who helped me to think more in theory. My interaction with Nívia Lopes and José Luis Camargo at the BDFFP was so fantastic that it resulted in chapter 4. They helped me tremendously by forcing me to think more about the life-history side of species coexistence and on the natural history of these trees. From the Tropical Forest Lab, at USP, I thank Alexandre A. de Oliveira, and especially Jennifer Euler, who helped me tremendously by reviewing and discussing chapter 1. Kyle Harms (LSU) and Ben Turner (STRI) also helped me a lot to conceive this chapter. Finally, the EcoEvoPub seminars and many other seminars and meetings were also an excellent place to get feedback from dozens of peers.

For so much emotional support and love, I am eternally grateful for the many great friendships I was gifted with during the past seven years. Starting at UMD, my life would have been impossible without my friends Gaurav, Daniel, Rong, Benoit, Ian, Nicola, Elske, among many others. I could also probably not have survived my transition to UCLA if it was not for the most diverse, and thus the best cohort the EEB department will ever see. Rachel, Camila, Alayna, Chris, Leila, Scott, Zack, Shyla, Dita, Rita, Aji, Audra, Shawn, Bruno, Gaurav, Tiara, Brandon, Emily, Hayley, Clive, Mabe, Tina, and Page are all people

I wish I still had around me. Life in Los Angeles was also made tractable with the help of older cohorts, especially Gabi, Ana, Rita, Mairin, Christine, Meghan, Jonathan, Taylor, Daniel, Charlie, Katelyn, and Grace. Newer cohorts were of course crucial to renew our energy and I found life-long friends among them too, in especial Ioana, Marvin, Maddi, Elizabeth, Mary, Marissa, Rosa, Nisha, Alec, Liz, Nick, Mars, Jules, Samuel, and Eva. Postdocs and visiting scholars helped me glimpse what my next steps could be, so I am really thankful for Santiago, Amanda, Maura, Rui Hua, Andy and Jane (who lended me the camera with which I took most of the photos that illustrate this dissertation), Nitika, Lei, Yi, Victor, Zeqing, Luke and Grace, Ian and Jasmin. I am also grateful for all UMD and UCLA staff, in particular to Magna Grey, who helped tremendously to adapt to live in the US, Jocelyn Yamadera, who received me from Maryland, Kelly Zuniga, who has saved me so many times with my visa issues, and above all, Tessa Villasenor, without whom I would have fallen through the cracks. I will never forget how amazing my roommates Maddi and Gaurav were during those disturbing times of confinement. Not less important were all the great people that made even the most disastrous days in the field to seem fun: Vitec, Aline, Mariana, Nívia, Seu Jairo, Aninha, Felipe, among many others whose stay overlapped with mine at the Km41 camp, as well as Germán and Ricardo, with whom I shared a beautiful field trip to Costa Rica. I also thank the great friends I made ahead of the Latin American and the Caribbean Chapter of the Ecological Society of America, such as Ayanna, Felipe, Diogo, Enzo, and Jenn, but especially Alejandra and Arona, who created this writing group that has helped me to focus on my dissertation. Finally, I cannot express how grateful I am

for my family, Maria do Carmo, José Otávio, and Fernanda, and Talita who all helped me keep my sanity during extreme hardship. Talita also provided great logistic support during my expeditions back home and my stay in Manaus. She was the one that would always come at my rescue. Without her help this work would definitely have not happened.

I could write a whole dissertation just describing how each small section of this dissertation is the product of collaboration and the generous help of many "strangers". I will never be able to do justice to all of you that in a way or another helped pave the way for the making of this dissertation. My faulty memory does not also help remembering the people, facts and events of many years into the past. These have been long, well-lived seven years, rocked by many impactful events, so I heartily apologize for leaving anyone short of a proper acknowledgement. Acknowledged or not, you too were fundamental for bringing this project to life.



Figure 0.1: Just another day in the field. Manoel Fróes (foreground) has been helping me to collect plant functional traits since 2009. Together, we sampled over 4,000 trees, mostly saplings, between 2016 and 2019. Some species, however, are not so easy to find, like the *Miconia* I was trying to sample (background). Saplings of pioneer saplings are nearly absent in the plot: the ones in recent gaps, like the one in the photo, grow very rapidly and become adults fast, while most of those growing in the shade have not survived since the first census, done in 2006-2007. The more we progressed with the sampling, the more it felt like a scavenger hunt.

Curriculum vitae - Marcel Vaz

Education

Ph.D. Ecology and Evolution (2015-2021) University of California, Los Angeles (UCLA). Supervisor: Nathan Kraft

M.Sc Ecology (2009-2011) Universidade de São Paulo, Brazil. Supervisor: Alexandre A. de Oliveira

B.Sc Biological Sciences (2004-2008) Universidade de São Paulo, Brazil. Supervisor: Alexandre A. de Oliveira

Teaching and mentoring

Teaching Assistant (2015-2021) UCLA: 1) *Introduction to Life Sciences* (2 quarters); 2) *Plant Physiology Lab*; 3) *Plant Ecology* (3 quarters); 4) *Life: Concepts and Issues*; 5) *Field Tropical Ecology*; 6) *Community Ecology*; 7) *Tropical Ecology*; 8) *Plant Diversity and Evolution*; 9) *Ecology*; 10) *Plant Physiology*.

Undergraduate Research Mentor (2015-2021) UCLA: 1) Grace Kumaishi; 2) Kimars Edalati; 3) Jiayu Li; 4) Celina Nishioka; 5) Magdalene Lo; 6) Sarah Williams; 7) Jiahui Li; 8) Carly Pomeroy.

Guest Lecturer (2019-2020) UCLA: 1) Resources and niches of Amazon trees, presented for the course *Ecology*; 2) Diversity of plant life-forms, for *Plant Diversity and Evolution*; 3) Biotic Interactions in Tropical Forests, for *Tropical Ecology*; 4) Habitat Selection, for *Community Ecology*.

Teaching Assistant (2014-2015) University of Maryland (UMD), College Park: *Cell Biology and Physiology* (2 semesters)

Grants and Fellowships

- Departmental Fellowships - UCLA (2019-2021) \$20,000 (stipend).
- Departmental Research Grants - UCLA (2017-2020) \$10,600 (consumables).
- ForestGEO Research Grant (2018) \$10,000 (consumables)
- PhD Fellowship - CAPES (2014-2018) \$91,000 (stipend, tuition, and consumables)
- Thomas Lovejoy Research Grant (2016) \$5,000 (consumables)
- Dean's Fellowship - UMD (2015) \$5,000

Service and Outreach

Reviewer (2018-2021) 1) *Frontiers in Plant Science*; 2) *Annals of Botany*; 3) *FLORA*; 4) *Science of the Total Environment*; 5) *Ecology and Evolution*.

...

Conferences and Events (2019-2021) 1) Panelist for ATBC webinar on applying for graduate school; 2) Moderator of session at the ESA 2021 meeting; 3) Co-organizer of symposium at the ESA 2021 meeting; 4) Co-organizer of the webinar on the Future of Biodiversity in Latin America the Caribbean; 5) Organizer and moderator of oral session at the ESA 2020 meeting; 6) Organizer of symposium at the ATBC 2020 meeting; 7) Reviewer of Inspire Session proposals for the ESA 2020 meeting.

Scientific Societies (2019-2021) 1) ESA's Tellers Committee member; 2) ESA's Ad Hoc Council Leadership working group; 3) Webmaster for ESA's Latin American and the Caribbean chapter (LAC); 4) ESA's Subcommittee on Governance; 5) Vice-chair of ESA's LAC; 6) Co-chair of ESA's LAC; 7) Student liaison at the UCLA EEB departmental Faculty Teaching Award committee.

Education (2019-2021) 1) Mentor for the Community College Field Biology Alliance at UCLA; 2) Developer for EcoEvoApps, educational apps for ecology and evolution; 3) Splash course The Ecology of the Tropics for high school students at UCLA; 4) Volunteer helper at the UCLA Software Carpentry workshop; 5) Middle school science fair judge at the Episcopal School of Los Angeles.

Publications

1. McGuire, R., and 5 others including Vaz, M.C. (pre-print) EcoEvoApps: interactive apps for teaching theoretical models in ecology and evolutionary biology. *bioRxiv*, 449026.
2. DeLucia, E., and 9 others including Vaz, M.C. (2021) Governance changes for a rapidly expanding society: recommendations to facilitate ESA's transition into its new centennium. *Bull. Ecol. Soc. Am.*, 102:e01912.
3. Mello, F.N.A., Bender, A., Martínez-Blancas, A.; Vaz, M.C.; Provete, D.B. (2021) Human Dimensions: The Latin America and the Caribbean Chapter of ESA - Embracing our diversity during adverse times. *Bull. Ecol. Soc. Am.*, 102:e01883.
4. Kandlikar, G.S.*, Vaz, M.C.*, and 8 others (2018) Contrasting patterns of taxonomic, phylogenetic, and functional variation along a Costa Rican altitudinal gradient in the plant family Melastomataceae. *J. Trop. Ecol.*, 34:204-208.
5. Bastias, C.C., and 9 others Vaz, M.C. (2017) Intraspecific leaf trait variability along a boreal-to-tropical community diversity gradient. *Plos One*, 12:e0172495.
6. Finegan, B., and 13 others including Vaz, M.C. (2015) Does functional trait diversity predict aboveground biomass and productivity of tropical forests? Testing three alternative hypotheses. *J. Ecol.*, 103:191-201.
7. Gomes, A.C.S., and 12 others including Vaz, M.C. (2013) Local plant species delimitation in a highly diverse Amazonian forest: do we all see the same species? *J. Veg. Sci.*, 24:70-79.

Introduction

Tropical rainforests have been an endless source of awe and inspiration. Forests from South America had a particularly crucial role in sparking the scientific revolution that led to the foundation of Ecology as a discipline. Many of the founders of this discipline had passages through these luxurious and teeming forests, usually at a young age, and thus not much different than what interns and graduate students do to this date when they go to the tropics to do field work. To name a few, Humboldt, who would come to write on plant geography [3], Darwin and Wallace, who would come to propose the theory of evolution "by means of natural selection" [4], Warming, who would later write the first textbook on plant ecology [5], and Schimper, that would lay the foundations of plant ecophysiology and coin the term "tropical rainforest" [6], all of them spent some years in their twenties or early thirties exploring these tropical forests before returning to Europe. Although essential to develop the discipline of tropical forest ecology, this scientific process was charged with the colonialist mindset of disregarding local wisdom and producing knowledge thousands of miles away from where it is needed the most [7]. Although there is still much work to be done

on this front, we have been luckily moving away from this scientific colonialism system since then [8].

One key aspect of tropical rainforests that must have catalyzed such revolutionary ideas is the extraordinary biodiversity of these forests. One can perhaps only appreciate similar levels of diversity in coral reefs [9], which however are much older than tropical forests. As corals are in the reefs, trees are the main structural component of tropical forests and their incredible diversity can be promptly appreciated by travelers, as Columbus describes: "[The mountains are] filled with trees of a thousand kinds" [10]. In a similar account, Wallace reminds us of how this tree hyperdiversity can make futile any attempt to have decent sample sizes for each of these species: "If the traveler notices a particular species and wishes to find more like it, he may often turn his eyes in vain in every direction" [11]. This was in striking contrast to the impoverished forests they knew in Europe. Before these travelers, a similar impression was likely held by the first people to arrive in South America as they descended from higher latitudes or altitudes, but unlike Europeans, these people quickly learned to capitalize on the tree hyperdiversity of these forests. If for newcomers forest hyperdiversity can be mind blowing, for someone born and raised in the wet tropics there is nothing surprising about it.

Why are there so many tree species in the tropics? This Eurocentric problematization of tropical hyperdiversity may have led ecologists astray for many decades and unfortunately it is still quite vivid in many ecologists' minds. Recent progress on understanding latitudinal diversity gradients is showing that the question that we should be pursuing is why higher

latitude forests are so impoverished [12]. For example, when migration rates were modeled together with speciation and extinction rates, it became clear that the tropics are both cradle and museum, i.e., species not only originate and are maintained in the tropics, but are also exported to higher latitudes [13]. Specifically for plants, e.g., there is growing consensus that a major barrier to diversity in higher latitudes is the challenge of evolving freeze tolerance, which was only achieved by a small subset of tropical clades [14–16]. Far from being abnormal, therefore, tropical hyperdiversity might just be the natural course of biomes who have fortuitously escaped from being erased by large scale disturbances such as the uplift of mountain chains, volcanism, or glaciations [17]. That said, an even more intriguing question remains: how could so many tree species have persisted in these forests? In other words, what maintains relatively low extinction rates in tropics?

As the world’s largest tropical forest, the Amazon naturally occupies the center of the stage in any discussion about biodiversity. In spite of this being one the least studied corners of our globe, with only 0.00035% of its area having been systematically sampled, it is estimated to harbour over 15,000 species of trees [18], of which about only two thirds are currently known to science [19]. Given that samples from new species that accumulate in herbaria may take over 50 years to be finally described by science [20] and that finding the type of fertile sample that helps with plant identification is relatively rare, it rests clear that 15,000 species is still a conservative estimate. The Amazon, however, is not an homogeneous landscape, as many may think, and tree diversity can vary substantially across the basin.

Curiously, it is in one of the most unfertile sites in the whole basin that we find what

might be the richest forest in the Amazon, and perhaps in the world. A recent report from a formidable permanent plot network shows that their 25-ha plot in the Central Amazon bears ca. 1,519 tree species followed by similarly impressive species richness in plots in Amacayacu (Colombia) and Yasuní (Ecuador), which have 1,133 and 1,114 species, respectively [21]. In contrast to these Eastern Amazon forests, however, the terra firme forest in Central Amazon is located on ancient and extremely weathered soils [22]. The Central Amazon hyperdiversity therefore aligns with what is observed in Mediterranean vegetation, where the most diverse sites, such as the Fynbos in South Africa, and the Kwongan in Western Australia, are found on nutrient-depleted soils [17]. This is actually one of the reasons why the Central Amazon forests are particularly susceptible to deforestation, as most of the nutrients are stored within tree biomass.

Deforestation, logging, and fires are bringing this immense forest to the brink of collapse. Recent relaxation of forest policy enforcement in the Brazilian Amazon has caused deforestation rates to resurge at levels only seen a decade ago, causing great impact to plant species [23]. The threat of extinction due to habitat loss is especially acute for those species adapted to very specific local conditions and that therefore are rare and have small-range distributions, which were estimated to make up about half of all Amazonian trees [24]. To make it worse, it is thought that a great deal of these species on the brink of extinction, or already extinct, are still unknown to science [25]. We thus may be losing these species at a faster rate than we can describe them.

Climate change, in turn, is causing droughts to become longer, more intense, and more

frequent. Recent extreme events, such as the El Niño droughts of 1997 and 2015-2016, had a great impact on tree mortality in the Amazon [26, 27]. Although in those cases no clear evidence was found that tree size affects the likelihood of tree mortality, other studies point to large trees being especially vulnerable to the impacts of climate change. It has been shown, for example, that large trees that were experimentally subjected to a rain exclusion treatment have suffered significantly higher mortality due to hydraulic failure than smaller trees [28]. Other effects of climate change may pose new threats to these large trees: thunderstorms are predicted to increase in frequency in the Amazon, and with them lightning damage, one of the main causes of large tree mortality in the tropics [29]. Finally, increasing frequencies of wind storms and even rising temperatures per se may also affect tree survival [30]. Therefore, even the few protected areas of intact and preserved forest might already have started the transition into savannas, a process that is certainly accelerated by the loss of the forest's large trees (Fig.0.3).

Taken together, human encroachment and climate change may brew the perfect storm for the Amazon and all its invaluable biodiversity. Simulation studies point out that a combination of longer dry seasons and increase in fire frequency may cause most of the Amazon to become savanna [31]. Dry season length is a function of hydrological cycles, which can be deeply affected by deforestation: the tipping point is believed to be at 20-25% of deforestation [32]. In the whole basin we have already lost ca. 17% of the forest, but in Brazil this figure is rapidly approaching the dangerous mark of 20% [33].

This dissertation, therefore, represents a desperate attempt to shed some light on the

mysterious and complex processes that rule the existence of so many tree species. It also reflects the sense of urgency of those working against the clock to salvage as much natural history information that we can before this immense living library is burned to the ground. In that spirit, it is with great pride that I present a modest, yet substantial glimpse on the ecology of the Central Amazon rainforest. And it is with immense sorrow that I realize that this work may contain the last piece of information ever gathered for many of the tree species studied here.

Why are there so many kinds of trees?

If asking why the tropics are so biodiverse makes little sense, there is nonetheless one fundamental and still unanswered question: Why are there so many species? Like just any such question in Biology, it is more helpful to break it down into its proximate, eco-physiological component and its ultimate, evolutionary. Although fundamental and extremely interesting, addressing the later question, on the evolutionary mechanisms and historical contingencies that led to the origination of so many tree species in the Amazon forest, is out of the scope of this work. I rather focus on pursuing the proximate cause of tree hyperdiversity, i.e., how so many species can share the same forest. I do not think that these two main questions should be treated as independent from each other, as there is no doubt at this point that biodiversity is a product of eco-evolutionary dynamics, but confronted with the choice, I decided to focus on the ecological mechanisms that can explain species maintenance in natural



Figure 0.2: ZF-3, the road that links the reserves of the Biological Dynamics of Forest Fragments Project (BDFFP) to the Manaus-Caracas highway. Roads like this are the main catalyzers of human encroachment in the Amazon, with 95% of deforestation occurring within 5.5 km of roads [34]. 42 years ago, when the BDFFP was created, ranchers had to be highly subsidized to establish in an area with such infertile soils. This photo shows the yellow latosol (oxysol) typical of the region's plateaus. Following deforestation, productivity dropped over only a few years, causing many of these rural properties to be abandoned. With the development of new techniques of soil correction and new heat-tolerant crops, however, new properties are spontaneously being opened at a fast rate along this road. Wealthy people from the nearby towns hunting along the road became a more common sight as well. Big game like this red brocket (*Mazama americana*), who capitalize on the tender leaves of the pioneer plants growing on the roadside are easy targets for these recreational poachers.

communities.

Over 60 years have passed since Hutchinson posed the famous question "Why are there so many kinds of animals?" [35], yet we still lack a satisfactory answer. The issue became even more interesting when the question was extended to autotrophs, as many species of phytoplankton were often found living together in relatively homogeneous and nutrient-poor environments, despite requiring the same basic resources to survive [36]. This is precisely the case of the hyperdiverse tree communities growing on the poor soils of the Central Amazon. The coexistence of multiple species of autotrophs was taken as a paradox, as it was clearly going against the principle of competitive exclusion, which stated that "complete competitors cannot coexist" [37]. This principle, however, was based on unsolid assumptions, such as environmental homogeneity and constancy, which was required for a stable equilibrium to be reached, i.e., the competitive exclusion of all species, except for the best competitor. Moreover, the axiom of inequality was invoked, but only to justify species fitness differences [37], not niche differences.

In practice, the exclusion principle assumes that any two pairs of species would always differ in their fitness, even if only by the slightest margin, and that environmental constancy would allow only the species with the competitive advantage to remain in the system. The paradox of the plankton, therefore, can be solved by relaxing the unrealistic assumption of environmental homogeneity and by applying the axiom of inequality also to species' niches. An early and eloquent empirical test of these ideas came when MacArthur showed that five sympatric bird species, that seemed ecologically identical, were actually partitioning their

common foraging grounds both spatially and temporally [38]. First, this shows that when species appear to be ecologically equivalent, like tree species in a forest, it is often because not enough is still known about their natural history. Second, it shows that as long as competing species differ in their niches, and as long the environment is not homogeneous, coexistence may be possible.

If on one hand species always differ in their niches, and no environment is perfectly homogeneous, niche differences and/or environmental variation are not always enough to promote species coexistence. Even if two competing species respond quite differently to environmental gradients, they can only coexist if the temporal scale of environmental variation is smaller than the scale at which fitness differences would lead to competitive exclusion [36]. For example, a stronger and a weaker competitor species can coexist if disturbances are capable of reverting their competitive ranks for a while, and if disturbances are frequent enough to prevent the exclusion of the weaker competitor, but not frequent to the point of excluding the stronger competitor. This is the basis of the intermediate disturbance hypothesis, created as an attempt to explain tree diversity in the tropics [9]. Overall, it rests clear that coexistence is both a function of species' niche and fitness differences [39].

Coexistence is impossible without niche differences, but it can happen even in the absence of environmental heterogeneity or even when species show no differential responses to environmental gradients. This is why, for example, stable coexistence is possible under even very simple models such as the Lotka-Volterra one, i.e., population dynamics itself can create heterogeneity. In such apparently homogeneous landscapes, coexistence may happen

when there are life-history trade-offs among species or negative density-dependence [40]. For example, when demographic traits that maximize competition, such as longevity, trade-off with traits that minimize competition, such as the ability to disperse to vacant sites, coexistence can occur (competition-colonization trade-off) [41]. As a matter of fact, treefall gap dynamics has been pointed as one of the most important sources of niches for tropical trees [42]. Other coexistence mechanisms do not even require life-history trade-offs, as long as the spatial scale at which interspecific competition takes place is smaller than that of intraspecific competition (heteromyopia) [43]. For example, host-specific natural enemies can limit the density of conspecifics near established individuals, which may open space for heterospecifics (Janzen-Connell hypothesis) [44]. Conspecific negative density dependence has been widely invoked to explain the diversity of trees in tropical forests, although this is still a contentious topic [45]. Nevertheless, it is important to notice that even though interspecific differences in responses to environmental gradients or life-history trade-offs are not strictly necessary for coexistence, niche differences still are, i.e., competing species must limit conspecifics more than they limit heterospecifics (stabilization) [39].

Niche differences may be necessary for stable coexistence, but they are not necessary to explain the maintenance of species diversity. In reality, coexistence mechanisms often require so many conditions to be met that models of unstable coexistence may be more parsimonious. These models are based on the theory of island biogeography, which states that species diversity may be maintained through a dynamic equilibrium caused by the interplay between immigration and local extinction rates [46]. The most famous and successful application of

these principles to tropical forests was the neutral theory, which can explain not only the high tree diversity found in these forests, but even the patterns of species abundance distribution [47]. Although this model violates the inequality axiom twice, by assuming there is no niche nor fitness differences among species, it remains as a crucial demonstration of the importance of priority and rescue effects in the assembly of tree communities.

A question that persists is how the balance of niche and fitness differences operates to shape the remarkable biodiversity in Amazonian forests. Are these tree species stably coexisting or slowly being competitively excluded while new species originate? This is one of those questions that may never be answered: even if generations of scientists could track the performance of organisms that outlive us by centuries (even the longest permanent plots in the Amazon are now just 40 years old), and even if we knew the natural history of these tree species in enough detail to predict their competitive abilities and sensitivities (many species are still unknown to science), it would still not matter, as climate warming is rapidly and dramatically changing the environmental conditions trees have to endure and as a great chunk of the forest may be lost to fire and deforestation in the near future. Nevertheless, there are some shortcuts that may help us derive important insights about the ecology of trees in this forest. Below I discuss three main steps that allowed me to make inferences about the coexistence mechanisms that help to explain the maintenance of Amazonian tree hyperdiversity.

First, in order to reduce the ecological dimensionality of such complex forests, we can simply shift our attention away from species and focus on functional groups. Therefore, instead



Figure 0.3: Canopy trees are especially susceptible to climate change. In the left, a vulture perching on a dead tree ominously glare at our camp while drying out its wings on the sun. In the right, an ancient giant slowly falls victim of increasingly severe droughts or thunderstorms. Standing dead or dying trees like these have become a disturbingly common scene in the past years.

of trying to make inferences about the coexistence of a thousand species, one may focus, e.g., on the coexistence of pioneer and late-successional species, canopy and understory species, or nitrogen-fixing and non-fixing species. This functional or emergent group approach has the advantage of being a middle ground between the purely niche or neutral approaches, as it assumes species within functional groups to be ecologically equivalent, while groups themselves occupy distinct and well-defined niches [48]. At the same time, though, this hybrid approach requires a wealth of natural history information on each species, something we simply do not possess for the vast majority of Amazonian tree species. It was only thanks to the revolution brought by phylogenetic- and trait-based approaches that the ecological niches of hundreds of species could be estimated [49]. This approach provided ecologists with a set of key traits of easy measurement, such as leaf size, or not so easy to measure, but phylogenetically conserved traits, such as wood density or seed size, that could thus be measured or estimated for several hundreds of species at a relatively short amount of time [50]. Trait-based approaches, however, cannot deal alone with the rarity of the vast majority of tree species in the Amazon.

A second revolution, this time statistical, permitted dealing with this deficiency in sampling sizes for most species. This statistical revolution can perhaps be compared to the advent of microscopes in the 17th century, when we became aware of the microcosmos that surrounded us [51]. Like a magnifier lens, mathematics can unveil patterns in the data that we would otherwise never be able to detect, especially for ecological data, which is usually very noisy. Hierarchical Bayesian inference, in particular, has been of utmost importance

to interpret empirical ecological studies, especially observational studies: this approach not only allows complex models to be fit, but by treating every variable as a random one it also allows uncertainty to be estimated and propagated from individuals to whole communities [52]. Therefore, if before only the few species that are relatively abundant in tropical forests could be included in ecological studies, now all the information contained in data collected across all species, no matter how small their sample sizes are, can be used to make insightful inferences and useful predictions.

Third, and lastly, because experimentation on community assembly is not a possibility in this system, inference by exclusion is a must. Most coexistence mechanisms described to date require proper experimentation to be tested, something that can be unfeasible even for much more tractable communities, such as grasslands with only a handful of species. Allow me to take the spatial storage effect as an example. According to theory, in order for storage effect to be important in species coexistence three conditions must be met: 1) species have contrasting responses to environmental gradients; 2) sites that are suitable for a particular species should sustain high densities of that species and consequently high intraspecific competition, thus causing environment and competition to be correlated; and 3) population growth should be buffered against declines due to competition in unsuitable sites [39, 40]. Deprived of the ability to perform experiments, how could one test for spatial storage effect? First, it can be assumed that population growth of forest tree species are somewhat buffered, as short-lived species such as *Cecropia* (Fig.0.4) often maintain seed banks [53], while in long-lived species the adults themselves may serve as the resistance form [39],

although shade-tolerant species may also maintain seedling banks in the forest understory [54]. Second, covariation between environment and competition may be inferred by modeling species density as a function of environmental gradients, which can be afforded by large permanent plots whose trees and environmental variables such as soil fertility and topography are mapped [55]. Third, and most challenging, is to demonstrate species differential responses to environmental gradients. This is only possible when demographic rates such as growth, recruitment, and mortality are available. As discussed above, functional groups may be used instead of species, but it is crucial to demonstrate that their performance metrics vary as a function of both environmental factors and functional traits before storage effect can be invoked to explain coexistence.

Given the challenges of studying such a diverse and remote forest, my objective was to harness distribution, growth, and trait data for over a thousand tree species in a large permanent plot to test for coexistence mechanisms that could explain the maintenance of tree diversity in the Central Amazon forests. The most obvious ways that tropical trees diverge in their niches is along the vertical and horizontal light gradients of the forest, and also along topo-edaphic gradients [53], so these are the environmental gradients I focused on in this dissertation. In chapters 3 and 2 I look into niche differentiation along the horizontal light gradient and in chapters 3 and 4 I also look at the vertical light gradient. Chapter 4 also deals with coexistence mechanisms associated with life-history trade-offs. Finally, in chapter 1 I focus on habitat association along a topo-edaphic gradient. Linking all these chapters is my attempt to understand the underlying mechanistic basis of the trait-environmental

correlations that may promote the coexistence of species or at least functional groups. It was only after putting these chapters together that I could visualize the overall conceptual framework that guided the confection of each chapter separately, which I explain in more detail in the section below.

Allocation trade-offs as the bases of niche partitioning

The main thesis of this dissertation is that interspecific differences in resource allocation trade-offs can lead to: 1) species-specific responses to environmental variation, and 2) life-history trade-offs, both of which promotes coexistence via spatial niche partitioning. Resource allocation trade-offs emerge when the same limiting resources subsidize the development of two or more performance traits, i.e., traits that are under natural selection [56]. Soil nutrients, for example, are needed to produce photosynthetic tissues aboveground, but may also be needed to recruit root symbionts (Ch.1). Also, any energetically demanding function in a tree, such as growing taller, will come at the expense of another function, such as reproduction, when light is limiting (Ch.4). These conflicting demands within individual plants require resolutions, or allocation decisions, which are a function of the interaction between a genetic program and internal or external cues. This means that individual plants may be able to alter their allocation decisions ontogenetically (Ch.4) or in response to their internal or external environments, such as plant water status or light availability (Ch.3). In practical terms, this plasticity should manifest in the form of intraspecific negative cor-

relations between two performance traits, such as size and number of leaves (Ch.2). More interesting, however, from an eco-evolutionary point of view, is the variation in the genetic program that drives allocation responses in plants. If there is a limit to the plasticity in allocation decisions, and if there is no strong stabilizing selection in favor of a given allocation response, the accumulation of mutations within lineages may cause them to diverge in their allocational strategies. Therefore, if we can take into account the factors believed to drive allocational plasticity, such as plant size (Ch.3,4) or soil nutrient availability (Ch.1), then we would be able to see interspecific trade-offs as well.

Interspecific allocation trade-offs can have profound ecological ramifications. The conventional wisdom is that allocation trade-offs operate to reduce fitness differences between species (equalizing trade-offs) [39, 57]. This is an important mechanism that prevents any single species from being a master of all trades (aka a Darwinian demon) and thus dominating the community. However, this mechanism alone does not fully capture the potential for allocation trade-offs to maintain species diversity, as it only works within a given environment. When environmental factors or resource availability vary over space, as do soil toxicity and fertility (Ch.1) and light levels (Ch.3,4), the fitness of a species with a given allocation strategy may vary along these spatial gradients. This happens whenever the trait favoured by the allocation strategy of a species is positively selected in one point of the gradient, but negatively selected in another point [56]. For example, having few, large leaves, as opposed to multiple, small ones, may improve a plant's fitness in shaded and wet habitats due to increased light interception, but decrease its fitness in dry and exposed areas due to exces-

sive transpiration (Ch.2). Therefore, if species with contrasting allocation strategies perform differently in different habitats, regional or spatial coexistence may be possible [58]. Viewed in this context, we see that what are commonly termed performance trade-offs between species [59] are, in reality, differential responses to spatial environmental variation. All in all, this conceptual framework allows for integrating life-history theory on allocation trade-offs, driven ultimately by resource limitation, with the modern coexistence theory framework of niche partitioning via species-specific responses to environmental variation [39].

While fundamental to all organisms, resource allocation trade-offs can be quite difficult to detect in nature. Part of this difficulty comes from the fact that a multitude of resource allocation trade-offs must affect plants, but only a few usually can be examined at a time [60]. This may result in an apparent lack of correlation between traits A and B when, e.g., a third trait C is also involved in a resource allocation trade-off. Under these circumstances, species with low values of both A and B can exist [61], but because they likely have high values of C. Finally, negative correlations between traits may be obscured by ample variation in fitness and, if variation in traits is not wide enough, even an apparent positive correlation might be produced [62]. In forests, for example, the lucky few trees that managed to reach the canopy, and thus have unlimited access to light, can reproduce while still growing, while the trees in the understory often can do very little of either (Ch.4). Because tropical forests notoriously lack strongly dominant tree species, which indicates fitness differences may vary little [47], at the same time that can harbour an incredible diversity of plant traits, such as leaf sizes and adult heights, I suspected that a hyperdiverse tropical forest would be the ideal

grounds to test for allocation trade-offs. Moreover, if on one hand sampling size is limited in these forests due to the rarity of most species, on the other hand species hyperdiversity provides a plethora of species to test for interspecific trade-offs. Therefore, in an attempt to solve the biodiversity paradox created by the apparent lack of trade-offs in nature [60], I used the above mentioned conceptual framework to elucidate the mechanisms by which a forest in the Central Amazon maintains one of the highest levels of taxonomic and phenotypic diversity on the planet.

I chose four different resource allocation trade-offs, common to all plants, that encompass levels of organization from leaves to whole-plants. I made four key findings. First, differences in nutrient allocation trade-offs between legumes and non-legumes help explain the puzzling observation that legumes do not dominate the forest despite their nitrogen-fixing advantage (Ch.1). Specifically, legumes have to allocate calcium to their roots to recruit rhizobia, which likely comes at the cost of having leaves that are more susceptible to physical damage. These differences lead to differential responses by these two functional groups to a soil fertility gradient, allowing for spatial niche partitioning. Second, I found that species-specific differences in a trade-off between leaf size and number causes differential sapling performance along a light gradient, allowing for light partitioning on the leaf size axis (Ch.2). Third, I show that interspecific differences in a trade-off between height gain and crown expansion at the sapling stage can allow for niche partitioning along horizontal, but not vertical light gradients (Ch.3). Fourth, I show how a trade-off between growth and reproduction can explain adult height diversification in forest trees (Ch.4). In this case, interspecific differences in the size

at the onset of reproduction cause demographic trade-offs involving fecundity and generation times, resulting in vertical niche divergence among species. Importantly, these insights would not have been possible but for the broader conceptual framework that I used to guide my empirical work. This framework is both general and powerful, and can be applied to literally any resource allocation trade-off that might affect plant performance. Elucidating the niche partitioning mechanisms that arise when species differ in such trade-offs allows us to both understand the mechanistic basis of high dimensional coexistence and explain the hyperdiversity of some tropical forests.



Figure 0.4: *Cecropia sciadophylla*: the most successful pioneer species in the study site. This is a fast-growing plant, with tiny seeds that can be dispersed by birds and bats and can stay dormant in the soil until a new trefall gap opens. They also have a especial mutualism with ants, especially the quite aggressive *Azteca*, to whom the plant provides both shelter, in their hollow stems, and food, produced by a specialized gland.

Chapter 1

Leaf nutrients and habitat selection

1.1 Introduction

The great diversity of tropical plants has intrigued many generations of scientists, and yet the challenge to understand the mechanisms that create and maintain such diversity has persisted to this date. One of the reasons why plant coexistence is so challenging to understand is that they require similar resources [63, 64], so the possible mechanisms of niche differentiation are restricted compared to animals. For example, species may diverge in the set of environmental conditions they can tolerate, and because these conditions tend to vary across space, spatial coexistence might be possible [40]. Spatial coexistence can happen as species diverge to become so specialized into contrasting habitats that they become more likely to compete with conspecifics than with heterospecifics [39]. Indeed, the high diversity of trees found in tropical forests such as the Amazon is driven to a significant extent by habitat specialization

[65–68]. However, the mechanistic basis of habitat specialization remains unclear for most parts of this gigantic forest and for the vast majority of its tree species.

In the non-flooded forests of Amazonia, one of the main axes of environmental variation for plants is soil fertility, which is intrinsically related to topography. Such topo-edaphic gradients have been shown to affect tree species distributions at all spatial scales: whole-basin [69], regional [70], and local [71]. In fact, for a large portion of the Amazon, such as the Central Amazon, topography may vary at the local scale as much as it does across large distances leading to low beta [72], but high alpha diversity [2]. This further emphasizes the importance of understanding the mechanisms driving habitat specialization at local scales, as these local topo-edaphic gradients may be the only source of future microrefugia for many tree species [73].

Earlier attempts to understand the mechanisms that drive specialization along soil fertility gradients have identified many plant traits potentially involved in habitat selection. Some of these traits include leaf anti-herbivory defenses [67], specific leaf area, leaf size, wood density, seed size [74], and even leaf drought resistance traits [55]. However, the trait that should be most obviously related to soil fertility has been largely ignored: it is known that leaf nutrient content varies across the basin-wide soil fertility gradient [75], but little is known about its role in the habitat specialization of trees. We thus quantified six leaf nutrients for almost a thousand species of trees growing in one the poorest soils in the Amazon. The study forest is situated in a plateau intercut by two stream gullies and it presents the ideal place to test tree habitat specialization as a function of leaf nutrients, as soil fertility

varies widely with topography.

1.2 Conceptual framework

Simple models of species interactions are powerful because they derive from first principles and can thus generate important insights about species coexistence in natural settings. The Lotka-Volterra consumer-resource model, e.g., can be used to compare the competitive ability of different plant species, as it takes into account species' efficiency to acquire and use a given resource. In its simplest form, the model assumes resource uptake to be a linear function of resource availability (type I functional response), which should be a good representation of root absorption of soil nutrients. The model is as follows:

$$\frac{dC}{dt} = RAE \times RUE \times R \times C - m \times C \quad (1.1)$$

where C is the number of consumers, R is the amount of resource, and m , RAE , and RUE are constants that represent, respectively, mortality rate of consumers, resource acquisition efficiency (capture rate), and resource use efficiency (conversion rate). When C is at equilibrium ($\frac{dC}{dt} = 0$), we can derive the following R^* rule:

$$R^* = \frac{m}{RAE \times RUE} \quad (1.2)$$

where R^* is thus the minimum amount of resource R required to stabilize the consumer's population. When two or more consumer species compete for a same resource, the species with the lowest R^* will drive the others to extinction [76, 77]. As there are many ways for

species to arrive at a similar R^* value (eq.1.2), trade-offs between RUE and RAE can lead to fitness equalization of highly divergent phenotypes [57]. For example, adult trees may have much lower m compared to herbs, but herbs have much higher RUE than trees due to their small sizes (lower non-photosynthetic to photosynthetic tissue ratios). If m and RUE are positively correlated, then differences in competitive ability (R^*) between trees and herbs should be reduced. Therefore, any such interspecific trade-offs involving these three rates has the potential to reduce fitness inequalities among plant species.

As shade tolerant adult trees in tropical forests vary little in mortality rates (m) [78], it is probably most important to consider trade-offs between RUE and RAE. So, if we assume for a moment that mortality rates are constant across tree species, then trees growing in poor soils can be competitive either by maximizing the acquisition of the scarce nutrients present in the soil or by maximizing Carbon assimilation per unit of soil nutrient absorbed. One way soil nutrient acquisition can be improved is via association with microbial mutualists, such as nitrogen-fixing bacteria (rhizobia) or mycorrhizal fungi [79]. Nutrient use efficiency, in turn, can be maximized by increasing nutrient retention times within photosynthetic tissues and by maximizing resorption rates when leaves senesce [80]. Improving nutrient acquisition and use efficiencies, however, involve energetic and opportunity costs. For example, recruiting and maintaining soil mutualists requires photosynthates and even some limiting nutrients [81], whereas maintaining long leaf lifespan requires the production of tough leaf tissues with low nutrient content, which in turn limits photosynthetic capacity [17, 82]. Therefore, there should be an allocation trade-off between RAE and RUE for soil nutrients similar to

what was described for light [57]. If this trade-off is strong enough it may help reduce the fitness differences between high *RAE*, low *RUE* trees and low *RAE*, high *RUE* species, thus making coexistence between these contrasting strategies more likely in poor soils [39]. This hypothesis, however, only makes sense if soil nutrients are a limiting factor to plant growth. Would these same strategies still be competitive in more fertile soils?

Across soil fertility gradients in wet forests, where water availability is often not limiting, from first principles we expect that competition for light becomes more important for plant growth in more fertile areas. When competing for light, plants that can overtop their neighbors get a twofold advantage: unrestricted access to full light as well as preemption of neighboring competitors' access to one of their most limiting resources [57, 83]. In order to win this race, however, trees have to grow fast, even though this may come at the cost of increased mortality rates [84]. To grow fast, trees must deploy large quantities of nutrients into their leaves, especially nitrogen and phosphorus, as they upregulate their photosynthetic machinery [82]. In terms of soil nutrient use, therefore, those species capable of keeping large leaf nutrient contents and exposing these leaves to direct sunlight will have large photosynthetic capacity and thus large nutrient use efficiency.

Slow-growing, conservative species should have a hard time establishing in such a competitive environment, and not even their high nutrient retention times may be advantageous if nutrients are readily available in the soil. This means that nutrient acquisition efficiency will now be higher for species that invest little into their roots, as opposed to species that invest lots of energy recruiting soil mutualists, like some legumes do. While it is true that

tropical nitrogen-fixing legumes have facultative symbiosis with rhizobia [85], they may still have costs associated with preventing reinfection from these mutualists when their services are not needed. Nitrogen-fixing legumes therefore should have their competitive advantage negated as soil fertility increases.

In summary, because nutrient acquisition gets cheaper and the cost of nutrient losses becomes less important as soil fertility increases, the strong allocation trade-off between *RAE* and *RUE* that takes place in poor soils should get relaxed in rich soils. Therefore, the most competitive species in fertile sites will be those capable of maximizing both *RAE* and *RUE* at the same time. In other words, *RAE* and *RUE* should be a function of the interaction between soil fertility and species traits. Below we list these hypotheses followed by some predictions that can be tested in our study system, assuming the gullies have more fertile soils than the plateaus:

1. In habitats where soil nutrients are more limiting compared to light, the trade-off between *RAE* and *RUE* is strong, but as soil fertility increases and light becomes relatively more limiting, this trade-off is relaxed and species converge into a fast lifestyle with high *RAE* and *RUE* (Fig.3.1a);
 - a) In the plateau, non-fixing species should have lower leaf nutrient content compared to nitrogen-fixing legumes;
 - b) In the gullies, there should be little difference between the leaves of nitrogen-fixing legumes and non-fixing species.

2. Association with nitrogen-fixing bacteria may help plants maximize RAE in poor soils, but in fertile soils the cost of curbing these microbial mutualists causes nitrogen-fixing legumes to have lower RAE than non-fixing species (Fig.3.1b);
 - a) The distribution of nitrogen-fixing legumes should be more associated with the plateau, while non-fixing species should be more associated with the gullies;
 - b) Nitrogen-fixing legumes should have higher relative abundance and basal area in the plateau than in the gullies.

3. When soil nutrients are limiting plant growth, a high RUE can be achieved by maximizing nutrient retention time, which requires a slow lifestyle, but when soil nutrients are abundant, the cost of producing well-defended leaves may be larger than the cost of nutrient loss; furthermore, in fertile soils RUE is maximized by increasing leaf photosynthetic capacity and exposure to direct sunlight, which require fast growth rates (Fig.3.1c);
 - a) Plants growing in the plateau should have lower leaf nutrient content than plants growing in the gullies;
 - b) Species with lower leaf nutrient content should be more associated with the plateau, while species with higher leaf nutrient content should be associated with the gullies;

c) Community weighted mean leaf nutrient content should be higher in the gullies compared to the plateau.

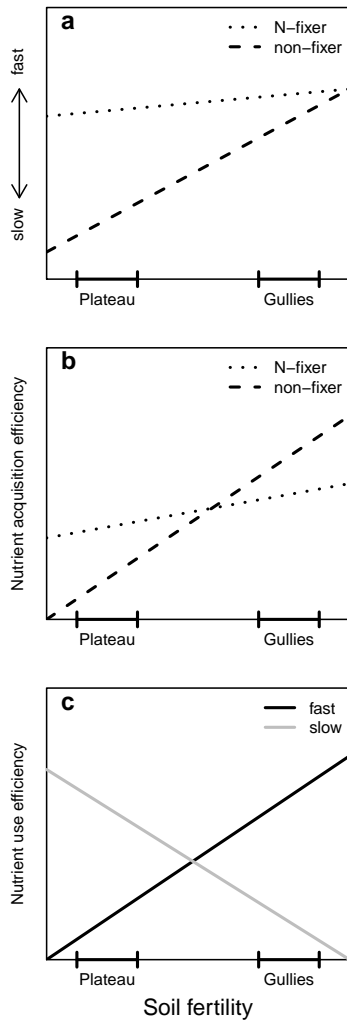


Figure 1.1: Conceptual figure depicting the three main hypotheses tested in this study. While soils on the plateau are poor and toxic, the gullies receive the nutrients washed down-slope and are thus more fertile. (a) N-fixation allows some species to have productive leaves and live fast lifestyles, while the leaf nutrients of non-fixers rely more on soil fertility. (b) While N-fixers have higher nutrient acquisition efficiency (RAE) compared to non-fixers in poor soils, due to their symbiosis with rhizobia, non-fixers should have higher RAE than N-fixers in more fertile soils because small investments yield high returns there. (c) When soil nutrients are abundant, plants with high leaf nutrient content have higher photosynthetic capacity and can thus grow fast and intercept more light, which allow them to have higher nutrient use efficiency (RUE) than slow plants; where soils are nutrient-depleted, and light is relatively less limiting, RUE depends more on the conservation of nutrients within the plant, which requires leaves to have longer lifespans and lower leaf nutrient content, which in turn causes plants to grow slowly.

1.3 Methods

Study site

The study site is a 25-ha permanent plot located in a non-flooded, pristine area of forest in the Central Amazon (2°30'S, 60°W). This is the most species-rich and diverse site within the ForestGEO network (> 1,500 tree species) [21], but this is in sharp contrast with the extremely infertile soils where it occurs. Soils in this region, classified as xanthic ferralsols (FAO/UNESCO system), are intensely weathered Tertiary deposits with low field capacity and low nutrient concentration, especially P, Ca, and K [86]. Soil properties, however, can greatly vary locally and often covary with topography, which in this region is dominated by plateaus and numerous stream gullies (Fig.A.1). The soil in the plateaus has a fine texture, with clay particles that are rich in iron and aluminium, but as runoff rainwater downflows to the gullies most of these fine particles are carried away, thus causing gully soils to be sandy, but less toxic (Fig.A.1,1.9) [87]. Previous chemical analysis of the plot soil has shown that availability of phosphorus in the gullies is on average higher than in the plateau (Fig.A.1). Gully forests also tend to have smaller standing biomass, with palms being more dominant compared to the forest in the plateau (Fig.1.2) [88]. Higher tree turnover rates mean that surges in nutrient availability derived from deceased trees will be relatively common, thus increasing the average soil fertility of the gullies. High mean annual temperatures (26.7°C) and humidity in turn promote rapid decomposition of decaying organic matter, but frequent and heavy rains can wash most of these nutrients away if plants fail to absorb them quickly.

Annual rainfall in the area is 1900-3500 mm annually, with a pronounced dry season between June and October, but monthly precipitation rarely drops below 100 mm [70].

Sampling design

To have a representative sample of the hundreds of tree species that make up this forest we took a sampling strategy that maximized the number of species sampled in the two most contrasting habitats in the plot. This was only possible because within the permanent plot all trees with a stem diameter at breast height (*DBH*) of ≥ 1 cm were mapped between 2004 and 2008 and then identified to species, totaling 150,739 trees. Given the vast number of trees and species available, we took three decisions to make sampling feasible. First, we only considered plants with *DBH* < 10 cm, as their leaves are more accessible for collection. Second, we divided the plot into two habitat types: plateau, with elevations ≥ 35 m, stream gullies, with elevations < 15 m; and slopes, with intermediate elevations (Fig.A.1). We decided to focus our sampling efforts on the plateau and on the western gully only, and avoid the slopes, in order to maximize the contrast between habitats. Third, we ranked the plot quadrats (20x20 m) according to their number of species and started sampling the richest ones until we had sampled all the species that account for $\geq 90\%$ of all stems found in each habitat (sampling coverage was 91% for the gullies and 95% for the plateau). In order to estimate intraspecific variation we sampled some common species up to three times in each habitat. Although some species could be sampled in both habitats, most species



Figure 1.2: The contrast between plateau and gully forests: on the plateau (upper panels) forests grow taller and denser, and stemless palms dominate the understory; in the gullies (lower panels), the canopy is much more open and dominated by large palms.

were sampled only once and thus in a single habitat. To avoid pseudoreplication, only one individual per species was sampled in each quadrat. Sampling was made more difficult due to plant mortality in the 10 years prior, and due to the deplorable state of many individuals, which were largely defoliated or whose leaves were highly damaged to the point that they could not be included. In spite of these difficulties, we managed to sample 1,182 individual plants (874 in the plateau and 308 in the gully) from 978 different species (782 in the plateau and 237 in the gully) and across 225 quadrats (190 in the plateau and 35 in the gully). These differences reflect the fact that the plateau and gullies occupy very different areas within the plot (61 and 10%, respectively; Fig.A.1).

Quantifying leaf nutrient content

In order to estimate foliar nutrients for each individual plant, we collected the least damaged leaves in each plant, dried them, and sent them for chemical analysis in a plant nutrition lab. We first collected one representative branch with healthy leaves (or a single leaf for large-leaved species such as palms) for each of the individual plants sampled. Once harvested, these branches were left to rehydrate overnight, as we also measured several other traits in these leaves. We then sampled 1-30 leaves per branch, depending on the size of the leaf, always selecting the least damaged, but mature leaves. These leaves were carefully cleaned with a paper towel to remove epiphylls, insects, and any other debris on the leaf surface. We then removed petioles and petiolules and dried the leaves to a constant mass. The samples

were then stored for up to three years until the field sampling was completed. Leaf sampling was done between July and October from 2016 to 2019. These samples were then ground to particles that could pass through a 2 mm mesh sieve, and then shipped to the Plant Mineral Nutrition lab (Agronomical School Luiz de Queiroz, Brazil), where the concentration of six macronutrients (nitrogen, phosphorus, potassium, calcium, magnesium, and sulfur) was quantified. Part of each sample was digested with sulfuric acid and then N was quantified by titration. The remainder of the sample went through nitric-perchloric digestion, and the other nutrients were then quantified through colorimetric analyses (P and S) or through atomic absorption spectroscopy (K, Ca, and Mg).

Modeling leaf nutrient content

As leaf nutrient content can vary substantially within a given species according to soil fertility [89], we chose to model intraspecific variation across soil habitats in order to better understand the effect of soil on leaf nutrient content. Estimating such sources of uncertainty, however, would require large sample sizes for each species, which is both unfeasible and unnecessary in hyperdiverse forests due to the extreme rarity of most species [90]. To counter that limitation, we used hierarchical Bayesian models that allowed us to capitalize on the unprecedented wealth of data we collected in a meaningful way. By modeling both within-species, within-habitats variation and within-species, across habitat variation, we could estimate species- and habitat-specific leaf nutrient content, which we later used to

correlate with species' habitat association. Finally, because leaf nutrients tend to be correlated to each other [82], we modeled leaf nutrients using a multivariate approach. So we started modeling the log-transformed leaf content of all six macronutrients for each plant i from species j (\mathbf{M}_{ij}) as a multivariate normal distribution as follows:

$$\log_e(\mathbf{M}_{ij}) \sim \mathcal{N}_6(\boldsymbol{\beta}_j + \boldsymbol{\gamma}_j \times H_{ij}, \boldsymbol{\Sigma}_w) \quad (1.3)$$

where $\boldsymbol{\beta}_j$ is the species-specific leaf nutrient content in the bottom of the gullies ($H_{ij} = 0$; random species effect); $\boldsymbol{\gamma}_j$ is the habitat effect (H) that is added to $\boldsymbol{\beta}_j$ to yield the amount of leaf nutrients in the plateau ($H_{ij} = 1$; species-specific slope); and $\boldsymbol{\Sigma}_w$ is the covariance matrix that describes the intraspecific correlations among the nutrients (residuals). To account for the effect of nitrogen-fixation on the leaf nutrients of some legume species, we further modeled intercepts ($\boldsymbol{\gamma}$) and slopes ($\boldsymbol{\beta}$) together ($\boldsymbol{\Gamma}$) as random draws from a multivariate normal distribution as follows:

$$\boldsymbol{\Gamma}_j \sim \mathcal{N}_{12}(\boldsymbol{\theta} + \boldsymbol{\phi} \times F_j, \boldsymbol{\Sigma}_b) \quad (1.4)$$

where $\boldsymbol{\theta}$ are the species-specific parameters ($\boldsymbol{\Gamma}$) for non-fixing species ($F_j = 0$); $\boldsymbol{\phi}$ is the amount added to these parameters for nitrogen-fixing legume species ($F_j = 1$). Species' ability to fix nitrogen (F_j) was taken at the genus level from a thorough compilation presented elsewhere [91]. Lastly, $\boldsymbol{\Sigma}_b$ is the covariance matrix that describes the interspecific correlations between species-specific parameters. ($\boldsymbol{\Sigma}_b$ can also show, e.g., if the species that have higher leaf nutrient content are also the ones who respond more strongly to changes in soil fertility,

or if there are any interspecific trade-offs among leaf nutrients.) Finally, we predicted the across-species leaf nutrient content in each of the habitats as follows:

$$\hat{\mathbf{M}} = \boldsymbol{\theta}_\beta + \boldsymbol{\theta}_\gamma \times H + \boldsymbol{\phi}_\beta \times F + \boldsymbol{\phi}_\gamma \times F \times H \quad (1.5)$$

The determination of prior distributions for the hyperparameters $\boldsymbol{\theta}$ and $\boldsymbol{\phi}$, as well as proof of model convergence are given in the supplementary material for chapter 1. All analyses were done in or through R v.3.5.3 [92], with the help of the package `rjags`, to run the Markov Chain Monte Carlo (MCMC) simulations in `JAGS` [93], and the package `coda` to extract and run MCMC convergence diagnostics [94].

Habitat association

In order to estimate species' association with either the gully or the plateau, we run spatial point pattern analyses based on topography for a subset of the species sampled for leaf nutrients. It was shown before that in the study area soil physico-chemical properties covary tightly with topography [87], and we could further confirm this for our own study site (Fig.A.1), so we chose to use elevation within the plot as a proxy of soil fertility. Furthermore, treefall disturbances cause soil properties to oscillate dramatically over time, thus making any attempt to describe soil fertility in greater detail within these major elevational habitats to be superfluous. We thus used elevation data collected at a 5 m-grid within the plot as a proxy for soil fertility, assuming there is a fertility gradient going from the toxic, clayey soils of the plateau to the fertile, sandy soils of the gullies (Fig.A.1). We then interpolated

elevation data to estimate each individual plant's elevation within the plot, and used these values as the predictor variable to test for species' habitat association, which we did using the analytical method described in Shen2013. This method is a two step modeling approach that measures how much of spatial aggregation of a given species is explained by environmental variables (α) while taking into account the effect of other unknown clustering processes, such as dispersal limitation. Plateau specialists, therefore, should have significantly positive α (density increases with elevation), while gully specialists should have negative α (density decreases with elevation). Because this kind of analysis may be sensitive to sample size, we only tested species with ≥ 70 individuals in the 25-ha plot, i.e., 359 species in total.

Community weighted means

To estimate the competitive advantage of high leaf nutrient content across the soil fertility gradient, we estimated community-level metrics of leaf nutrient content. Our metric of choice is the traditional community weighted mean (CWM) because it takes into account the ecological success of each species. A species' ecological success in this context can be estimated either by the number of individuals in a community (CWM_a) or by the sum of individual biomass of these individuals (CWM_b). Tree biomass in turn can be estimated by tree basal area ($A_B = \pi \times (DBH/2)^2$). CWM_a and CWM_b are complementary to each other, so we used both abundance and total basal area for each species to weight community-level trait values. To control for intraspecific variance in leaf nutrients and have

unique point-estimates of leaf nutrient content for each species across the plot, we averaged point-estimates for each species in each habitat (gully and plateau). Finally, we calculated *CWM* for each habitat (gullies, slopes, and plateau) in the plot and for each 20x20 m quadrat within these habitats (625 quadrats total: 65 in the gullies, 181 in the slopes, and 379 in the plateau). The sampling coverage for each of these habitats was as follows: 91, 92, and 95% of all individual trees and 89, 86, and 90% of the total basal area in the gullies, slopes, and plateau, respectively.

1.4 Results

We found a great diversity of leaf nutrient stoichiometry across species and habitats (Fig.A.5-A.6), but also within species (Fig.A.2). Across species, most leaf nutrients were positively correlated to each other, while within species there was some evidence of a trade-off between Ca and N, P, and K contents (Tab.1.1). A principal component analysis of the leaf nutrient content of all plants sampled reinforce these results, with the first principal component representing a general gradient of leaf nutrient content (only sulfur had a relatively small loading on this axis), and the second component indicating a trade-off between two groups of nutrients (S, N, and P against Ca and Mg; Fig.1.3). This trade-off may in part be explained by the differences in leaf nutrient content between N-fixers and non-fixers (Fig.1.3). Lastly, the foliar N:P ratio found across almost all species in the study site is well above the Redfield ratio for terrestrial ecosystems, i.e., the ratio above which P is considered to be acutely

limiting (Fig.A.7).

Several of the sampled species can likely associate with rhizobia to fix atmospheric nitrogen. In the study plot, there are at least 147 nitrogen-fixing legumes, which make up 10.15% of all species recorded, 7.28% of all trees, and 8.39% of the total basal area. As a contrast, there are only 43 species of non-fixing legumes, which make up 2.97% of all species, 1.26% of all trees, and 4.26% of the total basal area in the plot. These proportions between fixers and non-fixers practically does not change across the plot habitats, except for total basal area, which goes from 7.93% in the plateau to 11.61% in the gullies (Fig.A.4).

Table 1.1: Correlations among the six leaf nutrients quantified in this study. Values below and above the matrix diagonal correspond to intra- and interspecific variation, respectively. Parameters presented here derive from the variance-covariance matrices Σ_w and Σ_b in eq.1.3-1.4.

| | N | P | K | Ca | Mg | S |
|----|-------------|--------------|-------------|-------------|-------------|--------------|
| N | - | 0.27 | 0.21 | 0.05 | 0.17 | 0.33 |
| P | 0.17 | - | 0.36 | 0.07 | 0.13 | 0.17 |
| K | 0.12 | 0.34 | - | 0.44 | 0.43 | 0.14 |
| Ca | -0.13 | -0.14 | -0.11 | - | 0.77 | -0.14 |
| Mg | 0.06 | 0.00 | 0.00 | 0.37 | - | 0.03 |
| S | 0.15 | 0.12 | 0.03 | 0.04 | 0.16 | - |

In bold are parameter values whose probability of being larger than zero is $> 97.5\%$ or $< 2.5\%$.

Leaf nutrients, habitats, and N-fixation

Both the ability to fix nitrogen and the habitat where plants grow had significant effects on leaf nutrient content, but these effects varied across the different nutrients (Tab.1.2).

Our first prediction (1a) that leaf nutrient content would be smaller for non-fixing plants

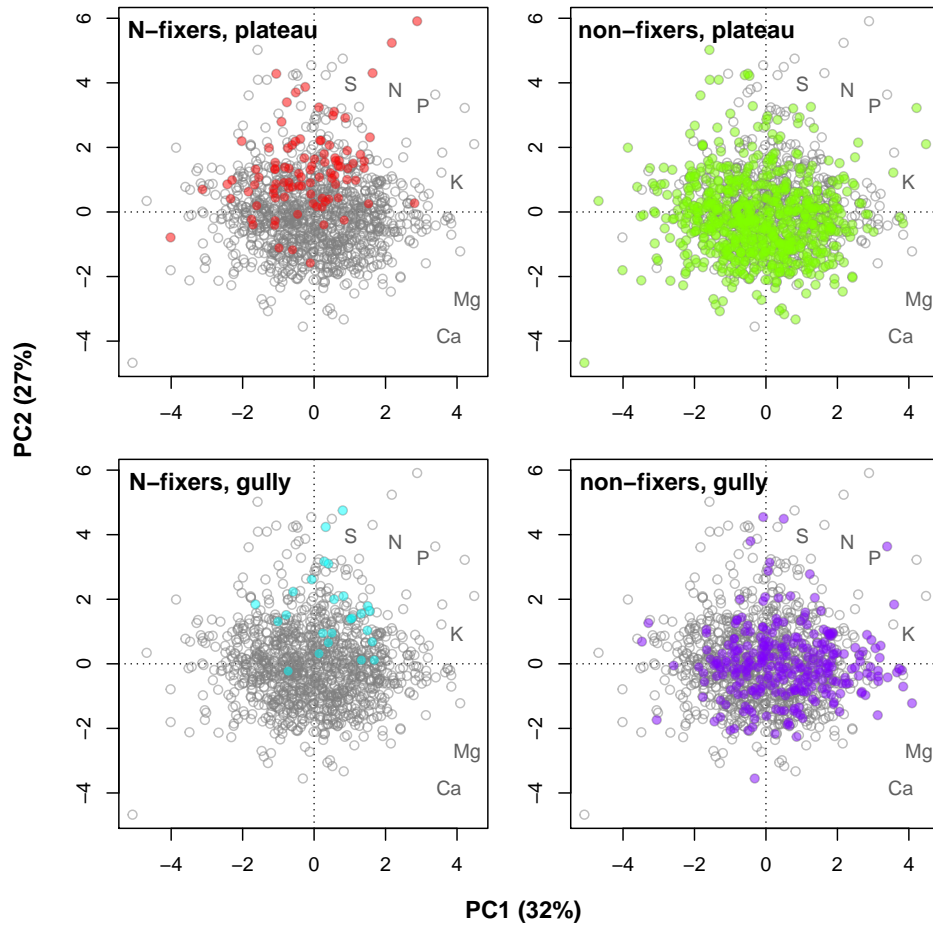


Figure 1.3: Principal component analysis of the observed leaf content of six macronutrients (N, P, K, Ca, Mg, and S) for 1,182 plants from 978 different species (106 N-fixing legumes) sampled in two contrasting soil habitats (308 plants in the gully and 874 in the plateau). The first principal component (PC) differentiate species with high contents of all leaf nutrients from those with low leaf nutrient content. PC2 reflects the trade-off between leaf N, P, and S (high in N-fixing legumes) and leaf Ca and Mg (low in N-fixing legumes). Together PC1 and PC2 explain 59% of all the variance found in the leaf nutrient data. The position of nutrient labels represent their loadings onto the two PC axes.

Table 1.2: Effects of habitat, N-fixation, and their interaction on the leaf content of six macronutrients. The median and credible interval ($CI_{95\%}$) refers to the posterior distribution of across-species parameters (hyperparameters; eq.1.4), and p is the probability that these parameters are positive (except for the intercepts, which were defined a priori to be positive). A positive habitat effect means that leaf nutrient content in the gully is larger than in the plateau (Fig.D.2). Bolded values refer to parameters that were significantly different than zero.

| Nutrient | Parameter | symbol | median | $CI_{95\%}$ | p |
|-------------------|--------------------|------------------------|--------------|---------------|------|
| Nitrogen | intercept | θ_{β_N} | 16.51 | [16.12;16.89] | NA |
| | habitat | θ_{γ_N} | 0.02 | [-0.03;0.06] | 0.74 |
| | N-fixation | ϕ_{β_N} | 0.30 | [0.24;0.37] | 1.00 |
| | habitat*N-fixation | ϕ_{γ_N} | 0.01 | [-0.15;0.16] | 0.53 |
| Phosphorus | intercept | θ_{β_P} | 0.66 | [0.65;0.67] | NA |
| | habitat | θ_{γ_P} | 0.11 | [0.08;0.14] | 1.00 |
| | N-fixation | ϕ_{β_P} | 0.17 | [0.13;0.22] | 1.00 |
| | habitat*N-fixation | ϕ_{γ_P} | 0.01 | [-0.08;0.11] | 0.56 |
| Potassium | intercept | θ_{β_K} | 3.09 | [2.95;3.22] | NA |
| | habitat | θ_{γ_K} | 0.38 | [0.31;0.46] | 1.00 |
| | N-fixation | ϕ_{β_K} | -0.05 | [-0.17;0.07] | 0.22 |
| | habitat*N-fixation | ϕ_{γ_K} | 0.12 | [-0.12;0.38] | 0.84 |
| Calcium | intercept | $\theta_{\beta_{Ca}}$ | 3.38 | [3.24;3.55] | NA |
| | habitat | $\theta_{\gamma_{Ca}}$ | 0.18 | [0.10;0.27] | 1.00 |
| | N-fixation | $\phi_{\beta_{Ca}}$ | -0.38 | [-0.52;-0.24] | 0.00 |
| | habitat*N-fixation | $\phi_{\gamma_{Ca}}$ | -0.07 | [-0.37;0.22] | 0.33 |
| Magnesium | intercept | $\theta_{\beta_{Mg}}$ | 2.05 | [1.97;2.14] | NA |
| | habitat | $\theta_{\gamma_{Mg}}$ | 0.16 | [0.08;0.23] | 1.00 |
| | N-fixation | $\phi_{\beta_{Mg}}$ | -0.41 | [-0.53;-0.28] | 0.00 |
| | habitat*N-fixation | $\phi_{\gamma_{Mg}}$ | -0.11 | [-0.39;0.15] | 0.22 |
| Sulfur | intercept | θ_{β_S} | 1.75 | [1.67;1.83] | NA |
| | habitat | θ_{γ_S} | -0.01 | [-0.08;0.07] | 0.43 |
| | N-fixation | ϕ_{β_S} | 0.27 | [0.13;0.40] | 1.00 |
| | habitat*N-fixation | ϕ_{γ_S} | -0.08 | [-0.33;0.19] | 0.26 |

compared to N-fixing legumes growing in poor soils (plateau) was only confirmed for N, P, and S, while Ca and Mg actually showed the opposite pattern (Fig.D.2). Contrary to our second prediction (1b), the differences in leaf nutrients between N-fixers and non-fixers were still significant in the rich soils of the gully, except for K and S (Fig.D.2). This is because for no nutrient there was a significant interaction between habitat and N-fixation (Tab.1.2). Nevertheless, leaf nutrient content was indeed smaller in the plateau (3a), except for N and S, which did not vary significantly across habitats (Fig.D.2). Interestingly, this habitat effect was stronger for non-fixers, while N-fixers had much less steep drops in nutrient content in the plateau; for K the difference was comparable to non-fixers, while S actually showed a opposite, albeit insignificant trend to increase in the plateau (Fig.D.2). Lastly, the N:P ratio was only significantly larger for N-fixers than for non-fixers in the plateau, although the difference was comparably large in the gully as well (Fig.A.7). In summary, N-fixers seem to have: 1) a less variable stoichiometry across habitats; 2) consistently higher leaf contents of N, P, and S; but 3) consistently lower contents of Ca and Mg; and 4) a stronger limitation by P compared to non-fixers.

Habitat association

The spatial analysis of species distribution in the plot shows that, as predicted (P_{3b}), species with inherently lower leaf nutrient contents are more associated with poor soils, except for nitrogen-fixing legumes (Tab.1.3). N-fixers did show a tendency to be more associated

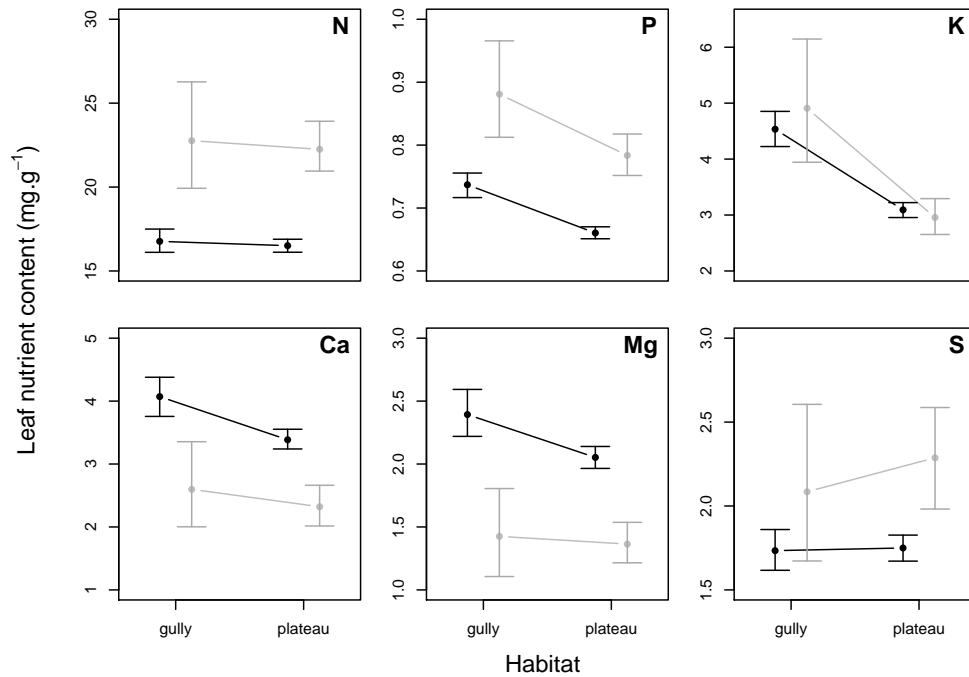


Figure 1.4: Differences in foliar content of six macronutrients (N, P, K, Ca, Mg, and S) between the gully and the plateau and between nitrogen-fixing legumes (grey) and non-fixing species (black). Points represent the median of the posterior distribution of the predictions based on hyperparameters. Error bars correspond to 95% credible intervals.

with the poor soils of the plateau, as predicted (P_{2a}), but non-fixing legumes showed an even higher association with the plateau; none of these differences were significant though (Fig.1.5c). Despite the much larger area of plateau within the plot compared to that of the gullies (Fig.1.5a), 44.5% out of the 359 species analyzed showed significant associations with one of the habitats: 107 species are associated with the plateau and 53 with the gullies (Fig.1.5b). For 199 species there was no evidence of habitat association, which does not necessarily mean they have no habitat preferences (generalists); many of them may be specialists, but it will be impossible to tell if they are distributed in just a few large clumps

in only one of the habitats.

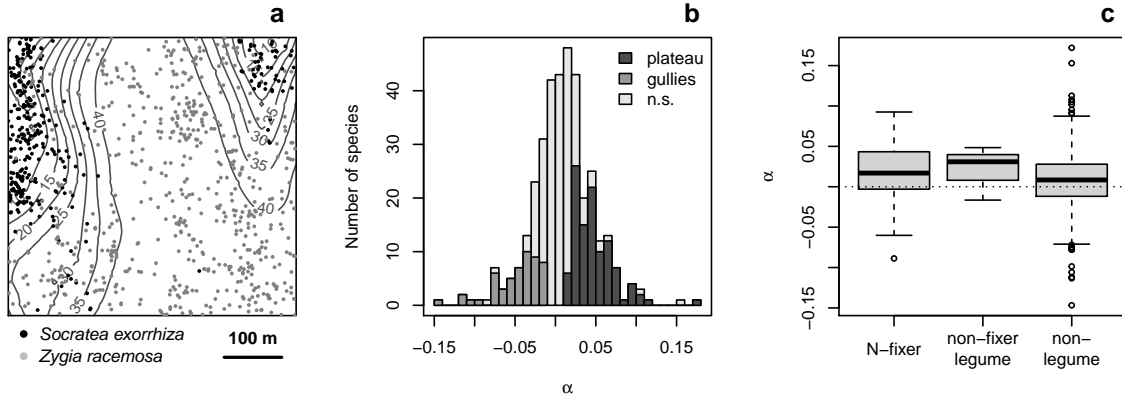


Figure 1.5: Habitat association analyses show the partitioning and sharing of soil habitats among 359 tree species. (a) Plot map showing the distribution of two habitat specialists: the gully specialist *Socratea exorrhiza* ($\alpha = -0.15$) and the plateau specialist, N-fixing legume *Zygia racemosa* ($\alpha = 0.05$). (b) Distribution of the habitat association metric (α), which is positive when a species distribution is associated with the plateau and negative when it is associated to the gullies (*n.s.* refers to species that did not show significant association with either habitat). (c) Differences in α between N-fixing legumes, non-fixing legumes, and non-legumes.

Community structure

Taking community structure into account mostly reinforced the previous results, but it also detected some new trends. For example, N-fixers had indeed higher relative abundances in the plateau than in the gullies (Fig.1.6a), which is according to our prediction (P_{2b}), but the pattern was reversed when we took tree size into account (Fig.1.6b). This is because N-fixing trees tend to be larger than non-fixer ones in the gully, but this difference decreases towards the plateau (Fig.A.8b). Another important finding was that community weighted mean (*CWM*) values of leaf nutrient content confirms that species with lower leaf nutrients

Table 1.3: Correlations between leaf nutrient content and habitat association. Nutrient content was estimated as the average of the species-specific values across habitats (plateau and gully). The metric α was used to represent habitat association. Negative correlations mean that species with low leaf nutrient contents tend to be associated with the plateau.

| | N | P | K | Ca | Mg | S |
|------------|--------------|--------------|--------------|--------------|--------------|------|
| N-fixers | -0.22 | -0.25 | -0.08 | -0.09 | -0.16 | 0.01 |
| non-fixers | -0.12 | -0.13 | -0.14 | -0.05 | -0.11 | 0.01 |
| all | -0.10 | -0.11 | -0.14 | -0.06 | -0.12 | 0.02 |

In bold are parameter values whose probability of being larger than zero is $> 97.5\%$ or $< 2.5\%$.

dominate the poor soils of the plateau, while those with higher leaf nutrients dominate the fertile gullies (Fig.1.7), in accordance with our expectations (P_{3c}). This is true for all nutrients except for sulfur, which showed the reversed pattern. These patterns did not change qualitatively when we used tree basal area instead of abundance (Fig.A.9), or when we calculated CWM for the whole area occupied by each habitat instead of doing it for each quadrat separately (Fig.A.10-A.11). The only benefit of the quadrat-level analysis is that it can show how variable CWM can be at smaller spatial scales and that the ranges of CWM in the plateau largely overlap with the ranges in the gully (Fig.1.7-A.9). Additionally, using species' average nutrient content allowed us to predict CWM in the slopes, a habitat we had not sampled leaf material from. The key finding was that, just as they do in terms of soil fertility, quadrats in the slopes showed CWM values intermediate between the gullies and the plateau.

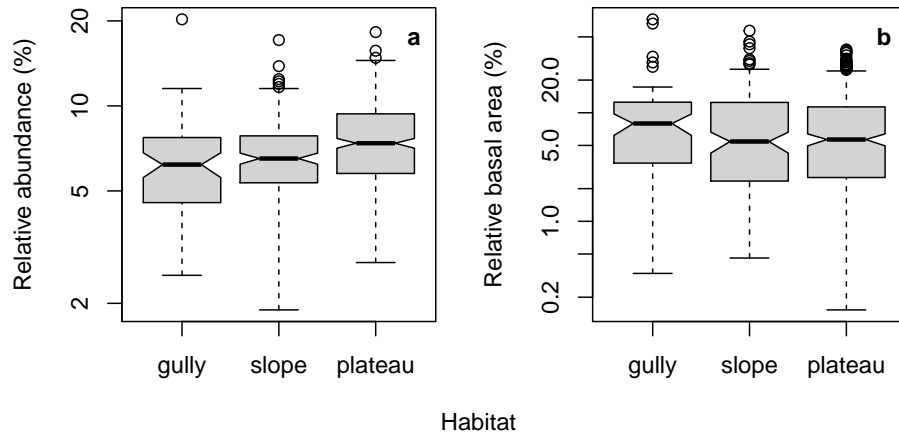


Figure 1.6: Relative abundance (a) and basal area (b) of nitrogen-fixing species across the three main habitats found in the forest plot. Values refer to each of the 625 quadrats of the plot. The notches in the boxes represent the non-parametric equivalent of 95% confidence intervals, i.e.: $\pm 1.58 \times IQR/\sqrt{n}$, where IQR is the interquartile range of the distribution and n is the sample size.

1.5 Discussion

Our study aimed to test if leaf nutrient content and ability to fix nitrogen could reflect species strategies for acquiring and using soil nutrients and thus predict species' abundance and distribution along soil fertility gradients. We reasoned that species can adapt to surviving in poor soils by either maximizing nutrient acquisition efficiency (RAE) or nutrient use efficiency (RUE). We hypothesized that: 1) N-fixing legumes excel at acquiring both N, due to their symbiosis with rhizobia, and other soil nutrients, due to an increased production of root enzymes compared to non-fixing plant species; 2) species could maximize nutrient use efficiency by reducing the amount of nutrients allocated to their leaves, which should come at the cost of photosynthetic capacity. These main hypotheses were tested at three different

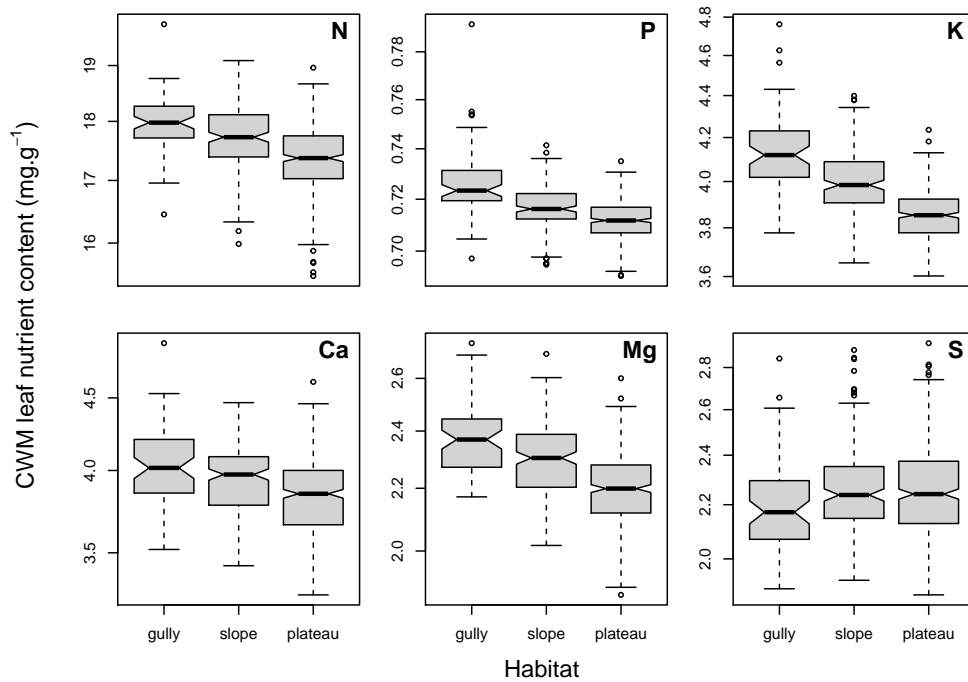


Figure 1.7: Mean leaf nutrient content weighted by species's abundance in each quadrat of each major habitat type. Values refer to community weighted means (*CWM*) based on the point-estimates of species' leaf nutrient contents averaged across habitats.

organizational levels along a soil fertility gradient: 1) within species and functional groups; 2) across-species differences in spatial distribution and relative abundance; and 3) turnover of community-aggregated trait values.

We found that leaf nutrient content varied widely across individuals, species, functional groups, and habitats. In spite of all this variance, we found strong patterns compatible with the hypothesis that plants with lower leaf nutrient contents are better adapted to growing on the nutrient-poor soils of the plateau. For example, plants growing in the more fertile soils of the gullies tended to have higher leaf nutrient contents than those found in the plateau (Fig.D.2, Tab.1.2). Moreover, species with lower average leaf nutrient content

were more associated with the plateau, while species with higher leaf nutrients were more associated with the gullies (Tab.1.3). Lastly, the communities on the plateau were more dominated by species with low leaf nutrients compared to the gully communities (Fig.1.7). In contrast, our hypothesis that N-fixing legumes being more competitive in poor soils proved more controversial. Although N-fixing species tended to be more abundant (Fig.1.6a) and associated with the plateau (Fig.1.5c), the relative dominance of these species was higher in the gullies than on the plateau (Fig.1.6b). This was in spite of their higher leaf content of N, P, and S compared to non-fixing species, which in turn had higher leaf Ca and Mg (Fig.D.2, Tab.1.2). Overall, these results reinforce the role of variation of soil nutrient availability in the differential performance and thus coexistence among species with contrasting nutrient acquisition and use strategies.

Nutrient use strategies and habitat specialization

Our results supported the general idea that plants that can produce more leaf biomass with less nutrients are more competitive in nutrient-depleted soils. This is compatible with the R^* rule, according to which species that can maintain positive population growth rates when resources are scarce (low R^*) are the best competitors in oligotrophic systems [76, 77]. If this ability to survive low resource availability trades off with the ability to consume and thus deplete resources quickly, then we should also expect that species with higher R^* are more competitive where resources are plentiful [58]. Although these concepts have been repeatedly

demonstrated in simple systems, such as bacteria [76], phytoplankton, and annual plants [77], it was surprising to see how well they can also apply to a hyperdiverse tree community. The correlation between leaf nutrient content and soil fertility had also been previously observed in the Amazon, but at the basin-wide scale and over a much wider fertility gradient [75]. In such large-scale studies it is often impossible to know to what extent variation in leaf nutrient content is due to plasticity as opposed to intrinsic differences across species. It was only after taking this plasticity in leaf nutrients into account that we could discern the patterns described here.

Leaf nutrient contents are expected to increase with soil fertility, but mostly for slow-growing species adapted to poor soils; fast-growing species respond to flushes of soil nutrients by growing faster [95]. Fast-growing species can thus better capitalize on surges in soil nutrient availability, as by growing larger means they will be also having priority access to other limiting resources, such as light, water, and even other soil nutrients [95]. We believe this kind of flush in soil nutrients is more common in the gullies compared to the plateau because: 1) the forest there is likely more dynamic, so nutrients spend less time trapped in the standing biomass [88]; and 2) after storms, runoff water may wash nutrients down-slope, thus constantly fertilizing the gullies [10]. Both of these sources of nutrients should have the effect of increasing the supply rate of soil nutrients to the plants in the gullies compared to the plateau, which should select for fast-growing species with high leaf nutrient content [77]. In contrast, the plateau's only external source of nutrients might be atmospheric fixation and deposition, and surges in soil nutrient may only occur when large trees suddenly die, thus

releasing all the nutrients they had accumulated over centuries. The high spatial variation in community weighted mean of leaf nutrient contents reflects the somewhat stochastic nature of this nutrient supply dynamics.

Our findings lend support to the hypothesis that plants adapted to infertile soils can survive and grow under much lower resource supply rates, but that plants adapted to fertile sites are more competitive once soil nutrients become more abundant. This is of fundamental importance because in practice it shows that the competitive landscape is heterogeneous across the studied topo-edaphic gradient, a necessary condition for spatial coexistence to take place [40]. If species with contrasting nutrient use strategies can specialize into contrasting soil habitats, then their coexistence becomes more likely, as spatial aggregation leads to intraspecific competition being more important than interspecific competition [39]. Because in these soils most nutrients might be limiting, and trade-offs in use efficiency across different nutrients are likely, the creation of multiple soil niches becomes a possibility [77]. This could help to explain the huge diversity of tree species in Amazonian terra firme forests, in spite of its relatively modest topographic diversity [72]. The leaf nutrients analyzed here, however, responded to the topo-edaphic gradient in a very similar manner, except for sulfur.

While all other nutrients seem to be less limiting in the gullies, high foliar S may be important to survive in the plateau. The gradient in leaf nutrients, which increase from the plateau to the gullies, was found even for nitrogen, which is not supposed to be a limiting resource in tropical forests thanks to the high N-fixation of many legume species [96]. So much so that large amounts of N are constantly leaking out of tropical forests [85]. In

fact our results show no significant differences in leaf N content (*LNC*) between gully and plateau, but we did find *LNC* to affect species distribution and relative abundance. This would only make sense if species' performance in the plateau is mostly limited by the low availability of other nutrients, such as P, in such a way that allocating more N into the leaf would not result in a higher photosynthetic capacity. Therefore, species that minimize their *LNC* when growing in the poor soils of the plateau should have higher N use efficiencies and thus have a competitive advantage there. Indeed, not only the leaf content of P, but also of K, Ca, and Mg were much smaller in the plateau. These are all nutrients that, given how ancient the soil in this forest is, may only enter the system through atmospheric deposition (ashes, e.g.), and supply rates should thus be dictated by leaching from decomposing litter on the forest floor. To cope with this limitation and capture these nutrients before they are washed away by the frequent rains, plants in this forest produce superficial roots that form a mat just below the leaf litter [97]. P is an especially challenging nutrient for plants to capture, as most of it is usually trapped in organic forms that are not readily available for uptake and require digestion by phosphatases or solubilization through the secretion of organic acids by the roots [98]. Although possible mechanisms of soil P extraction, these are all energetically costly and may not be feasible, e.g., for plants already struggling to have access to light. Therefore, the most efficient strategy to cope with the scarcity of this nutrient might be to reduce leaf P content to a minimum and prolong leaf lifespan in order to improve this nutrient use efficiency (Fig.1.8d) [17]. Another strategy is to maximize reabsorption of nutrients from senescing leaves, but again this can be energetically costly for the plant [99]

and is not possible for immobile nutrients such as Ca. Finally, the only exception to the observed pattern was foliar S, which is more abundant in the leaves of plants in the plateau, especially N-fixer species. We unfortunately lack data on soil S, but we do know that S leaks more easily out of sandy soils, and that it tends to bind to Al and Fe when P is scarce [100]. Because the plateau soil is clayey and rich in both Al and Fe [87], S availability should be higher there compared to the sandy and Fe and Al poor soils of the gullies. These very same metals that can trap S in the soil, however, can be very toxic for plants. Once inside plant tissues, metals catalyze the production of reactive oxygen species, capable of wreaking havoc within plant cells unless the production of antioxidants is up-regulated [101]. Some of the most important antioxidants are organosulfur compounds such as glutathione, so the high leaf S content may reflect the need plants have to avoid metal poisoning [101]. (Leaf S is so concentrated that on the plateau, after a rain, it is possible to smell it in some parts of the forest, presumably coming from the leaf litter of N-fixing species; *pers. obs.*)

The nitrogen-fixation conundrum

Nitrogen-fixing legumes greatly diverged from the rest of the species in their leaf nutrient allocation patterns, but their responses to soil fertility were more subtle than that of the remaining species. This is not exclusive of the studied forest: in La Selva, e.g., the growth of legume trees did not show strong responses to soil fertility, while non-leguminous species did [102]. This can in part be explained by the fact that N-fixers can access the endless

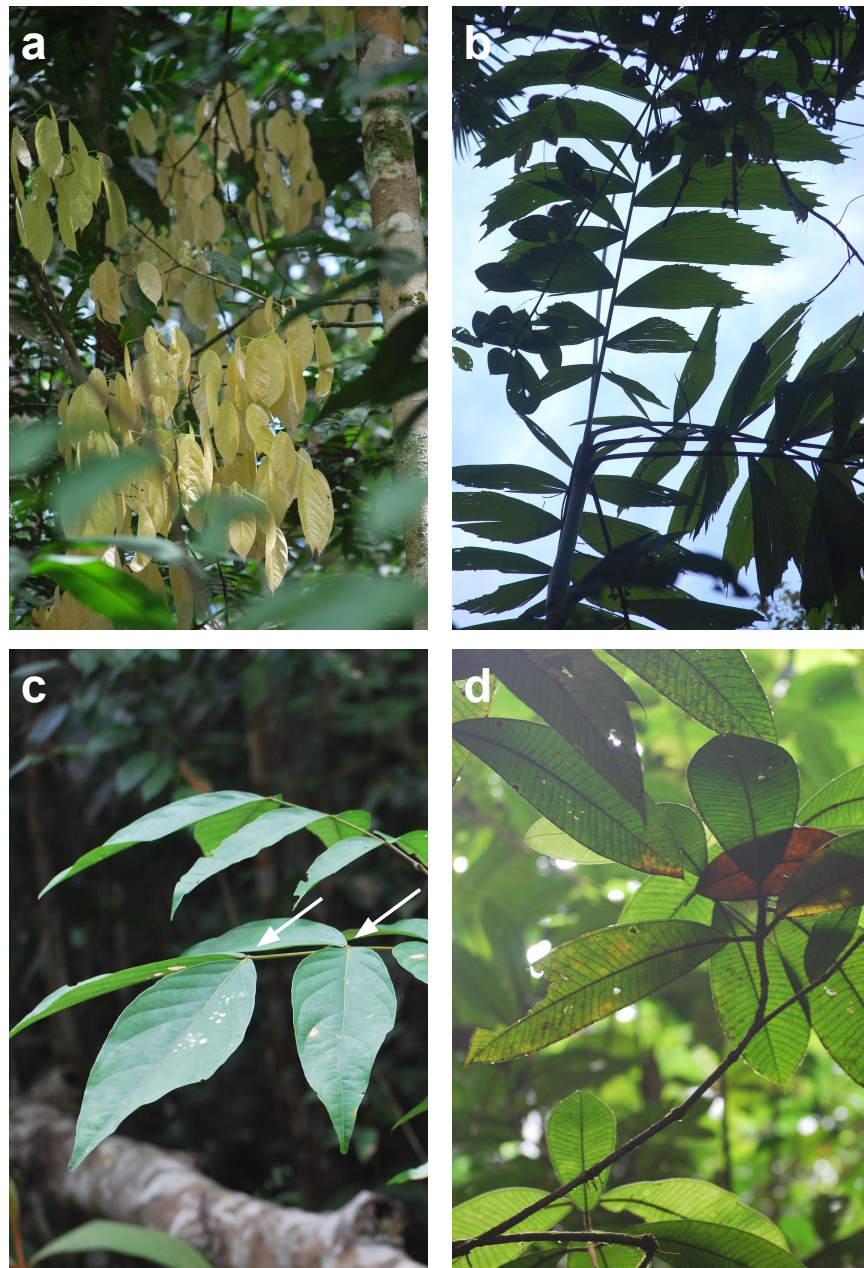


Figure 1.8: Common anti-herbivory defenses seen across tree species points to the importance of herbivory pressure in this forest. (a) Leaf flushing just before the onset of the rainy season, seen here in *Scleronema micrantha* (Malvaceae), can give enough time for leaves to fully develop before insect population peaks. (b) Mimicking herbivore damage, as seen in the ragged margins of intact leaves of *Socratea exorrhiza* (Areacaceae), may falsely indicate that induced chemical defenses have been deployed by the plant. (c) Ant-plant mutualisms are especially common in this forest, with many species showing adaptations such as the extrafloral nectaries (pointed by the arrows) in this *Inga* (Fabaceae), likely a nitrogen-fixer. (d) Sclerophylly may not completely prevent herbivory, like seen in the veiny leaves of this *Miconia eriodonta* (Melastomataceae), but they certainly reduce the cost-efficiency of feeding for herbivores.

pool of atmospheric N, and then use the surplus of N to produce root enzymes such as phosphatases, that will help them to acquire other limiting nutrients in the soil, especially P [96, 103]. In fact, our results show that N is so abundant for these plants that, despite the likely high allocation of N to the roots, they still manage to maintain high leaf N and P contents compared to non-fixing species. Being rich in N and P, the leaves of N-fixers likely have high photosynthetic capacity, which may produce the surplus Carbon necessary to feed their root symbionts, especially rhizobia, but also arbuscular mycorrhiza, who can further scavenge the soil for nutrients [79]. With such an aggressive nutrient acquisition strategy one may wonder what could then prevent N-fixers from becoming dominant over non-fixers in tropical forests, especially those growing on extremely infertile soils. Our findings may help to elucidate this question.

The allocation trade-off between leaf productivity and protection may be the mechanism preventing N-fixing legumes from turning into Darwinian demons. Our results shed some light on the underlying mechanism that may drive this growth-defense trade-off: although the leaves of N-fixing species are richer in N and P, they had substantially lower contents of Ca and Mg than non-fixers. Like P, Ca is also scarce in the soils of our study site, but the lack of leaf Ca and Mg in N-fixers might not be caused by a failure in nutrient acquisition from the soil. Instead, it is likely that N-fixers have to allocate a great portion of the Ca and Mg they uptake to their roots, as large amounts of Ca may be used to recruit rhizobia in the soil (via production of *Rhizobium* adhering proteins) and to signal nodulation (via Ca-binding messenger proteins) [81]. Both Ca and Mg are essential for the functioning of

nitrogenase, the bacterial enzyme responsible for fixing atmospheric N [104]. In plants, one of the most important functions of Ca is to strengthen the cell walls [105], but it can also be used in anti-herbivory defense in the leaves, when deposited as Ca-oxalate crystals, and even help with metal detoxification, especially Al [106]. N-fixing legumes may compensate for this lack of Ca with a surplus of S, which is also known to help with metal detoxification [101]. Therefore, the leaves of N-fixing species should be not only more nutritious for herbivores, but also less mechanically protected against them. A way to avoid herbivory would be for N-fixers to invest more into chemical defenses, but this does not seem to be the case [107]. There are other common anti-herbivory mechanisms in this forest, such as leaf flushing with delayed greening and mimicry of herbivore damage [108], but mutualism with ants seems to be especially important for N-fixers (Fig.1.8)[109]. The main role of leaf Mg, in turn, is to produce chlorophyll, whose content per mass needs to be high in plants growing in the shade in order to maximize light harvesting [110]. The constraints on leaf Ca and Mg imposed by N-fixation might have led these legumes to evolve fast lifestyles, with light-demanding, productive leaves, but with little protection against herbivores [82]. If additionally lower anti-herbivory defenses translate into higher mortality rates for N-fixers than for non-fixers, then these two groups could coexist via spatial niche partitioning [40]. Indeed, many N-fixers are persistent pioneers in tropical forests, i.e., they manage to persist as important components of the community long after the initial stages of succession [111]. Moreover, the nutrients that leak from the leaf litter produced by N-fixers may facilitate the establishment of non-fixer neighbors, who otherwise would not have access to this much soil nutrients [112].

In conclusion, if the high nutrient acquisition efficiency of N-fixers in infertile soils is offset by their low nutrient use efficiency, it would then make sense that N-fixing legumes are not dominant in the plateau, as was the case for the studied forest.

What about the fertile gullies? Why are N-fixers not dominant there either? In principle, N-fixing legumes should be more dominant where N is more limiting relative to other nutrients [77], and this is precisely what happens in the gullies, where P, K, Ca, and Mg tend to be more abundant. In a sense, this context reemulates the rapid evolution of N-fixer legumes in the Amazon following the large deposition of nutrients in the end of the Cretaceous, when an open vegetation dominated by gymnosperms gave space to a dense forest dominated by angiosperms [113]. Because nutrients are not as scarce in the gullies, light should be a more limiting resource there compared to the plateau, but the low leaf Mg of N-fixers might limit their shade tolerance. In fact, it has been shown elsewhere that N-fixer recruitment halts as succession proceeds [111], which could indicate a low probability of N-fixer saplings to survive in the shaded understory. Moreover, N-fixation is an energetically costly process, so saplings trying to survive in the shade may not benefit from the symbiosis with rhizobia. Moreover, N leaking from N-fixers will reduce their competitive advantage over non-fixers. In the end, the low shade-tolerance and short leaf lifespan of N-fixers creates a self-regulating feedback mechanism: when the soil is N-depleted and light is abundant (forest gaps), N-fixers have a great advantage, but as they grow and the forest floor becomes shaded and N-rich, non-fixers become more competitive. The fact that many legume lineages originated from majorly N-fixing clades, but then lost their ability to nodulate, such as *Parkia* and *Bocoa*, is

evidence of how tenuous the competitive advantage of N-fixing legumes is in this forest [91]. In conclusion, both the temporal and spatial variation in the relative availability of nutrients must create a heterogeneous competitive landscape for N-fixing and non-fixer species [40], which may allow for the coexistence of these two major functional groups.

Conclusion and future directions

Our study could clearly show the importance of plant nutrient acquisition and use strategies as adaptations to both fertile and infertile soils. Modulating leaf nutrient content in response to changes in soil fertility proved to be important both for acclimation and adaptation to specific habitats. While competitive ability in fertile soils seems to be dictated by a fast lifestyle, survival in infertile soils may require some specific adaptations, such as high nutrient use efficiency, which in turn leads to a slow lifestyle.

These conclusions are based on two core assumptions that must be addressed in future efforts to understand the role of nutrient acquisition and use strategies in species coexistence. First, we assumed that the content of nutrients in leaf tissues were a perfect reflection of the whole-plant nutrient status. This may not be true across species, as some may store nutrients in their roots or stems [95], which could benefit them by buffering against temporary shortages of soil nutrients, as well as stunt the growth of neighboring competitors, as a form of preemptive competition. Second, we assumed that mortality was more or less constant across species sharing the same habitat, but this is unlikely to be the case, as treefall gap

dynamics may select for some fast-growing, short-lived species. This growth-survival trade-off often interacts with soil fertility to produce habitat specialization [68], so taking mortality rates into account could yield important insights about this system.

Another very promising avenue for further inquiry is to take into account root competition for mutualistic microbes, as well as apparent competition among N-fixers driven by generalist herbivores. It is known that plant-soil feedbacks may cause niche differences, but also fitness differences, and therefore not always can promote stable coexistence [114]. If N-fixers have to compete for rhizobia in the soil, then this symbiosis could promote strong fitness differences and decrease the chances for stable coexistence among N-fixers. That is, unless N-fixers are particularly vulnerable to species-specific pathogens. Moreover, if N-fixer leaves are more herbivory-prone than non-fixers, then they may be more subjected to generalist herbivores, which are known to have a more negative effect on rare rather than abundant species, thus making coexistence less likely. This might explain why so many N-fixing legumes, especially those in the Mimosoideae clade, rely on ant recruitment through extrafloral nectaries to protect their leaves [109]. Tackling these fundamental questions could explain the high diversity of N-fixing legumes in some Amazonian forests.

A crucial follow-up study will be to test the effects of community-wide leaf nutrients on stand properties such as tree biomass and forest productivity. Leaf nutrients are directly associated with the photosynthetic capacity of plants and therefore their growth rates. Leaf nutrients are also correlated with other important leaf traits such as lifespan and resistance to herbivory, so they should also affect trees' survival probability. Tree mortality in turn causes

sudden increases in soil nutrients, which may select for fast-growing species at first, but as succession proceeds and soils become depleted again, slow-growing species may take over and become dominant. Leaf nutrients, therefore, could be the mechanistic link between individual tree performance and whole-forest processes, such as forest dynamics, productivity, and Carbon storage.



Figure 1.9: Example of soil erosion at the Km 41 camp. Rainwater runoff removes the small particles from the soil leaving only sand behind and creating a suitable habitat for lizards such as *Ameiva ameiva*.

Chapter 2

Leaf size-number trade-off

2.1 Introduction

Species coexistence has been a hot topic in Ecology for at least a century now [115], but nowhere it is more challenging to understand than in hyperdiverse plant communities [99]. This is so because plants happen to depend on the same basic resources [63, 64], which greatly reduces the niche space available for them to explore compared to animals for example. The main way plant species can differ is on the set of environmental conditions that they are able to tolerate and be competitive [42, 58, 64]. Therefore, whenever there is spatial and/or temporal variation in species relative competitive abilities, plants may specialize into different habitats, and stable species coexistence becomes possible [40]. But how can species diverge in their niches and specialize into occupying contrasting habitats?

Rapid evolution plays an important role in niche differentiation and thus in species co-

existence [116], but phenotypic diversification can only occur under certain conditions. One of the most important constraints to trait diversification is one-to-one mapping of form and function, i.e., when changes in a morphological trait drastically alters its function and thus organism performance [117]. In such a scenario, and once an adaptive peak has been reached, stabilizing selection may prevent any further trait change. Performance traits, however, often rely on multivariate morphological traits [117]. In this case, changes in one component trait can be compensated by changes in another component in such a way that fitness is buffered from any drastic change [117]. The mountain peaks of the adaptive landscape then give way to plateaus on top of which traits can evolve unimpeded: instead of a single optimum trait value, there is a whole surface defined by optimum combinations of trait values (many-to-one mapping). In nature, however, these flat adaptive surfaces are usually reduced to thin ridges, for the possible combination of traits are often constrained by resource allocation trade-offs.

Resource allocation trade-offs may not only enable phenotypic diversification, but they can also help maintain this diversity. The resources available for plants at any given point in time are finite, but because they can be used for many purposes by the plant, there will always be internal competing demands for these resources. The energy stored in sugar, e.g., may be used to produce new leaves or roots, but investment into one of these organs will come at the expense of investment elsewhere. If producing both new leaves and roots has a positive impact on plant performance, then allocation trade-offs will prevent any single plant from becoming a Darwinian demon, i.e., an organism that can maximize all performance components at the same time [56]. This important property of allocation trade-offs can help

reduce fitness differences among plants and to the limit make them ecologically equivalent [118]. Although ecological equivalence per se is insufficient to promote species coexistence, it can nevertheless make coexistence more likely [39]. Of course the effect of allocation decisions on plant performance is itself a function of environmental conditions. E.g., if the soil becomes too dry, the optimal strategy would favor resource allocation to the roots; but if light becomes more limiting than water, then the plant will benefit most from producing new leaves.

Although plants have the plasticity to change their allocation patterns in response to environmental fluctuations, this plasticity is limited by genetic and/or physiological constraints [119]. The natural implication of such constraints is that species will have a limited range of allocation decisions they can make, thus forcing them to assume a defined position along allocation trade-off axes. Desert plants that form rosettes, e.g., evolved in a context where water was so much more limiting than light, that they have lost the ability to produce branches and therefore are very limited in the number of leaves they can have at a time. This example is a useful reminder that a given trait combination may be particularly advantageous under a set of environmental conditions, but it will hardly be advantageous across environmental gradients. If phenotypic variation is also linked to variation in species' performance across environmental gradients (e.g. variation in soil moisture or light), then allocation tradeoffs can also promote niche differentiation.

Combined with the reduction of fitness differences among plants, the niche differences promoted by allocation trade-offs may result in stable species coexistence [39]. Allocation

trade-offs could therefore be an important mechanism promoting the maintenance of the large taxonomic and morphological diversity observed in tropical forests [120]. Many examples of allocation trade-offs linked to habitat specialization have been proposed, including: growth-defense trade-offs and soil fertility gradients [68, 121]; growth-reproduction trade-offs and the vertical gradient of light [122]; height-crown growth trade-off in saplings partitioning the horizontal light gradient in forests [123]. The most straightforward examples, however, are those between size and number of plant functional structures. One of the best studied trade-offs is that between seed size and number [124]: while having large, but few seeds is advantageous in undisturbed habitats, having many small seeds can help with dispersal to suitable sites in highly disturbed habitats [125, 126]. Another well-known case is the conduit size-number trade-off and its effect on species' drought tolerance [127]. For some reason the leaf size-number trade-off has not received the same attention, in spite of the great diversity of leaf sizes that can be found in tropical forests such as the Amazon, where simple leaves may range from 3 cm^2 to 1 m^2 [128]. The potential role of this trade-off in habitat specialization is reinforced by both the covariation of leaf size with irradiance gradients within forests and with rainfall gradients across forests [129, 130]. Although performance rank reversals across light gradients have been demonstrated in tropical plants before [59, 131], it is unclear if leaf size and number are involved.

We thus here address the role of the leaf size-number trade-off in the maintenance of tree diversity in an especially diverse forest in the Central Amazon. Our first hypothesis is that the leaf size-number trade-off is so strict that the total leaf biomass (M_T) is constant across

species with contrasting leaf sizes (Fig.3.1a-b), as found elsewhere [132]. If the interspecific variation in specific leaf area (SLA) is not too large, then total leaf area (A_T) should also be similar across species and therefore plant performance should not covary with leaf size. Alternatively, we hypothesize that small-leaved plants have to allocate more biomass into branching to avoid self-shading, which tends to be larger in small-leaved plants [83]. The biomass allocated into branching will be subtracted from the M_T , as has been demonstrated elsewhere [133], causing small-leaved plants to also have smaller A_T (Fig.3.1a-b), which was also shown before [134]. Having smaller A_T compared to large-leaved plants should reduce small-leaved plants' light interception efficiency, which is particularly important in shaded habitats [57]. Large-leaved species, therefore, should outperform small-leaved ones in the shade (Fig.3.1c-d). Conversely, small leaves can reduce a plant's transpiration cost in open areas by increasing heat loss through convection [135]. If light is no longer the most limiting resource, having a small light interception efficiency becomes less important than having a high water use efficiency, especially during droughts. It is thus expected that large-leaved species are outcompeted by small-leaved ones in gaps, but outcompete them in the shade (Fig.3.1d). Finding such a performance rank reversal in this forest would provide strong evidence that the leaf size-number trade-off may lead to habitat specialization and thus species coexistence.

Conceptual framework

All organisms have a limited amount of energy to allocate to growth, survival and reproduction. Such energetic constraints lead to allocation trade-offs that manifest as a negative genetic correlation between phenotypic traits that influence fitness. For example, a genotype that allocates energy to produce a large number of seeds is likely to do so at the cost of smaller seed size. Similarly, allocating energy to produce a large quantity of leaves comes at the cost of a smaller leaf size.

When species exhibit different allocation trade-offs (i.e., they occupy different positions on a trade-off curve; Fig.3.1a), these can manifest as negative correlations in different aspects of performance. For example, a plant species that produces a smaller number of large seeds will have an advantage in reproduction while a species that produces a larger number of small seeds will have an advantage in dispersal. In the absence of environmental variation and/or spatial structure, such species-specific differences in allocation trade-offs lead to competitive exclusion. For example, within a given site, a large seed will have a competitive advantage over a small seed. But, across a landscape of numerous sites, small seeds, due to their superior dispersal capability, may reach locations that are not accessible to large seeds. The key point is that in the presence of environmental variation species-specific differences in allocation trade-offs can allow them to coexist by partitioning niches in time or space [120].

Similarly, interspecific variation along the leaf size-number trade-off can lead to the partitioning of the light gradient and promote tree species coexistence. This is only possible

because the leaf size-number trade-off is related to the trade-off between water use efficiency and light interception efficiency. When a plant has its total photosynthetic surface split into several small units, its leaves can cool down through convection caused by even the slightest breeze [135]. This means the plant will have to use less water to cool off through transpiration, thus being more efficient at using water. Of course this adaptation only gives an advantage to plants exposed to the sun and where soil water is not unlimited. This can be the case for plants growing in canopy gaps of seasonal forests like the one studied here. Having numerous, but small leaves, however, comes with a disadvantage. For these plants to avoid self-shading, a much higher investment into branching is necessary compared to large-leaved plants, who often lack branches completely [83]. More biomass allocated to branches should reduce the amount of biomass allocated to leaves, thus leading to a smaller light interception efficiency (unless specific leaf area is high enough to compensate for this loss). This disadvantage must only be ecologically important where light is a limiting resource, i.e., in the shaded understory of mature stands. In conclusion, variation along the leaf size-number trade-off should cause species to partition the horizontal light gradient near the forest floor and thus promote spatio-temporal coexistence.

We can therefore make the following testable predictions about the ecological consequences of the leaf size-number trade-off:

1. Does the leaf size-number trade-off reduce fitness differences?
 - a) Total leaf biomass (M_T) or area (A_T) should be constant across different leaf sizes

- (unit leaf mass or area);
- b) Sapling performance (relative growth rate) does not vary with leaf size;
2. Does the leaf size-number trade-off promote niche partitioning?
- a) M_T or A_T covaries with leaf size;
- b) Performance covaries with M_T or A_T in at least one type of habitat (shaded or well-lit);
- c) There is a rank reversal in performance between large- and small-leaved plants as light conditions improve.

2.2 Methods

Study site

We chose to study in a 25-ha plot in the Central Amazon (2°30'S, 60°W) to capitalize on the great number of tree species present there ($\sim 1,400$) [21]. The climate in this pristine area is hot (MAT = 26.7°C) and wet (annual rainfall = 1.9-3.5 m), with a pronounced, but mild dry season annually, although El Niño droughts can be quite intense [70]. Most of the study is occupied by a non-flooded plateau covered by a tall (35-40 m) and evergreen forest with a deeply shaded understory dominated by saplings and stemless palms [136]. The forest

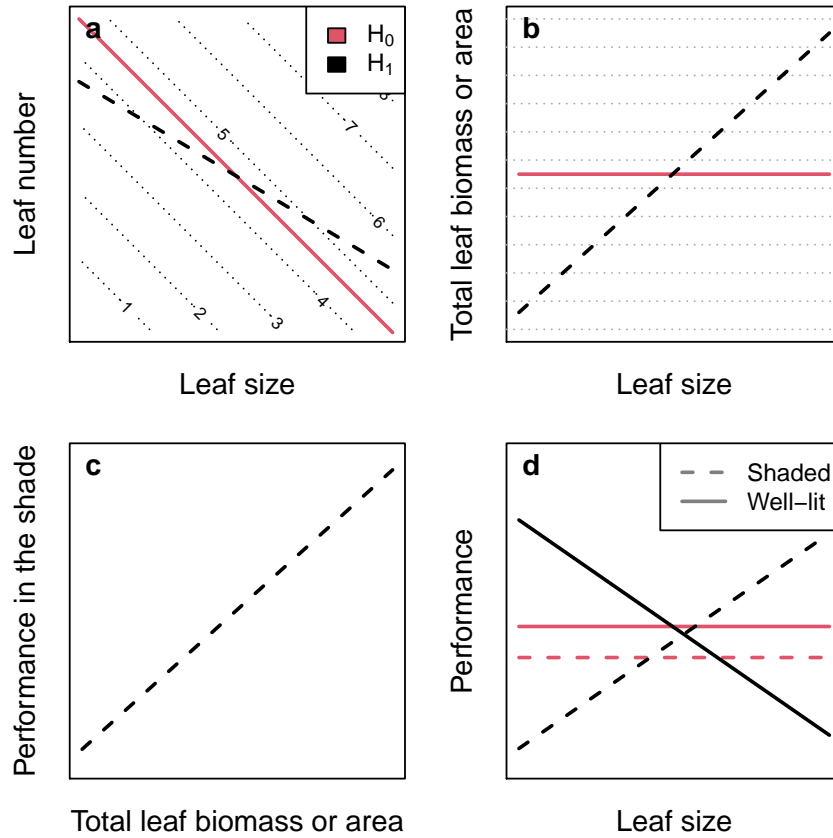


Figure 2.1: Conceptual figure depicting expected results under two alternative hypotheses: H_0 - size-number trade-offs serve as fitness equalizing mechanisms; and H_1 - size-number trade-offs promote niche differentiation. If the slope coefficient of the size-number relationship is close to unity (a), then total leaf mass (M_T) or area (A_T) should not covary with leaf size (b), and thus one should not expect performance to covary with leaf size (d). Conversely, if the size-number slope departs from one (a), then M_T or A_T must covary with leaf size (b). If sapling performance in the shade depends on A_T (c), then it should also covary with leaf size (d). Lastly, if leaf size (or A_T) confers differential advantages along the light gradient (if, e.g., large leaves are beneficial in the shade, but detrimental in well-lit habitats), then one should expect a rank reversal in performance between large- and small-leaved species across light habitats (d). This interaction between leaf size and light availability can promote niche partitioning and thus species coexistence.

has a small annual rate of tree turnover (1.2%) [136], and therefore large treefall gaps are relatively uncommon.

Sampling design

To sample the highest number of different species we could, we prioritized the 20x20 m quadrats from the permanent plot that had the highest number of species. To control for the effects forest structure, topography, and soil, we only sampled quadrats in mature stands on the plateau. To avoid pseudoreplication, we did not sample more than one sapling ($1 \leq D \leq 4$ cm) of each species per quadrat. To avoid adding noise to our data we only sampled saplings whose crowns were intact, not infested with lianas or epiphytes, and not entangled with the crowns of neighboring saplings, as these are factors that could alter sapling leaf output. In total we sampled 490 saplings from 283 different species in 41 quadrats. Field work was done between July and October 2017, i.e., ~ 10.7 years on average after the saplings were first censused, between 2006 and 2007. For each sapling, we measured stem diameter (D) to estimate growth and estimated crown illumination (L) using a visual method ([137]) to control for small, but significant variation in light conditions. We then counted or estimated the number of leaves (see details in the section below) and selected a representative branch to sample. Because large-leafed species are often branchless, we only sampled one or two leaves to minimize the damage inflicted to the sapling. For small-leafed species we would often sample up to 20 leaves to reduce the error in measuring dry mass.

Significantly damaged or malformed leaves, often due to herbivory or pathogens, were not selected, although finding leaves with no damage at all was nearly impossible. We only used leaves that were old enough to be clearly fully expanded, but we avoided using the oldest leaves in the branch for they were usually loaded with epiphylls. When only old leaves were available, we carefully removed all epiphyll material from the leaf to prevent it from interfering with the leaf dry mass.

Leaf traits

In order to quantify the great diversity of growth strategies found among saplings in the study site we measured three main leaf traits: total leaf number (N), unit leaf area (A), and leaf dry mass (M). Specific leaf area (SLA) was then derived from A and M . These traits were measured following standardized protocols [50], but with small adaptations to meet the specific conditions met in the field. The methodological details are described below.

Leaf area

To have a truthful estimate of the average leaf area of each sapling sampled in this study, we first made sure the leaves were fully hydrated before scanning them for subsequent image analysis [50]. The branches (or simply the leaves for large-leaved plants) selected for sampling were pruned in the field during the morning, then kept in a double black plastic bag, and brought back to the camp around midday. The leaves would hardly show any signs of wilting. Nevertheless, we would leave the branches rehydrating in a dark chamber during the rest of



Figure 2.2: A sample of the leaves sampled in this study shows the wide variance in leaf size among the single-leaved species found in the study site (scale = 1 inch).

the day and overnight. The cut end of the branches were again cut under the water to make sure air bubbles inside the xylem would not prevent the branch from uptaking water from the bucket. In the following day, each bucket at a time was brought to the lab and the pruned branch were taken from the bucket one by one, their leaves removed and immediately scanned at a 300 PPI resolution. At this point in the process, there was no noticeable difference in leaf turgidity compared to when they were still attached to the saplings. The petioles were removed prior to scanning the leaves, so leaf area in this study refers only to the leaf blade. The leaf images were then processed by the imageJ software [138], which quantified leaf area in $pixels^2$, later converted to cm^2 by using known area of the scanner window. Leaf areas estimated in this way were then averaged by individual sapling (A_{ij}) and by species (a_j).

Leaf dry mass

To estimate leaf dry masses, the same leaves that were previously scanned were dried in the field using a gas drying oven. The drying period was at least a whole day, but some species

with leaves with high water content required more time. All dried leaves were manually inspected to make sure they were completely dry before being weighted. We then weighted all leaves from each sapling together to reduce the scale error; scale resolution was 0.01 g.

Specific leaf area

Specific leaf area (SLA) is traditionally calculated as the ratio between leaf area (A) and leaf dry mass (M), which has the undesirable effect of making SLA colinear with M . We thus calculated saplings' SLA as the residuals of the power function that describes A as a function of M as follows:

$$\log_e SLA = \log_e A - \log_e \hat{A} \quad (2.1)$$

$$\log_e \hat{A} = \alpha + \beta \times \log_e M \quad (2.2)$$

where \hat{A} is the expected leaf area based on its dry mass and α and β are respectively the intercept and slope of this area-mass relationship. By solving eq.2.1 we find that $SLA = A/\hat{A}$ and thus SLA can be displayed as a percentage: an $SLA = 100\%$ means that a leaf's area is identical to that expected from a leaf with the same dry mass; likewise, leaves with $SLA = 50\%$ and $SLA = 200\%$ have areas that are, respectively, half and twice as large as that expected based on their M . While SLA estimated in this way is completely uncorrelated with M and only loosely correlated to A , it is still strongly correlated to its more traditional version (Fig.B.1).

Total leaf number

Total leaf number (N) was estimated in the field for each sapling by counting the total number of leaves, for large-leafed plants, or the number of branches, for small-leafed plants. To estimate N for these small-leafed saplings, we first chose one representative branch and counted the number of leaves it contained. We then counted the number of branches in the entire plant's crown taking into account the size of these branches compared to the reference branch (e.g. 42 leaves in the reference branch times 15.5 branches in the crown gives an N of 651). All leaf count estimates were done by a single person throughout the study to avoid perception bias.

Statistical analysis

To make use of all data we collected, including those from species sampled only once, we used a hierarchical Bayesian analysis. This approach also has the benefit of propagating errors from individuals to species to across-species models, estimating real marginal probability distributions for the fitted parameters, and being flexible enough to allow for very complex and modular models to be tested concomitantly [52]. We describe each of these models in more detail in the sections below. The parameters were fit using the Gibbs sampler algorithm based on Monte Carlo Markov Chain simulations and were performed by JAGS [93] through R v.3.5.3 [92], using the `rjags` package [139]. To improve model convergence, many observed variables were centered after being log-transformed; it also helped determining

prior distributions based on the range of values found in our own data (see supplementary material for chapter 2). To extract and analyze convergence on the MCMC output, we used the coda package [94]. All other data handling and graphical output was done in R.

Total number of leaves per sapling

To test the leaf size-number trade-off we modeled species-specific allometries of sapling total leaf number (N_{ij}) as a random sample of a lognormal distribution as follows:

$$\log_e N_{ij} \sim \mathcal{N}(\eta_{0_j} + \eta_{D_j} \times \log_e D_{ij} + \eta_{L_j} \times (L_{ij} - 1) + \eta_{M_j} \times \log_e M_{ij} + \eta_{S_j} \times SLA_{ij}, \sigma_N^2) \quad (2.3)$$

where η_s are the species-specific parameters (η) that estimate the species random effect (η_0), the effect of sapling size (D), crown illumination (L), leaf dry mass (M), and specific leaf area (SLA); and σ_N^2 is the intra-specific residual variation of N . The model intercepts (η_0) can also be understood as the N of species' standardized saplings, i.e., median-sized saplings ($D = 1.8 \text{ cm}$) growing in the shade ($L = 1$), and whose leaves are median-sized ($M = 0.62 \text{ g}$) with an SLA of 100%. To model interspecific variation in sapling allometries we modeled all species-specific parameters (η) as samples from a multivariate normal distribution as follows:

$$\mathbf{\Gamma}_j \sim \mathcal{N}_5(\boldsymbol{\mu}_\eta, \boldsymbol{\Sigma}_\eta) \quad (2.4)$$

where $\mathbf{\Gamma}_j$ is the matrix containing all five η ; $\boldsymbol{\mu}_\eta$ is the vector with the means of the hyperparameter distributions for each η , and $\boldsymbol{\Sigma}_\eta$ is the variance-covariance matrix containing the interspecific variations and correlations among η .

Sapling total leaf area

To understand the effects of leaf unit size on sapling architecture we estimated total leaf surface area (\hat{A}_T) for the standardized saplings of each species as a function of leaf size (M) and SLA as follows:

$$\hat{A}_{T_j} = \hat{N}_j \times a_j = e^{(\eta_{0_j} + \eta_{M_j} \times m_j + \eta_{SLA_j} \times sla_j)} \times a_j \quad (2.5)$$

where a_j , m_j , and sla are the species' average leaf area, dry mass, and specific leaf area, respectively.

Relative growth rate

To test for the effects of both total leaf area (A_T) and leaf traits on sapling performance, first we modeled relative growth rate (R) for each individual sapling as a function of A_T . Second, we modeled the effect of A_T on R as a function of leaf traits (M and SLA) for each species in our study. To estimate R for each sapling, we modeled current sapling size (D) as a function of its former size (D_0) and the time period between the measurement of D_0 and D (Δt) as follows:

$$\log_e D_{ij} \sim \mathcal{N}(\log_e D_{0ij} + R_{ij} \times \Delta t_{ij}, \sigma_D^2) \quad (2.6)$$

where σ_D^2 represents measurement error in D . Although Δt was over a decade on average, the saplings used in this study grew so little that for many of them $D < D_0$. Although some stem shrinking is possible due to differences in plant water status, cases of negative growth rate are often attributed to measurement error, which becomes important for plants

that grow slowly. Instead of discarding these data, as it is often done, we assumed diametric growth to be always positive and forced R in the model to be positive by modeling it as a lognormal distribution as follows:

$$\log_e R_{ij} \sim \mathcal{N}(\delta_{0_j} + \delta_{D_j} \times \log_e D_{0_{ij}} + \delta_{L_j} \times L_{ij} + \delta_{A_j} \times \log_e A_{T_{ij}}, \sigma_R^2) \quad (2.7)$$

where δ_{0_j} is the R of a median-sized sapling from species j growing in the shade; δ_{D_j} , δ_{L_j} , and δ_{A_j} are respectively the effects of initial size (D_0), crown illumination (L), and total leaf area (A_T) on R ; and σ_R^2 represents the uncertainty around the estimated R . The set of all species-specific parameters (δ) are represented by the matrix Δ_j . Lastly, to test the effects of species average leaf traits (m and sla) on R , we modeled δ as samples from a multivariate normal distribution as follows:

$$\Delta_j \sim \mathcal{N}_4(\nu_0 + \nu_M \times m_j + \nu_S \times sla_j + \nu_{MS} \times m_j \times sla_j, \Sigma_\delta) \quad (2.8)$$

where ν_0 are the deltas for species with average M and SLA ; ν_M , ν_S , and ν_{MS} are respectively the effects of species' m , sla , and their interaction on Δ ; and Σ_δ is the variance-covariance matrix containing the interspecific variations and correlations among δ .

2.3 Results

Diversity of leaf traits

We found a great diversity of light capture strategies across the 283 species included in this study. Saplings ranged from having unbranched stems with only a handful of large

leaves to complex and highly branched stems with a multitude of tiny leaves. Leaf size varied dramatically, with leaf dry mass (M) varying > 300 -fold (0.04-12.33 g) and leaf unit area (A) ranging from 7 to 1300 cm^2 (Fig.2.3b-c). A second axis of variation was specific leaf area (SLA), which ranged from 46% to 371% (Fig.2.3d). Although SLA was positively correlated to A (Fig.B.1c), a wide range of combinations between leaf size and SLA could still be observed. Species ranged from having large and thin leaves (e.g., *Miconia tomentosa*, Melastomataceae) to small and thick leaves (e.g. *Eschweilera amazoniciformis*, Lecythidaceae), and from large and thick leaves (e.g., *Mouriri nervosa*, Melastomataceae) to small and thin leaves (e.g., *Pterandra arborea*, Malpighiaceae). Lastly, total leaf number (N) also varied substantially, from 7 to $\sim 2,500$, although a great deal of this variance can be attributed to variance in sapling size (0.6-4 cm) and crown illumination (1-3.5).

Leaf size-number trade-off and total leaf area

Our results strongly supported the leaf size-number trade-off and confirmed that large-leafed species invest more biomass into leaves compared to small-leafed species. Moreover, we show that this larger investment into leaf biomass is indeed converted into larger total leaf area (A_T). After accounting for variation in sapling size (D) and crown illumination (L), we saw a strong interspecific negative correlation between leaf dry mass (M) and total leaf number (N ; Fig.2.4a). Surprisingly, L had an insignificant effect on N whereas SLA had a significantly negative effect, but unsurprisingly N increases with D (Tab.2.1; Fig.B.4), and all the scatter

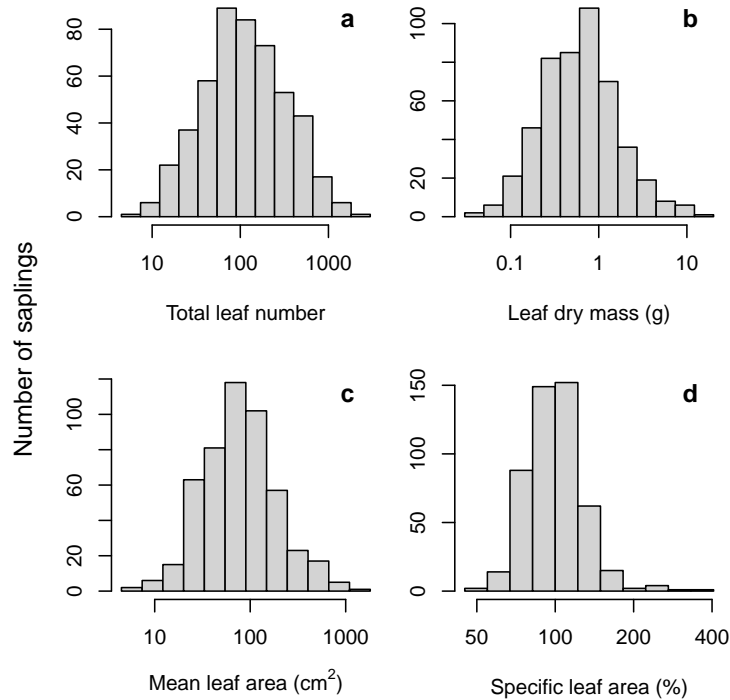


Figure 2.3: Distribution of leaf traits across the 490 saplings sampled in this study: total leaf number (a), leaf size as both leaf dry mass (b) and leaf unit area (c), and specific leaf area (d). All x-axes are presented on a logarithmic scale.

seen in Fig.2.4a is due to variation in SLA . Because the slope of N as a function of M is significantly below unity (Tab.2.1), we can point out that saplings from large-leaved species have on average higher leaf biomass than saplings from small-leaved species (Fig.2.4a). Our across-species model showed a high goodness of fit when we used it to predict N for the observed saplings ($R^2 = 0.74$; Fig.B.3), and can thus be considered reliable. Lastly, when we estimated A_T for the standardized saplings of all species we found that the higher leaf biomass maintained by large-leaved species also yields larger A_T compared to small-leaved species (Fig.2.4b).

Table 2.1: Best-fit parameters for the models fitted in this study: total leaf number (TLN ; eq.2.4) and relative growth rate (R ; eq.2.8) as a function of sapling size (stem diameter; D), illumination (L), leaf size (dry mass; M) and specific leaf area (SLA). Parameter estimates refer to across-species parameters (hyperparameters). Based on the posterior distributions of these hyperparameters we could estimate 95% credible intervals ($CI_{95\%}$), as well as the probability p that these hyperparameters are larger than zero (this does not apply for intercepts who were defined a priori to be larger than zero).

| Model | Parameter | symbol | median | $CI_{95\%}$ | p |
|---|-----------------|--------------------|--------|---------------|------|
| Total leaf number | intercept | μ_{η_0} | 105 | [96;114] | NA |
| | size | μ_{η_D} | 1.45 | [1.25;1.64] | 1 |
| | light | μ_{η_L} | 0.08 | [-0.14;0.29] | 0.77 |
| | M | μ_{η_M} | -0.81 | [-0.90;-0.71] | 0 |
| | SLA | μ_{η_S} | -0.72 | [-0.99;-0.45] | 0 |
| Relative growth rate (intercept) | intercept | $\nu_{0\delta_0}$ | 0.007 | [0.005;0.008] | NA |
| | size | $\nu_{0\delta_D}$ | -1.59 | [-2.10;-1.06] | 0 |
| | light | $\nu_{0\delta_L}$ | 0.01 | [-0.47;0.47] | 0.52 |
| | total leaf area | $\nu_{0\delta_T}$ | 0.48 | [0.26;0.71] | 1 |
| (M effect) | intercept | $\nu_{M\delta_0}$ | 0.01 | [-0.17;0.18] | 0.56 |
| | size | $\nu_{M\delta_D}$ | -0.03 | [-0.39;0.33] | 0.43 |
| | light | $\nu_{M\delta_L}$ | -0.04 | [-0.27;0.20] | 0.38 |
| | total leaf area | $\nu_{M\delta_T}$ | -0.02 | [-0.12;0.09] | 0.4 |
| (SLA effect) | intercept | $\nu_{S\delta_0}$ | 0.09 | [-0.59;0.75] | 0.60 |
| | size | $\nu_{S\delta_D}$ | 0.03 | [-1.19;1.27] | 0.52 |
| | light | $\nu_{S\delta_L}$ | -0.04 | [-0.82;0.76] | 0.47 |
| | total leaf area | $\nu_{S\delta_T}$ | -0.04 | [-0.43;0.33] | 0.41 |
| (MxSLA effect) | intercept | $\nu_{MS\delta_0}$ | 0.09 | [-0.83;0.96] | 0.57 |
| | size | $\nu_{MS\delta_D}$ | -0.64 | [-2.73;1.47] | 0.28 |
| | light | $\nu_{MS\delta_L}$ | -0.30 | [-1.99;1.36] | 0.35 |
| | total leaf area | $\nu_{MS\delta_T}$ | -0.04 | [-0.80;0.73] | 0.47 |

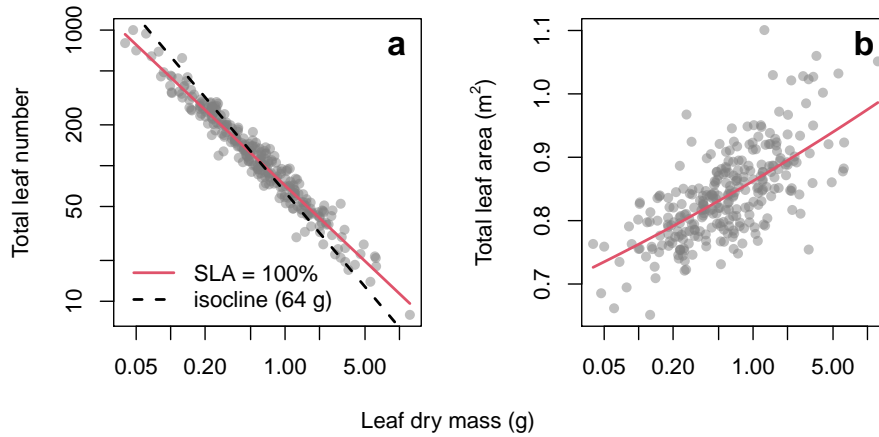


Figure 2.4: Interspecific trade-off between leaf size and number and its effects in total leaf area. In (a) each point represents a species with a given leaf dry mass and specific leaf area (SLA) and the predicted number of leaves and total leaf area for median-sized saplings ($D = 1.8\text{ cm}$) growing in the shade ($L = 1$). The red line represents the across-species model ($SLA = 100\%$) and all variation around this line is due to variation in SLA . The dashed line is the isocline along which the combination of leaf number and mass equals the median total leaf dry mass (M_T) across all sampled saplings (64 g). Panel (b) shows the advantage of large-leaved species in terms of A_T . The scatter around the across-species model (red line), in this case, can be attributed both to variation in SLA and variation in M_T .

Effects of total leaf area on sapling performance

We found that sapling performance in the shade was to a great extent determined by total photosynthetic area, as predicted. Again, light (L) had no detectable effect on relative growth rate (R), but sapling initial size (D_0) had a strong negative effect and total leaf area (A_T) had a strong positive effect on R (Tab.B.1; Fig.B.7). Also worth of notice is the very slow growth of these saplings: a median-sized individual ($D_0 = 1.8\text{ cm}$) growing in the shade ($L = 1$) and with a median total leaf area ($A_T = 0.9\text{ m}^2$) will, after a whole year, have grown only $70\text{ }\mu\text{m}$ in stem diameter (intercept δ_0 in Tab.B.1). R varied substantially around this basal growth rate among the observed saplings (Fig.2.5a), but the estimated across-species

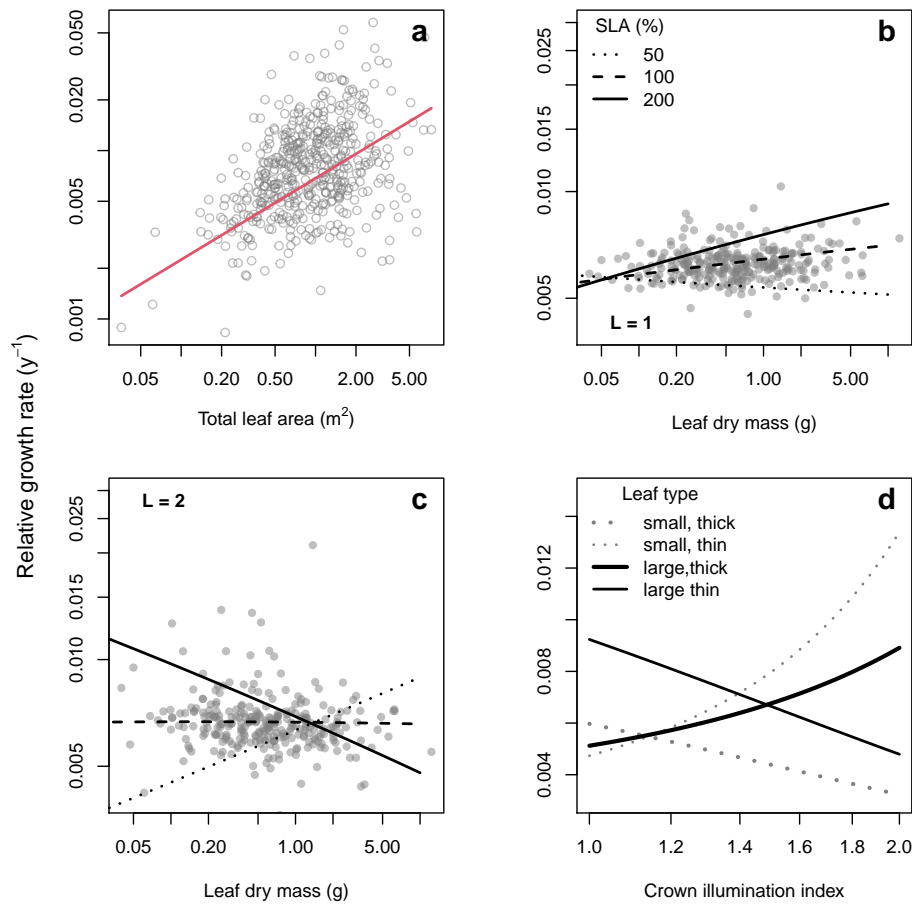


Figure 2.5: Individual and species level growth models. The first graphic (a) shows predicted relative growth rate (\hat{R}) for each individual sapling as a function of its observed total leaf area. The red line represents the generalized model for saplings with median leaf dry mass ($M = 0.6 g$) and median specific leaf area ($SLA = 100\%$). The remaining graphics show \hat{R} of each species as a function of its average M and SLA in the shade ($L = 1$; b) and on improved light conditions ($L = 2$; c). Lines represent the across-species models for standardized saplings, i.e., median-sized saplings growing in the shade.

variance among standardized saplings was naturally much smaller (Fig.2.5b). The individual growth model (eq.2.6) had a relatively high predictive power ($R^2 = 0.61$; Fig.B.6a) compared to the species growth model (eq.2.7; $R^2 = 0.36$; Fig.B.6b).

Performance trade-off

Although we found no significant effect of leaf size on relative growth rate (R), our model's predictions confirm the expectation that species trade performance ranks across light gradients. If traits individually had no detectable effect on R (Tab.B.1), it is their interaction that seems to allow for such rank reversals in R . There is a trend for plants with large leaves and high specific leaf area (SLA) to grow faster than small-leafed species in shaded conditions (Fig.2.5b). But this trend is reversed when saplings are growing in better-lit environments (Fig.2.5c). This reflects the fact that saplings with large and thin leaves are the ones with the largest predicted total leaf area (A_T) regardless of the light conditions (Fig.2.6a,c). As shown above (Fig.2.5a), maintaining a large A_T when growing in the shade ($L = 1$) positively affects R , which is thus highest for plants with large and thin leaves (Fig.2.6b). Surprisingly, however, having leaves that are either large and thick or small and thin is somehow worse than having small and thick leaves (Fig.2.6b). Now, when light conditions improve ($L = 2$), our model predicted a radical change in the performance landscape: large and thin leaves are no longer the best leaf trait combination, although it is not as bad as having small, thick leaves; and plants with small, but thin leaves now have the highest R , followed by those whose leaves are large and thick (Fig.2.5d, Fig.2.6d). These predictions from our model thus points toward a trait-mediated performance trade-off along the light gradient.

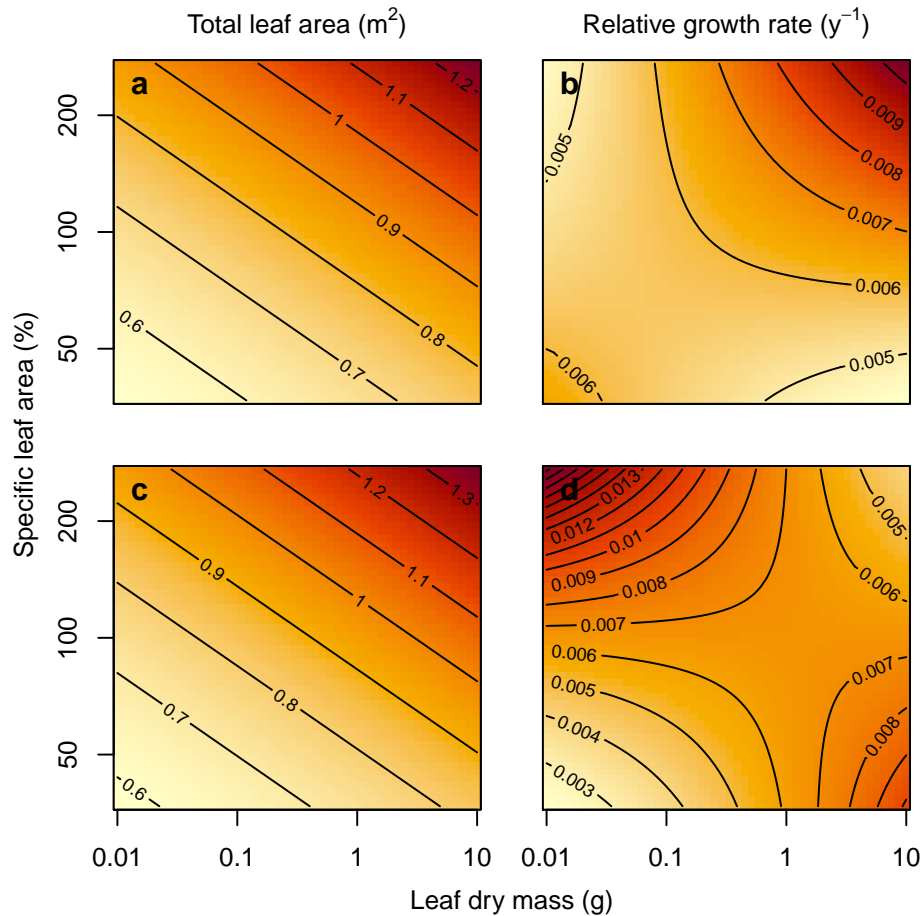


Figure 2.6: Total leaf area and relative growth rate as a function of leaf dry mass and specific leaf area. The patterns shown here were derived from all the models fitted in this study. While the upper panels (a-b) refer to saplings growing in the deepest shade found in the forest ($L = 1$; no direct radiation), the bottom panels (c-d) refer to better illuminated saplings ($L = 2$; some direct radiation from small lateral canopy gaps). Heated colors indicate higher values of total leaf area and relative growth rate, which are also indicated by the isoelines, but are specific for each panel. The consistency of the pattern for total leaf area across the illumination gradient (a,c) indicates it is produced by internal, context-independent constraints, while the radical change in relative growth rate patterns indicates it is context-dependent.

2.4 Discussion

After studying saplings from hundreds of different species we could assess the potential role of the leaf size-number trade-off in promoting the great tree diversity seen in the Amazon rainforest. To test the role of this resource allocation trade-off on the coexistence of species with contrasting leaf sizes, we tested two non-mutually exclusive hypotheses: 1) allocation trade-offs function as fitness equalizing mechanisms by reducing differences in sapling performance; and 2) variation along allocation trade-offs axes interact with environmental gradients to produce niche differences among species. Although each of these mechanisms can make coexistence more likely, only the combination of both of them might be sufficient to maintain the high tree diversity found in the Central Amazon. Although we would not risk proposing whether these long lived tree species can truly coexist in such a complex study system, we could nevertheless provide evidence that is compatible with these main coexistence mechanisms.

Our results indicate that the interspecific leaf size-number trade-off is more involved in the partitioning of light gradients among species with contrasting leaf sizes, although it may also help reduce fitness differences among these species. If on one hand the trade-off is very strong, it is clearly insufficient to prevent large-leafed species to have significantly higher total leaf area compared to small-leafed species (Fig.2.4a-b, Tab.2.1). Higher total leaf area in turn proved to have a strong positive effect on sapling performance (Fig.2.5a, Tab.2.1), thus demonstrating the inability of the trade-off to equalize species fitness in the

shade. The effect of leaf size on sapling performance, however, is not direct, but strongly interacts with specific leaf area (*SLA*; Fig.2.5b-c). Moreover, the combination of leaf size and *SLA* interacts with the horizontal light gradient to produce rank reversals among species (Fig.2.5d, Fig.2.6b,d). This differential selection along an environmental gradient is exactly the sort of mechanism that can promote habitat specialization and thus spatial coexistence [120]. Next, we discuss each of these main results in light of the modern coexistence theory in order to assess if they are compatible with well-known coexistence mechanisms driven by trade-offs.

An imperfect fitness equalizing trade-off

Although the leaf size-number trade-off is not a perfect fitness equalizing mechanism, it is still strong enough to constrain species' fitness to a relatively narrow margin. We had hypothesized that if sapling leaf number (N) traded-off perfectly with average leaf mass (M), then the total leaf mass (M_T) of similar-sized saplings growing in similar conditions should be constant, in spite of the wide range of leaf sizes present in this forest (Fig.2.2-2.3). In practical terms, for M_T to remain constant across species the exponent x in $N = M_T \times M^x$ should be -1. We found that this exponent is significantly larger than -1 (-0.81; Tab.2.1), meaning that large-leaved species have an advantage in terms of M_T compared to small-leaved species (Fig.2.4a). This large leaf advantage likely comes from the limitations imposed by leaf size on sapling architecture (Fig.2.7) [140]. Small-leaved saplings, e.g., have to invest more



Figure 2.7: Leaf size effects on plant architecture. (a) Large-leaved plants invest little or nothing in branches as saplings, like this *Conceveiba martiana* (Euphorbiaceae), but rely on low-cost spacers such as long petioles to avoid self-shading. (b) Small-leaved plants, on the other hand, such as this *Sorocea muriculata* (Moraceae), have to construct branches.

into branching to avoid self-shading [83], thus reducing the amount of biomass available to be allocated to leaves [133]. Conversely, large-leaved saplings often lack any branches, which can be replaced by cheaper structures such as long petioles or by leaves with thin and elongated bases [141].

Another interesting finding about the leaf size-number trade-off is that it is little affected by illumination (Tab.2.1). While the positive light effect on N indicates that more exposed

saplings can afford to produce more leaves, the very small size of this effect indicates that these saplings may rather allocate biomass elsewhere, such as stems or roots [142, 143]. Now the strong and significant effect of specific leaf area (SLA) on N is clear evidence that the leaf economics spectrum is not completely detached from the leaf size spectrum as once thought [141]. SLA represents the efficiency with which a plant converts leaf biomass into leaf area, so high SLA plants could produce relatively high total leaf area (A_T) with a given M_T . Therefore, the negative effect of SLA on N means that these plants are keeping lower A_T than they can. This could be either to prevent self-shading or because high SLA saplings have higher rates of foliage loss [141, 144]. What really matters for plant performance, however, is that the leaf biomass advantage large-leafed plants have over small-leafed ones is translated into a A_T advantage (Fig.2.4b).

Total leaf area is an important trait that can greatly impact a sapling performance when light becomes limiting. In the shaded understory, saplings of a given size that manage to maintain larger A_T will harvest more light (high light interception efficiency) and may have larger ratios of photosynthetic to non-photosynthetic tissues (high light use efficiency; [57, 143, 145]). This should make large-leafed species superior competitors in the shade, but this large-leafed advantage can be at least in part offset by SLA (Fig.2.4b), which mediates the conversion of leaf biomass into leaf area. This variation in SLA thus explains why predicted M_T for standardized saplings varied ca. 5-fold (31 – 160;), while A_T varied less than 2-fold (0.65 – 1.10 m^2). Even among species with similar leaf sizes, A_T could differ by ca. 0.1 m^2 due to differences in SLA . Therefore, plants with thin and vulnerable leaves

will naturally be more efficient in producing a high total leaf area compared to plants that produce thick, sturdy leaves [143]. Having less protected leaves, on the other hand, greatly limits their lifespan, which may also affect a plant's performance as we will discuss next. In conclusion, despite the extra variation in A_T added by SLA , large-leafed species still have an advantage in the shade, which limits the importance of the leaf size-number trade-off as a fitness equalizing mechanism.

The indirect link between leaf size and performance

The total leaf area (A_T) advantage that large-leafed saplings have should translate into high performance, especially in the shade, but the link between A_T and performance is not straightforward. Instead, relative growth rate (R), one of the main components of sapling performance, covaries only very modestly with leaf size (Fig.2.5b). This is interesting because, besides sapling initial size, total leaf area was the most important predictor of sapling R (Tab.2.1). Among the many factors that may cause this $A_T - R$ link not be direct, the interaction of leaf size with specific leaf area (SLA) seems to be the most important one: not only SLA can drastically improve the performance of a sapling with a given leaf size in the shade, but it may also revert its effect once light conditions improve (Fig.2.5b-c). It is well known that SLA is positively correlated to R [145], both in the shade and in the sun [143], so why is this not always the case in this particular forest? As discussed in the previous section, high SLA helps saplings maximize their A_T which is very important for

light interception in the shade [143]. Interestingly, however, this positive effect of *SLA* is only important in large-leafed species; as discussed before, this may still be due to the fact that small-leafed saplings have to invest more into branching [140], which reduces their total leaf biomass.

When light conditions improve, having a higher *SLA* can help the plant to save energy on leaf construction in a context where old leaves in a rapidly growing shoot get quickly shaded by the younger leaves on the top [82]. In this case, however, only small-leafed saplings seem to benefit from having high *SLA*, while having low *SLA* is only advantageous for large-leafed saplings Fig.???. There are two main explanations for these patterns. First, large and thin leaves are likely more susceptible from suffering large damage from falling debris coming from newly opened canopy gaps, which are the primary causes of the improvement in light conditions to begin with. Falling debris and defoliation are common causes of mortality in tropical forests [121, 146], and should certainly impact plant growth too. Second, small leaves could be advantageous in better-lit conditions because small leaf sizes help reduce transpiration water loss during the dry season and promote transpiration during the wet season [135, 147]. Droughts have become longer and more intense in the Amazon, with devastating effects for the vegetation [148]. This study's field work was done just after one of the driest periods in the past decade (2014-2016), and in one the most severely impacted areas, so lack of water can be definitely an issue in this forest especially for saplings who might not have well-developed root systems yet. Therefore, because small-leafed saplings should have high water use efficiency in habitats where light is no longer limiting, they should

outcompete large-leafed species. An alternative explanation is that small-leafed saplings would have a higher number of lateral buds that could confer them a great plasticity to respond rapidly to environmental factors such as an increase in illumination or foliar damage [132]. Although this is likely true, one could argue that large-leafed saplings can easily overcome this limitation by producing really small scaly leaves, with negligible costs for the plant, but that nevertheless allow them to keep a considerable "bud bank". This is in fact common among large-leafed saplings (*pers. obs.*).

One last consideration about these saplings is that they are among the slowest growing saplings recorded for tropical forests. In a global plot network, the slowest growing species had an annual growth of 0.57 – 4.65% [78]; in the forest we studied, saplings had a median growth rate of only 0.7%. In other words, median stem growth resumes to an annual increment of only 70 μm . Given that typical plant cells range from 10 – 100 μm in diameter [149], there is at best the addition of 3.5 new cell layers every year in these sapling stems. With such slow growing saplings it is not surprising the high uncertainty levels associated with the patterns we observed. Much of the variation in growth rates may also come from differences in wood density; large, thin-leafed species e.g., may grow faster because they tend to have lower wood density [150]. Despite these uncertainties, however, the observed patterns led us to very important insights about species coexistence and the maintenance of morphological diversity in the studied forest, as we will discuss next.

Complex trait-mediation of habitat specialization

Complex trait-mediation of habitat specialization Regardless of what the actual selective mechanisms are, the most interesting prediction of our model is that there should be multiple performance rank reversals across illumination gradients (Fig.2.5d). These reversals act not only on leaf size, but on the diverse combination of leaf size and *SLA*, as discussed above, and can help the maintenance of both taxonomic and functional diversity in the studied forest. Because leaf size tends to be decoupled from *SLA*, both world-wide [150] and in this particular forest (Fig.B.1b-c), when we consider enough species we may find all possible trait combinations, such as large and thin or small and thick leafed plants. As shown here, these functional types respond differently to variations in the availability of crucial resources such as light and water, which is the first condition for spatial coexistence [40]. Then, if the relative performance of these functional types also covaries with environmental gradients, i.e., if the competitive landscape is heterogeneous, then stable coexistence is possible [40]. Although we could not provide irrefutable evidence for that, our best fit model clearly indicates the occurrence of multiple rank reversals among these functional types along the light gradient at the forest floor. Interestingly, we considered here only a small fraction of the total light gradient that can be found at this forest floor, as we did not sample any gaps in our study, so one could expect more such rank reversals occurring at other parts of this gradient. This clearly contradicts the notion proposed for seedlings that rank reversals among species are mediated solely by differential mortality rates, and not growth rates [151]. Although we

acknowledge that differential mortality may further enhance the patterns observed here, our model indicates that differential growth responses to light can on themselves cause such rank reversals, as proposed before [131].

This idea that resource allocation trade-offs may map into context-dependent performance trade-offs has been already illustrated elsewhere using simulations [120]. These simulations have shown that size-number trade-offs may cause species with different traits to specialize into contrasting habitats, which then can lead to the maintenance of both taxonomic and functional trait diversity in species-rich systems. With this work we could provide empirical evidence that this same idea can be applied to a different size-number trade-off and to, we argue, to any type of resource allocation trade-off. That we could find evidence for trait-mediated coexistence mechanisms in such a small fraction of a single environmental gradient is evidence for the great number of potential mechanisms that may help promote the great tree diversity seen in the Central Amazon and similarly diverse forests. Additionally, the complexity derived from the interaction between one environmental factor and only two traits makes it easier to understand why species often behave in such a unique way: if we consider all the plant traits that may affect performance and all the ways they could interact with each other and the environment, it is not hard to accept that species may say more about functional traits than vice-versa [152].

Conclusions and future directions

We have here proposed a mechanism that can explain the coexistence of contrasting plant functional types and therefore can help to maintain the great functional diversity of the studied forest. This mechanism is based on the interaction between internal (allocation trade-offs) and external factors (differential selection along environmental gradients). More specifically, we show that resource allocation trade-offs can provide the variation needed for divergent selection to act. Divergent selection, in turn, depends on the variation of limiting resources across habitats, but most importantly, in the spatial variation of species competitive abilities. That is, species that are more efficient at acquiring and/or using the most limiting resource at a given patch have a competitive advantage. Resource allocation trade-offs guarantee that no species will be the best competitors at all habitats. The specific coexistence mechanism proposed here, however, is likely not enough to maintain the large number of tree species found in most tropical forests. Nevertheless, similar mechanisms are likely to operate in the several other resource allocation trade-offs and along gradients of the many environmental factors that affect plant performance (soil fertility, pathogen load, etc). Depending on how decoupled these mechanisms are from each other, it is not hard to visualize how the coexistence of many hundreds of plant species may be maintained. Perhaps even more importantly, these mechanisms can help to explain both the origins and maintenance of the great morphological diversity in tropical plants.

A promising path forward is to take into account the highly dynamic nature of light

gradients. Although near the Equator light levels do not change much along the year, it can still vary substantially during the course of a single day (angle of incidence), from day to day (cloudiness), and at larger time scales (gap dynamics). Rainfall varies at different temporal scales too and is no less important, as both variation in light and humidity will affect the advantages and disadvantages of certain combinations of leaf traits. Understanding this environmental variation is crucial, for some additional coexistence mechanisms can emerge from this variation (storage effect and non-linearity, e.g.) and may also help understand the impacts of climate change in forest regeneration and dynamics. As the climate in the Amazon becomes drier, e.g., large-leafed species may decline or take refuge in moister areas in the landscape, like stream gullies.

Before we advance to these exciting new directions, however, it would be important to consider some important factors that had to be left out in this study. The most important one is sapling mortality, which is perhaps an even more important component of sapling fitness than growth rates. (Unfortunately the data for the second plot census was not available by the time this work was done, but given the difficulty in finding the saplings in the field, their mortality might not be negligible.) Another layer of complexity can be added by including species with more complicated leaves, such as lobed, compound, and bipinnated leaves, as plants with these special types of leaves may behave differently (Fig.2.8). Moreover, the framework delineated here may be used with adult trees, but we might have to rely on more refined methods such as the use of ground or airborne LiDAR techniques to 3-D scan the forest. Finally, we can still greatly improve the model used here by including saplings'

wood density and using biomass instead of stem diameter as a proxy for sapling size, or by modeling the within-plant variation in leaf area, as these could reduce the noise found in the data. Although these improvements are still on their way, our current model provides an empirical framework that can be used for future research on the many other allocation trade-offs that limit plant performance.



Figure 2.8: Bipinnate leaves of a canopy legume tree. Leaflets are so small that is difficult to even discern them from far away, especially when closed like this one. Including more complicated leaf types like this is one of the next challenges.

Chapter 3

Decoupling of adult and sapling niches

3.1 Introduction

How can hundreds of tree species co-occur in a single hectare of tropical forest? This is one of the longest standing questions in ecology, yet it remains unanswered. This question is especially challenging because, unlike animals, plants have to compete for a limited set of shared resources (light, water, soil nutrients, and CO_2 [63, 64]). As using different resources is not an option, plants may avoid competition by diverging in the ways they acquire and use these resources, i.e., species may vary in when and where they can survive, grow, and/or reproduce [40, 42, 58, 64]. A clear example is how plants can differentiate to occupy contrasting soil and topographic habitats [74], but within each of these habitats we can still find hundreds of tree species. Part of this diversity can be explained by differentiation along another important niche axis, defined by the sharp vertical light gradient found in tropical

forests [153]. Species differentiation along this niche axis is caused by divergent evolution of plant height, which is driven by the costs and benefits of growing tall [83]. For example, the disproportional advantage in competition for light that large trees have over their shorter neighbors is offset by the great cost of constructing and maintaining their large stems [57]. More importantly, life-history trade-offs mediated by plant height, such as the trade-off between fecundity and recruitment rates [154], can in theory promote stable coexistence between species with contrasting adult heights [155]. Despite its obvious importance in such a light-limited ecosystem, height differentiation alone is not sufficient to maintain the great diversity of trees observed in most tropical forests, where many species can have very similar adult heights [156, 157].

It has long been predicted that there is a limit to how finely species can partition a niche axis such as light, and that eventually, as community richness increases as we see in tropical forests, species will converge in resource use [158]. Therefore, as species richness increases we should have the emergence of groups of ecologically equivalent species, that is, species with very similar niches and whose per capita fitness is nearly identical [159]. On one hand, this should lead to neutral dynamics within these groups of species [47], which on itself cannot promote stable within-group coexistence. On the other hand, convergence along a key niche axes can help reduce fitness differences between species in such a way that subtle differentiation along another niche axis is all that is required for species coexistence [39, 160]. While spatial variation in light availability is a central feature of most discussions of forest diversity [155, 161], there are a number of other niche axes that may be important to tropical

trees, including soil fertility gradients [68], spatial variation in herbivore or pathogen pressure [121, 162], all of which may help explain tree species coexistence. However, many of these niche axes might be unlikely to operate on neighboring trees found within the same height strata of a forest, which begs the question- what might the niche differences be between species with similar adult heights in a tropical forest?

Light availability close to the forest floor may vary as much as it does vertically between the forest canopy and the deep-shaded understory of dense stands. This spatial variation in light is mostly maintained by gap dynamics, so horizontal light gradients are often quite patchy. This heterogeneous landscape, in turn, provides contrasting regeneration niches for pioneers and late-successional species [63]. Coexistence between these two groups of species can be promoted by competition-colonization trade-offs, with late-successional species excelling at surviving in the shade, and pioneers excelling at growing fast in full sun [163]. This mechanism, however, is unlikely to maintain the vast majority of tropical tree species, as only a small fraction of them are typical pioneer species [164]. At the same time, there are still plenty of finer grained variation in light quality and quantity in the shaded understory of mature stands of the forest [161]. This subtler spatial heterogeneity may still allow for further niche partitioning among species. Late-successional species, e.g., can either remain short and complete their whole life cycle in the shade (shade tolerance), or establish in the shade, but grow up to better-lit heights so that it can start reproducing (shade avoidance) [53, 119]. While shade tolerants are believed to outperform shade avoiders in deeply shaded patches, the opposite should happen in less shaded patches [123]. Provided they really

occur in nature, these rank reversals could define a new niche axis promoting tree species coexistence in tropical forests.

These regeneration niches could then help to explain the high number of species sharing the same vertical strata in mature tropical forests. A strong evidence in favor of this hypothesis is the great diversity of growth strategies found among saplings in tropical forests [165]. These different strategies are mainly produced by the differential expression of apical dominance, which promotes height-gain as opposed to branching and thus defines plants' architecture and crown-height allometries [166]. Therefore, contrasting saplings' architecture with their species' adult heights could generate important insights about species coexistence in tropical forests. Unfortunately, we still lack this basic information for the vast majority of tropical tree species.

Given the relative lack of data on these issues, we chose to explore how interspecific variation in adult height and sapling architecture might contribute to the richness of one of the most diverse forests on Earth, the Amazon, thought to be home to $\approx 15,000$ tree species [18]. Our study site is a 25-ha plot in the Central Amazon which contains $\approx 1,500$ tree species, making it perhaps the richest forest in the Amazon basin [21]. The hyperdiversity of this forest makes the issue of diversity maintenance even more intriguing and it likely takes many coexistence mechanisms for these many species to build up into a single community. Therefore, to test the role of regeneration niche partitioning on within-strata coexistence, we first compiled adult height (H_{max}) data from herbaria and the literature for ≈ 800 tree species. We then quantified three core architectural traits on $\approx 1,000$ saplings from ≈ 400

tree species, while controlling for sapling size and illumination. As hyperdiverse forests contain many rare species, finding enough individuals to have high confidence in species trait values can be challenging [90]. We therefore use a Hierarchical Bayesian framework that allows us to account for the uncertainty from rare taxa in our analyses [52]. We then fit species-specific allometric models that allowed us to compare sapling growth strategies with their species' H_{max} . Finally, using the plot data allowed us to test whether the spatial distribution of sapling traits were compatible with the partitioning of the understory between shade-tolerant and shade-avoider saplings.

3.2 Conceptual framework

If light is the most limiting factor in wet tropical forests, then stable coexistence must involve the partitioning of light gradients. Tropical trees notably diverge a great deal in their adult heights (H_{max}) to occupy different positions along the vertical light gradient (vertical segregation hypothesis [10]). Due to the high incidence angle of sunlight near the Equator, these forests are expected to have a large number of vertical strata [167]. Vertical partitioning of light, however, is likely insufficient to promote the coexistence of the hundreds of tree species found in equatorial forests, many of which are understory species [157]. Additionally, instead of being evenly spread vertically, trees may converge into a few local optima along the vertical gradient of light [156, 167]. Moreover, most trees have to start as seedlings on the forest floor, so the vertical niches of tall species are actually nested within

the niches of smaller species. Therefore, on top of vertical niche partitioning, the partitioning of horizontal light gradients should be essential for the coexistence of tree species, especially those with similar H_{max} .

Horizontal light gradients, such as those created by forest gap dynamics, could be partitioned by species with contrasting regeneration niches [63]. More specifically, spatial variation in light conditions should promote across-species divergence in sapling growth strategies, with species with shade-tolerant saplings regenerating in the shade and species with light-demanding saplings regenerating in the gaps [166, 168]. Now, if saplings with similar H_{max} establish in contrasting light conditions, thus causing species in the same strata to be spatially segregated, then within-strata spatial coexistence could be possible [40]. Two selective mechanisms could lead to such a spatial segregation of saplings based on their architectural traits: 1) limiting similarity; and 2) environmental filtering [74]. However, whether these mechanisms can promote within-strata coexistence or not depends on the coupling between H_{max} and sapling growth strategies.

We hypothesize that limiting similarity of sapling traits can promote within-strata coexistence provided there is a strong coupling between adult and sapling niches (the *adult-sapling coupling* hypothesis). Conversely, if species with similar H_{max} tend to have contrasting sapling growth strategies only environmental filtering could help with within-strata coexistence (the *within-strata divergence* hypothesis). The coupling between H_{max} and sapling architecture has been suggested to be a result of the strict allocation trade-offs between height gain and crown expansion in woody plants (*allocation trade-off* hypothesis [123]). According

to this idea, saplings that start branching prematurely produce short-statured adults (shade-tolerance or "pessimistic" strategy), while saplings that invest mostly into height growth can produce tall adults (shade-avoidance or "optimistic" strategy) [123, 166]. Because the overall shape of optimistic saplings tend to be complementary to that of pessimists, competition for light should be weaker between neighbors with contrasting architectures compared to similar-shaped neighbors, thus limiting how similar neighboring saplings can be (*optimal space filling* hypothesis [169]). This limiting similarity mechanism would segregate saplings with similar architectures and by extension with similar H_{max} , thus promoting the spatial coexistence of species that occupy the same strata as adults. Alternatively, if sapling growth strategies are independent of H_{max} , then limiting similarity would often fail to segregate saplings with similar H_{max} . On the other hand, if there is *within-strata divergence* in sapling traits, then environmental filtering could promote within-strata coexistence. Within-strata divergence along the regeneration niche axis would be expected if the partitioning of the vertical light gradient is not sufficient to relieve interspecific competitive pressures [160]. Additionally, if sapling traits are filtered by the often quite patchy light conditions, then saplings with similar traits, but with contrasting H_{max} , would be spatially aggregated (the *light habitat filtering* hypothesis). Indeed it has been suggested that optimistic saplings perform better on well-lit patches, but perform worse on shaded patches compared to pessimistic saplings [123].

We can therefore make the following testable predictions about species' spatial segregation and within-strata coexistence in the studied forest:

1. Adult-sapling coupling and limiting similarity:

- a) If vertical segregation occurs via an allocation trade-off between height gain and crown expansion, we predict a strong negative correlation between sapling height and crown size and a positive correlation between H_{max} and sapling architecture, with saplings from tall species being tall, but with small crowns compared to saplings from short species;
- b) If within-strata coexistence is promoted by limiting similarity of sapling architecture, we should find saplings with similar architectures co-occurring less often than would be expected by chance (negative spatial autocorrelation of sapling traits).

2. Within-strata divergence and environmental filtering:

- a) If there is within-strata divergence in regeneration strategies, we expect that species with the most similar H_{max} have saplings with the most different traits;
- b) If within-strata coexistence is maintained by environmental filtering, then saplings with similar traits should be spatially aggregated (positive spatial autocorrelation of sapling traits).

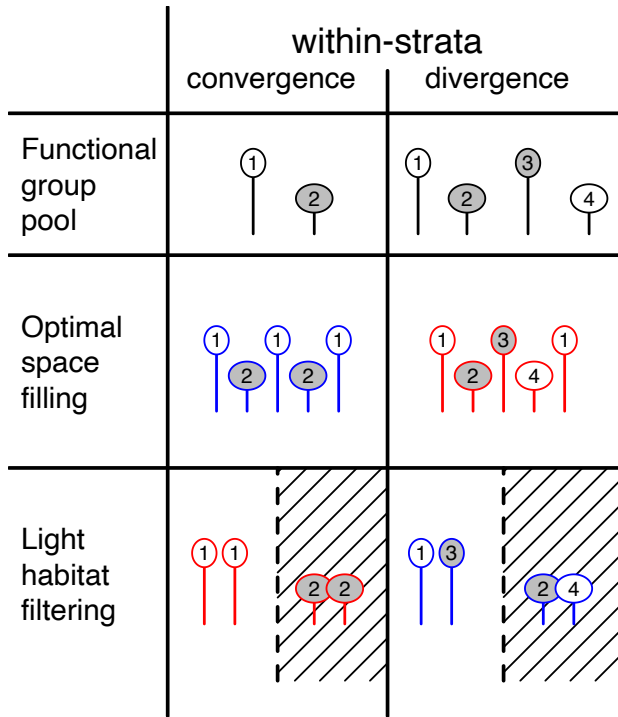


Figure 3.1: Conceptual figure describing the two main hypothesis of within-strata species coexistence: 1) adult and sapling niche coupling (a) associated with limiting similarity (c); and 2) ontogenetic niche shifting (b) and light habitat filtering (f). Other combinations are theoretically possible (d and e), but cannot promote within-strata spatial coexistence of all pairs of functional groups (pairs unlikely to coexist are shown in red). Saplings whose crowns are grey have short adult heights, while those with white crowns are from tall species. Functional groups are represented by unique numbers: 1 - tall optimists; 2 - short pessimists; 3 - short optimists; and 4 - tall pessimists. In the case of habitat filtering, shaded habitats are represented by the dashed area, contrasting to the clean, white space representing well-lit habitats.

3.3 Methods

Study site

The studied forest is situated in a 25-ha permanent plot located in the Central Amazon (2°30'S, 60°W). This is an ancient landscape with one of the oldest and thus poorest soils in the entire Amazon basin [22], yet 1,400 tree species can be found in the studied plot alone [21]. The climate is hot and wet, but with a dry season, with annual mean temperature of 26.7°C and annual rainfall of 1900-3500 mm [70]. Although most of the plot is situated on the top of a plateau, it is cut by two stream gullies. The forest in the area is pristine, non-flooded, evergreen, and has very slow dynamics (annual tree turnover rate is 1.2% [136]), meaning that gaps are especially rare in this forest. The forest canopy ranges from 35 to 40

m, with some emergent trees reaching $> 50 - m$ tall, while the understory is dominated by saplings and stemless palms [136]. All trees ≥ 1 cm in stem diameter at breast height (D ; $\sim 160,000$ plants in total) have been mapped and identified to the species level [21].

Maximum adult height

Given challenges in finding accurate data on species maximum height, we estimated maximum adult size (H_{max}) for species at our study site from three different sources: species descriptions found in the literature, notes from herbarium specimens, and the stem diameter (D) distribution for each species found in the permanent plot. Because H_{max} reported in the literature (H_{lit}) can be imprecise, for a subset of 290 species we compiled heights from records in an online consortium of herbaria [170]. We then used the 95th percentile of the herbarium record height distributions to estimate H_{herb} (Fig.C.1). As many species in the plot (give number or percent) are not yet described, we also estimated H_{max} from each species' stem diameter (D) distribution in the plot ($H_{D_{max}}$). Then, the 97.5th percentile of D distributions was chosen to estimate D_{max} (Fig.C.2). We estimated $H_{D_{max}}$ as a power-law function of D_{max} for the 290 species for which we had reliable H_{max} estimates, and then applied the same function to estimate the H_{max} of the remaining 1,200 species. Lastly, to have a consensus estimate (H_{cons}) of these three sources of information, we kept the $H_{D_{max}}$ values that were within ≤ 5 m from either H_{lit} or H_{herb} .

Sampling design

Given the large differences in abundance between common and rare species in the plot (ranging from 9,761 to 1), we employed a stratified sampling approach based on species relative abundance. Common species were sampled more intensely (≥ 10) than rare species (≤ 3) in order to help inform estimates of intraspecific variation. To control for the effects of forest structure, topography, and soil, we focused sampling on mature stands on the dominant plateau habitat (ca. 61% of the plot area). To sample the plateau's most abundant species in each forest vertical stratum, we first classified all species into four quartiles according to their estimated adult heights ($H_{D_{max}}$) and selected the 25 most abundant species from each of these groups. We then aimed to sample at least six saplings ($1 \leq D \leq 4$ cm) from each of these 100 target species, but due to high sapling mortality since the previous plot census this was not possible for most target species. To avoid pseudoreplication, we did not sample more than one individual per species in each 20x20 m quadrat. For efficiency in the field, we targeted quadrats with a high representation of our common focal species for sampling. To include rare species, we sampled any additional species found in any quadrat selected for sampling. Among common and rare species, sampling sizes ranged from 1 to 22. Finally, given our interest in architectural design of species rather than in the effect of disturbance or biotic interactions on architecture per se, we only sampled saplings that had an intact crown with no recent main stem breakage, that were not infested by lianas, and that did not have their crowns entangled with the crowns of neighbors, thus preserving the sapling

original shape. In total we sampled 1,041 saplings from 429 species in 100 different quadrats; together, these species account for $\sim 78\%$ of all the censused plants in the plot.

Sapling architecture

To describe sapling architecture we measured three traits: total plant height (H ; m); crown projected area (W ; m^2); and relative crown thickness (T ; unitless). We measured H as the distance between the ground and the tallest leaf in the sapling's crown. To estimate W , we measured two crown diameters: W_1 , the largest horizontal distance between the tips of the two farthest leaves in the crown; and W_2 , the largest diameter perpendicular to W_1 . We then approximated W to the area of an ellipse ($1/4 \times \pi \times W_1 \times W_2$). Crown thickness was the difference between the tallest and the shortest leaf in the crown (excluding occasional resprouts or isolated and small branches at the base of the plant). Because thickness is bounded by H , we divided it by H , resulting in the relative measure T . Additionally, to control for the variation in sapling size and light availability, we measured stem diameter (D ; cm) at breast height (1.3 m) and crown illumination index (L ; unitless), which ranges from 1 (no direct light) to 5 (completely exposed to direct light; following [137]). We measured D with a digital caliper (0.01 mm resolution) and all other sapling dimensions with a laser tape (1 cm resolution). While D , H and W were log-transformed, T had to be logit-transformed (Fig.C.3).

Sapling allometry

To test if species' early growth strategies are coupled with adult height (H_{1a} : *adult-sapling coupling*) we first had to make sapling architectural traits comparable across species. We thus modeled these traits as a function of sapling size (D) and crown illumination (L). To use all the information collected, even for species for which we had only one sample, we employed a multivariate, hierarchical Bayesian approach based on a previous work [171]. The three measured traits (H , W , and T) were analyzed together, assuming they were sampled from a multivariate normal distribution as follows:

$$\mathbf{A}_{ij} \sim \mathcal{N}_3(\boldsymbol{\beta}_j + \boldsymbol{\alpha}_j * D_{ij} + \boldsymbol{\phi}_j * L_{ij} , \boldsymbol{\Sigma}_w) \quad (3.1)$$

where \mathbf{A}_{ij} is the set of three trait values for each sapling i from species j , $\boldsymbol{\Sigma}_w$ is a covariance matrix describing the relationships among sapling traits, $\boldsymbol{\alpha}_j$ and $\boldsymbol{\phi}_j$ are species-specific parameters that describe the effects of D and L on architecture, respectively; and $\boldsymbol{\beta}_j$ are the intercepts. We centered D at the median and subtracted 1 from L , so that the intercepts represent the estimated traits of median-sized saplings growing in the shade ($L = 1$), henceforth referred to as standardized saplings. Then, to model the links between sapling architecture and H_{max} , we further modeled each of the nine species-specific parameters (α s, β s, and ϕ s) as follows:

$$\boldsymbol{\Gamma}_j \sim \mathcal{N}_9(\boldsymbol{\kappa} + \boldsymbol{\theta} * H_{max_j} , \boldsymbol{\Sigma}_b) \quad (3.2)$$

where $\boldsymbol{\Gamma}_j$ is the set of β s, α s, and ϕ s for each species; $\boldsymbol{\Sigma}_b$ is the covariance matrix that describes the correlations among these species-specific parameters; $\boldsymbol{\kappa}$ is the across-species

average parameters (hyperparameters); and θ describes the effect of H_{max} on each of these parameters.

To improve model convergence, we determined prior distributions based on the range of values found in our own data (supplementary material for chapter 3). All statistical analyses were done in JAGS [93] through R v.3.5.3 [92], using the `rjags` package [139]. To extract and analyze convergence on the Markov chain Monte Carlo simulations, we used the `coda` package [94].

Within-strata variance in sapling traits

To test the alternative hypothesis that species sharing the same vertical strata tend to diverge in their early growth strategies (H_{2a} : *within-strata divergence*), we correlated differences in H_{max} to differences in sapling traits across species. If there is *within-strata divergence* in sapling traits, then species with similar H_{max} should have sapling traits that are more dissimilar than expected by chance. We thus ran a Mantel correlation test using Euclidean distances among species' H_{max} and sapling traits. Sapling traits were derived from the allometric models, as described above, and represent the architectural traits of standardized saplings (β s), as well as their respective allometries (α s) and response to light (ϕ s). To determine which of the sapling traits were most responsible for the patterns found, we reran this test with all traits individually and in all combinations.

Spatial analysis

To test if species with similar adult heights could coexist through spatial segregation, and if this segregation is mediated by sapling growth strategies, we quantified spatial autocorrelation for both H_{max} and sapling traits. More specifically, to test if saplings with similar architectures are segregated at the neighborhood scale (H_{1b} : *optimal space filling hypothesis*) and/or aggregated at the forest stand scale (H_{2b} : *light habitat filtering hypothesis*), we ran a spatial autocorrelation (SAC) analysis using several different scales (1-200 m). To make use of the great deal of spatial data provided by the permanent plot, we extrapolated the nine traits derived from the allometric models (α s, β s, and ϕ s) to all the saplings in the plot that were identified as any of the 429 species we had sampled. Because the volume of data was too large ($> 80,000$ saplings), and because the spatial scales of the phenomena we were testing were likely < 100 m, we decided to run separate analyses in each of 25 1-ha subplots. Analysis consisted of estimating a SAC statistic (Moran's I) for each subplot using the `Moran.I` function from the R package `ape`. To check for SAC dependence on spatial scale we plotted correlograms using the `correlog` function from the R package `pgirmess` [172].

Table 3.1: Compilation of species' maximum adult height (H_{max}) shows the high number of species that can share the same strata (defined here by vertical 10-m intervals). Also shown is the abundance distribution across these strata, and the number of species whose saplings were sampled. H_{max} ranges refer to the most and least conservative estimates. Abundances were rounded to thousands. Associated percentages refer to the total number of species (~1,500) and individuals (~160 k) included in the 25-ha permanent plot used in this study.

| Stratum | $H_{max}(m)$ | Richness | Abundance | Sampled |
|--------------|--------------|-------------------------|-----------------------|-----------------|
| Shrubby | 1-10 | 76-298 (5-20) | 14-18 (9-11) | 32 (2) |
| Understory | 11-20 | 159-541 (11-36) | 36-74 (22-46) | 192 (13) |
| Subcanopy | 21-30 | 125-358 (8-24) | 27-45 (17-28) | 136 (9) |
| Canopy | 31-40 | 61-165 (4-11) | 6-12 (4-7) | 55 (4) |
| Emergent | > 40 | 10-50 (1-3) | 1-2 (0-2) | 14 (1) |
| Total | | 431-1412 (29-95) | 83-150 (52-95) | 429 (29) |

3.4 Results

Vertical segregation

While species' maximum adult heights (H_{max}) diverged widely (ranging from 4-47 m), we found substantial overlap in H_{max} , with hundreds of species occupying the same stratum (Tab.3.1). This overlap persisted regardless of the source of the height estimate (Tab.C.1). Because plants with $D < 1$ cm were not included in our sampling, the richness of the lowest stratum is likely underestimated in Tab.3.1. Nevertheless, 83-85% of the species have H_{max} shorter than the height of the forest canopy (30-40 m; Tab.3.1).

Allocation trade-offs and adult-sapling coupling

Contrary to the idea that adult height (H_{max}) and sapling traits were coupled (H_{1a}), H_{max} had little effect on sapling architecture and allometry (Tab.3.2). Interestingly, the strongest

effect of H_{max} was on the allometry of crown relative thickness (T), with taller species having saplings that grow disproportionately more in crown thickness through their growth trajectory than shorter species (Tab.3.2). As predicted by the adult-sapling hypothesis (H_{1a}), H_{max} positively affected sapling height (H), but this effect was weaker and less consistent (Tab.3.2). Surprisingly, many of the most abundant species in the plot, who were also the best sampled species in our study, had growth strategies that directly contradicted the expectation from the adult-sapling coupling hypothesis that tall species should have optimistic saplings while short species should have pessimistic ones (Fig.C.4). This lack of correlation between H_{max} and sapling traits was not due to a lack of variation in sapling growth strategies, for we found a great diversity of sapling architecture, allometry, and response to light (Tab.C.2). Some traits, however, varied more within rather than between species (Tab.3.3). Although we found evidence of allocation trade-offs between sapling H and crown size (W and T), the strongest trade-off ($H - W$) was intraspecific (Tab.3.3). Interestingly, W and T were strongly correlated, both intra- and interspecifically, indicating no trade-off between growing wide versus thick crowns (Tab.3.3). Finally, we could derive from our allometric models a description of the general architecture and behavior of the saplings in the studied forest: 1) saplings tend to be relatively tall (~ 4 m), but with small crowns (0.6 m wide and 1.1 m deep); 2) while W grows exponentially ($\alpha > 1$) with stem diameter (D), H and T show a logarithmic growth ($\alpha < 1$); and 3) while light had no effect on H , it slightly inhibits W and greatly promotes T (Tab.3.2).

Table 3.2: Effects of adult size (H_{max}) on sapling architecture: height (H ; m), crown projected area (W ; m^2), and crown relative thickness (T). Species-specific architecture parameters (β , α , and ϕ) were modeled as a function of H_{max} (SDL), where the intercepts (κ) represent the architecture (β s), allometry (α s), and response to light (ϕ s) of a median-sized sapling ($D = 1.77$ cm) growing in the shade ($L = 1$) and from a median-sized species ($H_{max} = 22$ m).

| Parameter | Intercept (κ) | H_{max} effect (θ) |
|------------|------------------------|-------------------------------|
| β_H | 3.95*** | 0.002* |
| β_W | 0.30*** | 0.000 |
| β_T | 0.28*** | -0.002 |
| α_H | 0.74*** | 0.002 |
| α_W | 1.50*** | 0.004 |
| α_T | 0.21*** | 0.013** |
| ϕ_H | -0.01 | -0.001 |
| ϕ_W | -0.05* | 0.001 |
| ϕ_T | 0.14*** | 0.006 |

* $p < 0.2$ or $p > 0.8$; ** $p < 0.1$ or $p > 0.9$; *** $p < 0.05$ or $p > 0.95$; where p is the probability that a parameter is greater than zero.

Table 3.3: Intra- and interspecific variances and correlations among the three architectural traits measured (H , W , and T). Parameters presented here correspond to the variance-covariance matrices Σ_w and Σ_b of our Bayesian model (KTH).

| | Trait | Intraspecific | Interspecific |
|---------------------|-------|---------------|-------------------|
| Variances | H | 0.03 | 0.04 [§] |
| | W | 0.18 | 0.11 [§] |
| | T | 0.44 | 0.31 |
| Correlations | HW | -0.14*** | -0.05 |
| | HT | -0.03 | -0.08* |
| | WT | 0.18*** | 0.57*** |

[§] significantly difference between intra- and inter-specific variances

Within-strata divergence in sapling traits

Although our results contradict the idea that there is within-strata divergence in sapling traits (H_{2a}), the largest differences in sapling traits were found among species with similar H_{max} (Fig.3.2). While species with large differences in H_{max} tended to have more dissimilar saplings (Mantel $r = -0.27$; $p = 0.001$), the saplings from species with similar H_{max} ranged from being as similar as possible from being as different as possible (Fig.3.2). Moreover, the bottom left empty corner in Fig.3.2 reveals an increasing minimum similarity in sapling traits as species diverge in their H_{max} , which is another evidence of the correlation between H_{max} and sapling traits. When we ran the same analysis with each trait individually and in all combinations, we found that the adult-sapling correlation was maximized by the allometry and response to light of T (Mantel $r = 0.66$; $p = 0.001$; Tab.C.3), thus further reinforcing the results shown above (Tab.3.2).

Spatial distribution of sapling traits

We found that saplings with similar growth strategies were spatially aggregated, supporting the light habitat filtering hypothesis (H_{2b}). On the other hand, we found no significant negative spatial autocorrelation (SAC) in sapling traits, implying no support for the optimal space filling hypothesis (H_{1b}). All sapling traits showed positive SAC across all 1-ha subplots, with only a few exceptions (Tab.C.4). When we investigated the scale at which these trait aggregation patterns were strongest, we found that they were occurring predominantly at

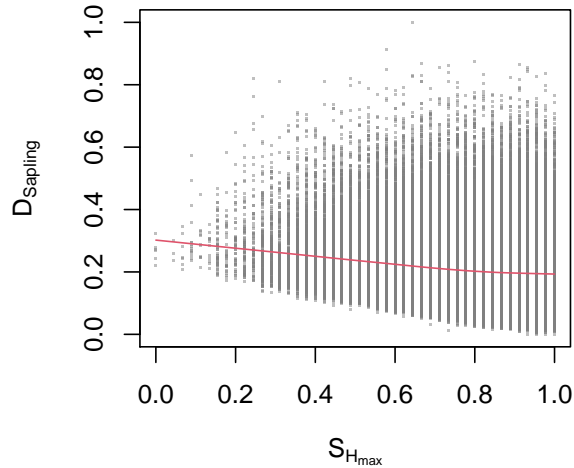


Figure 3.2: Interspecific similarities in adult size ($S_{H_{max}}$) and dissimilarities in sapling growth strategies ($D_{Sapling}$) are negatively correlated (trend line in red estimated from a locally-weighted polynomial regression). Although saplings from species with similar H_{max} can be very different from each other, the empty corner pattern found (lower left corner) is the reverse of the one that would be expected (lower right corner) if there was a strong within-strata divergence in sapling growth strategies.

small scales ($0-40 m$), although in some cases it would reappear at scales $> 100 m$ (Fig.C.5). Moreover, it was not uncommon for the positive SAC patterns to be followed by negative ones at scales $> 40 m$ (Fig.C.5). Although these negative SAC patterns were never significant, they indicate a "checkerboard" pattern of trait distribution, which could be seen clearly after these traits were mapped (Fig.3.3).

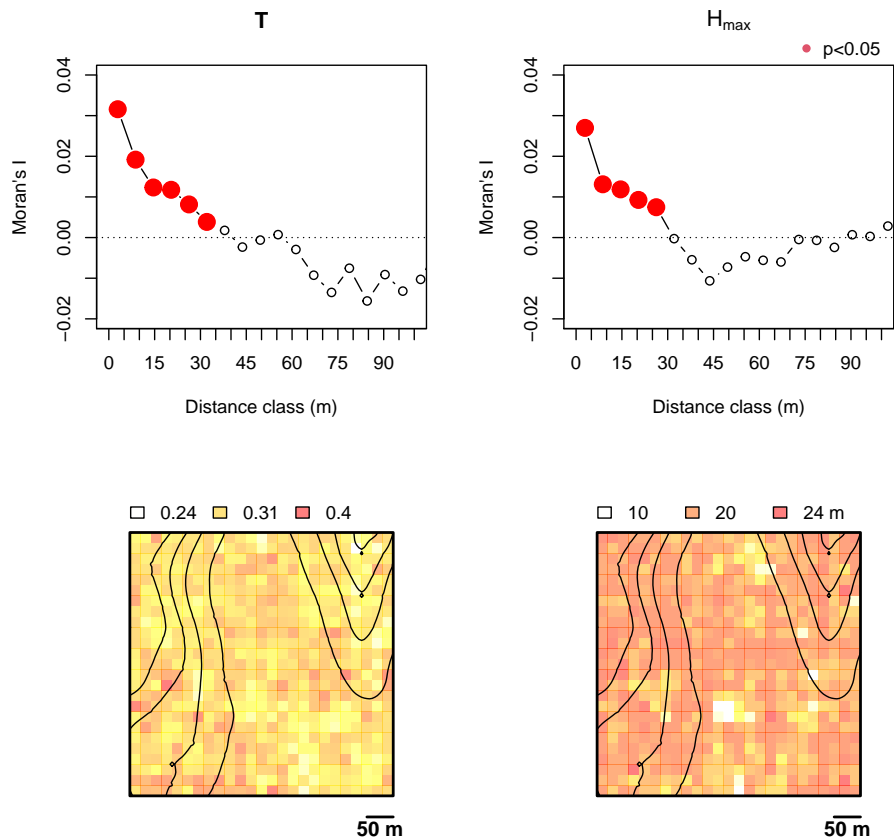


Figure 3.3: Both sapling architecture and adult size (H_{max}) were spatially aggregated at the local scale (up to 30 m). This is shown by the spatial correlograms above and the quadrat maps below. Crown relative thickness (T) is showcased here for being the sapling trait with the strongest spatial pattern. CRT and H_{max} was estimated for all saplings in the 25-ha plot that belonged to the > 400 species sampled in this study. Correlograms refer to one of the best sampled hectares in the plot. The maps show the median CRT and H_{max} for each of the 625 quadrats in the plot.

3.5 Discussion

Here we have tested two distinct mechanisms of spatial coexistence that can help to explain the huge tree diversity in the Central Amazon. We began by suggesting that the vertical partitioning of light is unlikely to be sufficient to maintain the high number of species occurring at most of the forest's vertical strata. We then proposed that if species sharing the same vertical strata as adults were spatially segregated when still saplings, then within-strata coexistence could be possible. This form of spatial coexistence would require some form of differentiation of species' regeneration niches. We thought of two selective mechanisms that acting on sapling traits could help promote within-strata coexistence: 1) limiting similarity, if adult height and sapling traits were coupled by allocation trade-offs; or 2) environmental filtering, if species with similar adult heights had divergent saplings. If we found support for either one of these mechanisms we could point a way through which tropical trees with identical adult niches could still coexist via the differentiation of their sapling niches. We showed that despite the large range of adult heights found in this forest, there are still many hundreds of species sharing the same strata, especially the lowest ones (Tab.3.1). This result further highlighted the importance of investigating how species diversity could be maintained within each of those strata. We then showed mixed evidence for both of our within-strata coexistence hypotheses, pointing that perhaps they are not mutually exclusive. First, we found that there is only a loose coupling between adult height and sapling traits (Tab.3.2), which in part can be attributed to the high plasticity of these traits (Tab.3.3). Next, we showed

that, although there is no evidence of within-strata divergence in sapling traits, saplings with identical adult heights can still be as different as saplings with the most contrasting adult heights (Fig.3.2). Lastly, we showed that saplings were spatially aggregated not only based on their current traits, but also on their potential adult heights (Fig.3.3). This last piece of evidence may seem to defy the very idea of within-strata spatial coexistence, but we argue that the spatial aggregation of adult height was so weak that there might still be enough room for spatial coexistence mechanisms mediated by sapling traits to take place. Overall, the mixed results found here indicates that the role of adult and sapling niche differentiation in promoting species coexistence is more complicated than anticipated. Below, we discuss each of these findings in more depth.

The incomplete nature of vertical segregation

Despite the great diversity of adult heights found in tropical rainforests, sharing of vertical adult niches seems to be as important as the partitioning of the vertical light gradient. According to the sunfleck model, equatorial forests should have the highest number of tree vertical niches, as light can penetrate at very steep angles into the forest (Fig.3.6) [167]. This vertical niche diversity should result in a wide distribution of maximum adult heights, which indeed varied 10-fold in the studied forest. Now, maximum adult height only shows the endpoint of a tree's growth trajectory, which can take many alternative paths [173], but necessarily have to start at the forest floor. I.e., the adult niches of tall species are nested

within the adult niches of all shorter species, thus severely limiting the potential for vertical segregation. This also means that the lowest strata are the ones most packed with species, so one would expect that only few species would have short adult heights. On the contrary, a large majority of species is restricted to the shaded strata that lie below the canopy (Tab.3.1). This is compatible with prior findings for tropical forests [157], and further reinforces our need to explore the mechanisms that can promote within-strata coexistence. Another prediction of the sunfleck model is that trees are not evenly distributed vertically, converging instead to certain optimum points between the forest floor and the canopy (these would be the intersection points between light cones from neighboring gaps [167]). This model provides a mechanistic response to the century-long debate about whether tropical forests are organized into discrete vertical strata or not [10]. Unfortunately, the height data from herbarium specimens we used lack the precision needed to run a reliable cluster analysis, but recent evidence from another tropical forest points to a clear vertical stratification [156]. In conclusion, forest stratification further limits adult niche differentiation further emphasizing the importance of within-strata coexistence.

Alternative mechanisms of height differentiation

There must be physiological mechanisms other than allocation trade-offs driving the differentiation of adult height in plants. Although we did find some evidence of the often assumed hypothesis that plants trade height gain for crown expansion [83, 123, 174], this evidence

is weak at best (Tab.3.3). This lack of support for biomass allocation trade-offs can be explained by the adaptive plasticity of sapling architectural traits [175]. Given how variable and unpredictable the light environment in the interior of tropical forests can be [161], it would only make sense for saplings to be highly plastic in their architecture. Because architecture is tightly related to plants' light interception efficiency in the understory [176], variation in these traits will cause significant variation in plant performance as well, which may obscure trade-offs even when they are strong [62]. Not less important might be the several confounding variables that certainly added noise to our data, such as interspecific variation in wood density, foliage density, and undetected breakage in the sapling crown, all of which could lead to the underestimation of plant investments into crown expansion. Therefore, even if there is a strong height-gain, crown-expansion trade-off, the above-mentioned sources of variation should limit the role this trade-off has in height differentiation. This idea is supported not only by the very presence of saplings with shifted growth strategies (pessimistic tall species and optimistic short species), but by the fact that some of these unexpected combinations are among the most abundant species in the forest (Fig.C.4, 3.4).

The case of short-statured species with optimistic saplings is easier to understand. This might be just a variation of the growth strategy of many tall species, which only expand their crowns after reaching the forest canopy [177]. Crown expansion might also precede the onset of reproduction in these trees, which should further slow down gains in height [122]. As with the onset of reproduction, there might be some minimum light level that serves as the cue for the switch from optimistic to pessimistic strategies. If this is the case, small

differences in this light threshold across species could lead to considerable differences in their adult heights. Now, the case of tall species with pessimistic saplings is more intriguing. The mechanism responsible for such an odd combination could be related to the plasticity of other shade-tolerance traits, such as light compensation point and maximum photosynthetic rate [176]. Tall species that regenerate in the shade should experience dramatic ontogenetic shifts in their photosynthetic traits, as they go from the understory's deep shade to the full light above the canopy [119, 178]. If this plasticity can also be manifested at smaller time scales, then saplings could use it to alternate between shade-tolerant phases when suppressed and shade-avoiding phases when light conditions improve. In fact it has been demonstrated theoretically that this could be a more successful growth strategy compared to a purely optimistic strategy [179]. Regardless of what these physiological mechanisms driving height differentiation are, the finding with the greatest implications for species coexistence is that adult heights are decoupled from sapling growth strategies.

Adult-sapling decoupling, habitat filtering, and spatial coexistence

On one hand we found support for the hypothesis that within-strata coexistence is promoted by the combination of adult-sapling trait decoupling (Fig.3.2) and environmental filtering of saplings traits (Fig.3.3). On the other hand we found evidence contrary to this spatial coexistence hypothesis, as saplings with similar adult heights tend to be spatially aggregated (Fig.3.3). These apparently contradicting results fit well at the center of the debate on

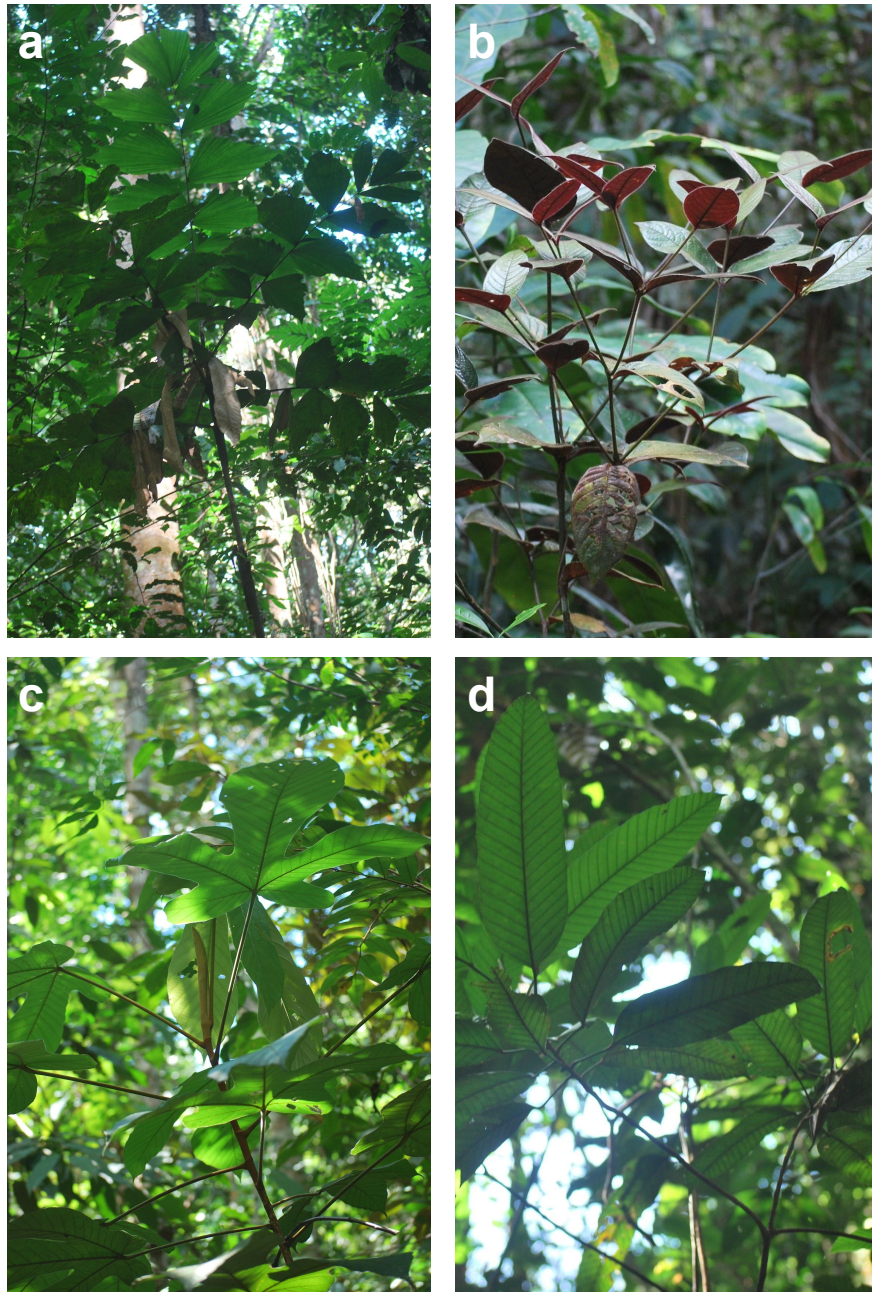


Figure 3.4: Sapling architecture can be decoupled from plant maximum height and even phylogeny. (a) Palms are the ultimate optimistic plants, completely refraining from branching even as adults, such as this understory palm (*Iriartella setigera*, Arecaceae), once used to make blowguns. (b) A completely opposite strategy is represented by this rare shrub (*Psychotria* sp., Rubiaceae), with its puzzling dichotomous branching pattern. (c) *Pourouma myrmecophila* and (d) *Pourouma ovata* are both members of the same family (Urticaceae), yet they have contrasting growth strategies: while the former relies on long petioles to compensate for the lack of branching, the latter invests into long plagiotropic branches to avoid self-shading. They also occupy different strata: *P. myrmecophila* is an understory tree, while *P. ovata* can reach the forest canopy.

whether saplings are more adapted to their current habitats [119] or to their future adult habitats [180]. Saplings' photosynthetic traits, e.g., may be retained at the adult stage if there is an upper limit to the potential to acclimate to increasing light exposure as the tree grows tall [119]. As a consequence, one would expect that saplings from taller-statured species would only be able to regenerate in better-lit habitats compared to short species, and indeed there is a correlation between adult and sapling light environments [180]. This could explain why the adult height of saplings was spatially aggregated in this study. This adult-sapling niche coupling seems to be stronger among shade-tolerant species [180], which are likely the bulk of the species used in this study. Sapling architectural traits, however, tell us a different story: not only are these traits poorly correlated to adult height, but they appear to be filtered by environmental factors other than those causing aggregation of future adult heights.

It is not a surprise that a plant's architecture may change dramatically as it grows; in fact, once a tree grows its architecture often becomes unrecognizable [165]. Moreover, architectural traits often compensate for mismatches between photosynthetic traits and the light conditions, e.g., by modulating the degree of self-shading within the crown [176]. There is therefore the possibility that photosynthetic traits are more "conserved" through tree ontogeny than architecture, and that it is actually the combination of these two types of traits that define a sapling's shade-tolerance and thus its light niche. If this is the main selective mechanism defining sapling niches, then it is unlikely that it can promote within-strata coexistence, at least not through the spatial segregation of saplings with similar adult heights

as hypothesized. Alternatively, the randomness introduced by dispersal and recruitment limitation [42], e.g., allied with the wide variety of adult niches (vertical strata), could be enough to lower the risk of neighboring saplings having similar adult heights. Environmental filtering of traits loosely connected to adult height, such as sapling architecture, could further add to this apparent spatial randomness. Another possibility is that we are actually looking at the ghosts of a past coupling: if initially species had their sapling niches coupled with their adult ones, then any species capable of breaking this constraint would be able to successfully invade the system. This is in line with the common theme in plant evolution of overcoming physiological constraints [61], and it would not take many evolutionary steps as plant architecture could to some extent compensate for a lack of shade-tolerance traits in the leaves (low light compensation point, e.g.). This could explain why some of the most abundant species in this forest are precisely the ones doing the unexpected (tall pessimists and short optimists); after all, if a canopy species could regenerate in patches previously dominated by saplings of understory trees, it would have a great advantage as it outgrows its neighbors and become an adult tree.

As for the absence of any evidence of *optimal space filling* among saplings, one explanation is that saplings occur in such a low density that competition between neighboring saplings is not a strong selective force [42]. Although there can be up to 300 saplings in a single 400- m^2 -quadrat in the study area, the cover area of all these saplings combined ranged from 11 to 40% per quadrat (cover). That definitely does not correspond to one's experience when walking through this forest, where one can see lots of foliage overlap. This is mostly due

to the fact that some of the most abundant forms of understory life were not included in this study, such as lianas and epiphytes, but especially stemless palms whose long fronds are often leaning against saplings (*pers. obs.*). Another explanation is that architectural traits are so plastic (as shown in Tab.3.3; Fig.3.5) that even if there is a selective force driving limiting similarity in sapling traits we would not be able to capture it with our species-focused approach. If that is the case, only by measuring the traits of neighboring saplings would we be able to properly test the *optimal space filling* hypothesis.

Future directions

Before we can move forward, some fundamental steps must be taken, starting with a more accurate depiction of tree species' adult and sapling niches. Maximum adult height and sapling architectural traits are just the ends of a continuum growth trajectory, and even two species with identical values for these traits can still diverge in many ways. Foliage, e.g., can be distributed in such a way that minimizes competition among neighboring trees, even if they have similar adult heights. As a matter of fact, this may occur with saplings too, and although we found no evidence for it, the great plasticity of architectural traits may have prevented us from detecting any patterns predicted by the optimum space filling hypothesis (negative spatial autocorrelation). This complementarity in foliage distribution could explain within-strata coexistence [155], but it would require a tremendous sampling effort [57]. As Lidar technology becomes more accessible, we will soon be able to 3-D scan the forest [181],



Figure 3.5: The many evolutionary contingencies in plant development and the solutions plants have found. (a-b) Plants with simple, opposite leaves, like *Miconia* (Melastomataceae), can either (a) arrange their leaves in a plane, such as *M. Longispicata*, which requires horizontal branches, or (b) they can twist their branches to produce a decussate phyllotaxy, such as *M. Splendens*. Both strategies have profound consequences for plant architecture as can be seen. (c-d) Trees often have to alter their strategies as they grow, as can be seen for *Hevea guianensis* (Euphorbiaceae). When young, they can simply rely on long petioles to spread their leaves (c), but as they reach a critical size they start launching long vertical branches (d). There are of course many other growth strategies. (e) Plants with large bipinnate leaves can also be arranged in horizontal branches, although the result seems a bit odd, as in this *Stryphnodendron pulcherrimum* (Fabaceae). (f) Another very common strategy in this forest is to grow by stacking tiers of branches (pointed by the arrows) that are widely separated from each other to avoid self-shading, like in this *Iryanthera* sp. (Myristicaceae).

but this will only help discern tree species niches if trees can be individualized within the cloud of points generated. In the meantime, investing into an integrative framework including other known traits (wood density, seed size, etc) will be fundamental to understand other important niche dimensions of these species. Lastly, a large enough collection of studies like this one has been produced that allows for intersite comparisons [182]. Some pressing questions are: Why do we find adult-sapling coupling at some sites, but not others? Is it related to the number of tree species or the forest latitude? Are these contrasting findings the result of bias in choosing the species that were sampled?



Figure 3.6: Light beams trespassing the forest canopy close to dusk. The visual effect is produced by barbeque smoke at the Km 41 camp. Near the equator, light incidence angle during a single day can vary as much as during the whole year in higher latitudes.

Chapter 4

Growth-reproduction trade-offs

4.1 Introduction

Tropical forests can harbor not only an immense diversity of plant species, but also great functional diversity [74]. Among the most apparent traits is plant size, which can vary from mosses growing on fallen logs all the way to giant emergent trees growing above the forest canopy. How all this taxonomic and functional diversity is maintained is still a very elusive question in Ecology. And it is an especially intriguing question in the case of plants because they have to rely on the same small set of resources to survive, grow, and reproduce [64]. Because diverging on the types of resources used is not an option, plants have to diverge in the ways they acquire and use these same resources [40, 42, 58, 64]. One major axis of variation is defined by plant life history, ranging from fast-growing, short-lived herbs to long-lived, slow-growing trees [183]. Even among trees, which are the most important contributor

to the plant diversity of most tropical forests, we can still find a very wide variation in life histories, with some pioneer species living < 40 years (*Cecropia obtusifolia*)[184] and giant emergents living more than 1,500 years (*Cariniana micrantha*)[185]. As it can be seen from these examples, the life histories of tropical trees are often closely related to their maximum size. To understand how the diversity of maximum sizes is maintained in these forests, however, we first need to understand the genetic constraints and environmental context that drive the evolution of tree size. A major factor seems to be the timing, and therefore the size, at which trees switch from juvenile to sexually mature.

If the onset of maturity in trees is a genetically determined response to illumination cues, then it should be subject to evolution. The evolution of this reproductive trigger, in turn, will be restricted by the environmental context in which trees evolve. In a forest, for example, having a low light threshold will result in a tree that can start reproducing at an early age, but that is still shaded by taller neighbors. Furthermore, because the resources allocated to reproduction are finite, especially photosynthates and soil nutrients, they will not be able to be invested elsewhere [186]. These competing demands become increasingly more dramatic as resources become more limiting, to the point that reproduction may come at the cost of vegetative growth [187]. Therefore, in shaded habitats such growth-reproduction trade-offs may cause tree growth to halt, sentencing trees that mature prematurely to a life in the forest understory. On the other hand, trees with higher light thresholds will forfeit early sexual maturity while still in the shade and may thus continue growing towards better-lit heights. Therefore, as long as there is a vertical light gradient, changes in the light threshold

that triggers sexual maturation should result in changes in tree size.

If trees with higher light thresholds can grow larger and taller, they should have a competitive advantage for light over neighbors with lower light thresholds [57]. With crowns fully exposed to the sun, these large trees will have plenty of energy to reproduce frequently and in abundance [154]. This higher fecundity should cause trees to engage in a vertical arms race, with taller species replacing shorter ones and causing forests to be as tall as possible [83]. Even in the tallest forests, however, we can still find a huge variation of tree sizes, from small treelets in the understory all the way to the tallest, emergent trees that rise above the forest canopy [83]. How can then this diversity in tree size be maintained? We hypothesize that smaller tree species have a demographic advantage over larger species: by starting to reproduce earlier than larger species, these short-statured trees should have shorter generation times and thus faster population growth rates. Therefore, if the fecundity advantage of large trees is offset by the shorter generation times of small trees, we could have a demographic trade-off capable of reducing otherwise large fitness differences between large and small trees. This particular fitness equalizing mechanism would add to several others that have been proposed, but even if there were no fitness differences among these species, stable coexistence would still not be possible theoretically [39].

The most interesting aspect of the mechanism proposed here is that it can also promote species niche differences. As species diverge in their light thresholds, they may tend to reproduce earlier or later in their growth trajectory along vertical light gradients. When a tree starts reproducing, especially if it is still in the shade, growth becomes increasingly slower,

thus defining the tree's vertical position in the forest [122]. Therefore, while prematurely reproducing species should occupy the forest understory, trees with delayed reproduction should occupy higher strata. Then, because species within the same strata tend to compete more intensely for light [167], any divergence in species' adult height should promote niche differences among these species. If these niche differences are larger than fitness differences between differently sized species, then stable coexistence would be possible [39].

We tested these ideas in a hyperdiverse tropical forest with a wide range of tree adult sizes. Our main hypotheses are that: 1) the demographic trade-off between fecundity and generation time acts as a fitness equalizing mechanism between large and small tree species; and 2) variation in light thresholds determine species' adult size, thus promoting niche differences between them. We predict that, if the proposed mechanisms are important for coexistence, then taller species should reproduce more frequently than smaller ones, but would also only reach maturity at much larger sizes. To test these predictions, we recorded monthly occurrences of reproductive events during three years for 626 trees found in a forest in the Central Amazon. Using hierarchical Bayesian analysis, we then modeled these reproductive events as a function of tree current and maximum size. With these species-specific models we could then estimate the size at the onset of reproduction and maximum probability of reproduction for each of the 261 species sampled. Together with strong evidence supporting our hypotheses, we show how our robust statistical framework can be used to compare the studied forest with other sites with comparable data. Such inter-site comparisons would allow us to ask more interesting questions such as the effects of soil fertility on the diversity

of reproductive strategies or how reproductive trade-offs relate to forest diversity.

4.2 Methods

Study site and sampling design

The study was carried out in the KM41 reserve ($2^{\circ}24'26''\text{S}$ $59^{\circ}43'40''\text{W}$), one of the control sites within the area of the Biological Dynamics of Forest Fragments Project (BDFFP) in the Central Amazon. Temperatures in the reserve range from $35\text{-}39^{\circ}\text{C}$ to $19\text{-}21^{\circ}\text{C}$, with an annual mean of 26.7°C , and annual mean precipitation is 2200 mm with a dry season from June to October [136, 188]. This area is covered by a pristine, non-flooded, lowland forest, with a complex vertical structure and a canopy height of 30-37 m, although emergent trees may reach 55 m [70]. Several 1-ha plots have been established in this forest and all trees ≥ 10 cm of stem diameter (D) were identified, resulting in one of the highest tree diversities ever recorded: 226-329 species per hectare [70, 189]. This forest diversity contrasts with the very infertile and acidic soils of the plateaus [190], where the four 50x50 m subplots used in this study were located. These subplots were > 200 m apart from each other, and contained in total 535 trees from 233 different species.

Data collection

To quantify the reproductive potential of each tree, we monitored the inventoried trees between November of 2017 and January of 2021. During this period we kept a monthly record of the presence of flowers and/or fruits on the tree crown (reproductive events). This data was later converted to a binary variable (R) indicating whether a particular tree had any evidence of reproductive events ($R = 1$) or not ($R = 0$) during the entire period. Stem diameter (D) was measured at breast height and in the first months of the monitoring period. We also estimated maximum size (D_{max}) for each of the species studied as the 95% quantile of all the trees from that species found in a nearby 25-ha plot [21]. In order to make species with contrasting D_{max} comparable, instead of D we used the relative measure $D_{rel} = D/D_{max}$ to describe each tree's current size.

Statistical analysis

In order to model how probability of reproducing, or $p(R = 1)$, changes ontogenetically, we fitted species-specific logistic regressions ($p \sim D$) using a hierarchical Bayesian (HB) approach. HB was the most appropriate analysis in our case because our sample had several species, most of them undersampled ($N < 10$). In this case, a HB approach allowed us not only to use all the information available in our data, but it also gave us the modeling flexibility to include the effects of species maximum size (D_{max}). Other advantages are that a HB analysis provides a straightforward way of making predictions and propagating uncertainties,

which is essential to scale up the estimated reproductive potential of individuals to that of the whole community. We fit the HB model using three Monte Carlo Markov Chain simulations and the Gibbs sampler provided by JAGS [93]. All the analyzes, however, were done through R v.3.5.3 [92], using the `rjags` package [139]. To improve the convergence in the MCMC simulations, we determined the prior distribution of each parameter using the ranges of observed variables (range method; see supplementary material for chapter 4). MCMC convergence was diagnosed with the `coda` package [94]. Below, we provide a more detailed explanation of the model we used.

Individual tree model

For each tree i from species j , sampled in plot l , we first modeled reproductive events (R_{ijl}) as a random sample from a Bernoulli distribution as follows:

$$R_{ijl} \sim \text{Bernoulli}(\pi_{ijl} \times \kappa_j) \quad (4.1)$$

where κ_j is a species-specific scale parameter constrained between zero and one that defines species j maximum probability of reproducing (P_{max}), and π_{ijl} is the expected probability of reproducing of tree i . π was further modeled as a function of the tree's current size (D_{ijl}) as follows:

$$\text{logit}(\pi_{ijl}) = \zeta_l + \beta_j + \alpha_j \times \log_e(D_{rel_{ijl}}) \quad (4.2)$$

where ζ_l is the plot location random effect, β_j is the species random effect (in practice they represent p of a tree from species j with $D_{rel} = 50\%$), and α_j is the fixed effect of D_{rel} on p .

Species model

Combined, α_j and β_j can provide a metric of reproductive threshold (D_{crit_j} ; [122], i.e., the size at which 50% of P_{max} is achieved (the inflection point of the logistic curve):

$$D_{crit_j} = \exp\left(\frac{-\beta_j}{\alpha_j}\right) \quad (4.3)$$

While ζ_l was simply modeled as a random sample from a normal distribution centered at zero, $\zeta_l \sim \mathcal{N}(0, \sigma_z^2)$, the species-specific parameters (κ , β , and α) were further modeled as a function of species' D_{max_j} as follows:

$$\kappa_j \sim \mathcal{N}(\theta_k + \phi_k \times D_{max_j}, \sigma_k^2) \quad (4.4)$$

$$\beta_j \sim \mathcal{N}(\theta_b + \phi_b \times D_{max_j}, \sigma_b^2) \quad (4.5)$$

$$\alpha_j \sim \mathcal{N}(\theta_a + \phi_a \times D_{max_j}, \sigma_a^2) \quad (4.6)$$

where θ s are the intercepts (representing the species-specific parameters for median-sized species), ϕ s are the slopes (effects of D_{max} on the species-specific parameters), and σ^2 s are the residual interspecific variation.

4.3 Results

At the end of 3-year period of monitoring, a total of 255 trees had at least one reproductive event, meaning they had already reached reproductive maturity. Among these mature trees, 45% flowered, but only 36% fruited. The average proportion of mature trees was 48%, although across plots this figure varied considerably (47-59%). Out of the 233 species in our subplots, 93 had no reproductive individual in the period, while 78 species had all their individuals reproducing; the median proportion of reproducing individuals was 50%. Size of the sampled trees ranged from 10-100 cm in stem diameter (D ; median = 16.1 cm), while species maximum size (D_{max}) ranged from 10.3 to 210 cm (median = 33.4 cm). D and D_{max} varied in such a way that D relative to their D_{max} (D_{rel}) range from 11 to 100% (median = 53%).

Diversity of reproductive strategies

Species varied widely in their reproductive threshold (D_{crit}) and on their maximum probability of reproduction (P_{max}). Unsurprisingly, all species showed a significant positive reproductive response to size (α), i.e., the predicted probability of reproduction (\hat{p}) always

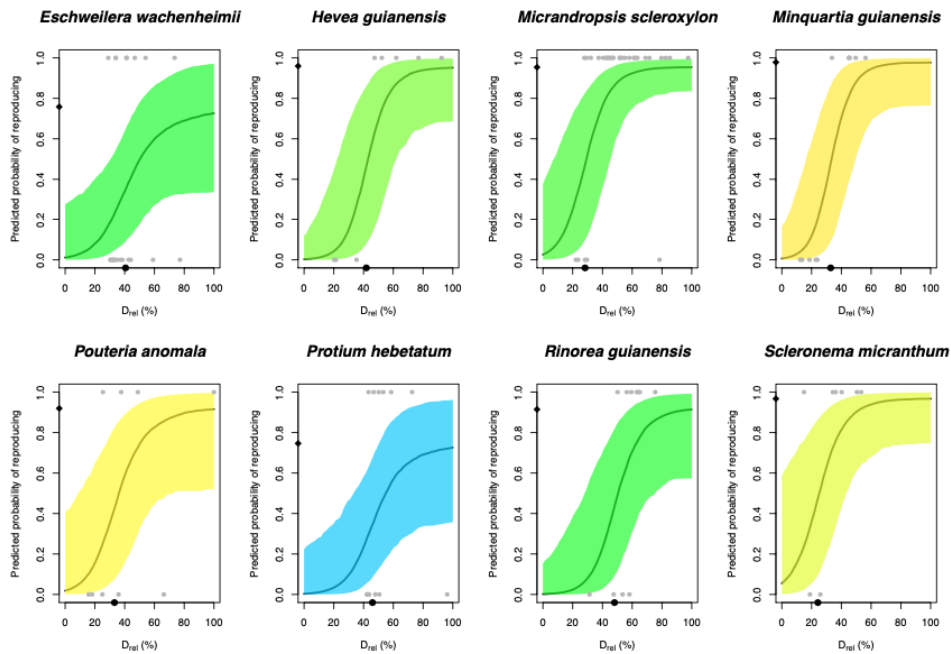


Figure 4.1: Predicted probability of reproduction as a function of trees' diameter at breast height (D) for each of eight common species in the studied forest. D is given as a percentage relative to a species' maximum D (D_{max}) to make species's curves comparable. The 95% credible envelope is represented by the shaded areas. Raw observations were binary (1 = reproductive trees; 0 = non-reproductive trees) and are represented by grey dots. The maximum probability of reproduction (P_{max}) is represented by a black diamond on the y axis, while the the critical D at which half of P_{max} is achieved (D_{crit}) is represented by a black dot on the x axis. Hotter colors represent larger species (legend in Fig.4.2).

increases with a tree's size, but α itself varied little among species (Tab.D.1). The other two parameters (β and κ) varied much more across species (Tab.D.1) and were responsible for the great diversity of reproductive responses seen here (Fig.4.1-4.2). Although also largely variable (13-68%), D_{crit} was about half the D_{max} for most species (median = 48%), while P_{max} ranged from 3.5 to 99.9% (median = 85%; Tab.D.1). Interestingly, while some species such as *Hevea guianensis* and *Miquartia guianensis* had a very sharp threshold, in species like *Eschweilera wachenheimii* and *Protium hebetatum* this threshold was not so well-defined

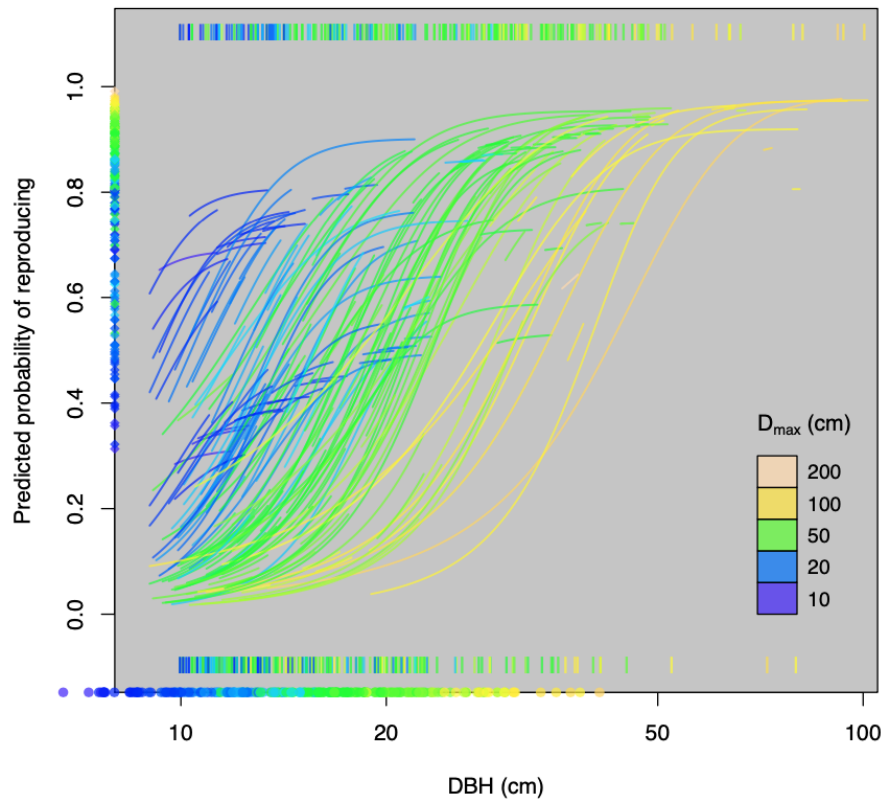


Figure 4.2: Predicted probability of reproduction as a function of tree’s diameter at breast height (D) for the average species and for the most common species. The maximum probability of reproduction (P_{max}) is represented by diamonds on the y axis, while the the critical size at which half of κ is achieved (D_{crit}) is represented by dots on the x axis.

(Fig.4.1). This happens because for *Hevea* and *Minquartia* reproductive events were only observed in trees whose D were larger than the species’ D_{crit} , while for *Eschweilera* and *Protium* this is clearly not the case, with many instances in which trees smaller than D_{crit} have already reproduced (Fig.4.1).

Species' maximum size effects

Species reproductive strategies were clearly affected by their potential maximum size (D_{max}). D_{max} had a positive effect on species-specific parameters, but this effect was only significant for β and κ (Tab.D.2, Fig.D.1a-c). These D_{max} effects resulted in larger reproductive threshold sizes (D_{crit}) for large species compared to small species (Fig.4.2,D.1e). Interestingly, the pattern is reversed when species' D_{crit} was analyzed in relation to their D_{max} , as larger species may already start to reproduce with less than a third of their potential final size (Fig.D.1d). More importantly, the maximum probability of reproducing (P_{max}) increases linearly with D_{max} , but it starts to level off as D_{max} reaches ca. 50 cm (Fig.D.1c). Understory species ($D_{max} \leq 20cm$) were clustered into two groups, one with high and the other with low P_{max} . The formation of the group with the lower P_{max} can be explained by the lack of reproductive individuals of some species in our sample, which further demonstrates that reproduction of smaller species is not as consistent as it is for larger species.

Size-mediated demographic trade-off

Species reproductive thresholds (D_{crit}) were tightly correlated to their maximum probability of reproduction (P_{max}), and this relation is clearly mediated by species maximum size (D_{max}). If on one hand large species have to grow to larger sizes to reach their reproductive threshold (large D_{crit}), on the other hand they reach higher P_{max} compared to smaller species (Fig.4.3). The correlation between species point estimates for D_{crit} and P_{max} was 0.21 ($p(\rho > 0) = 0.91$)

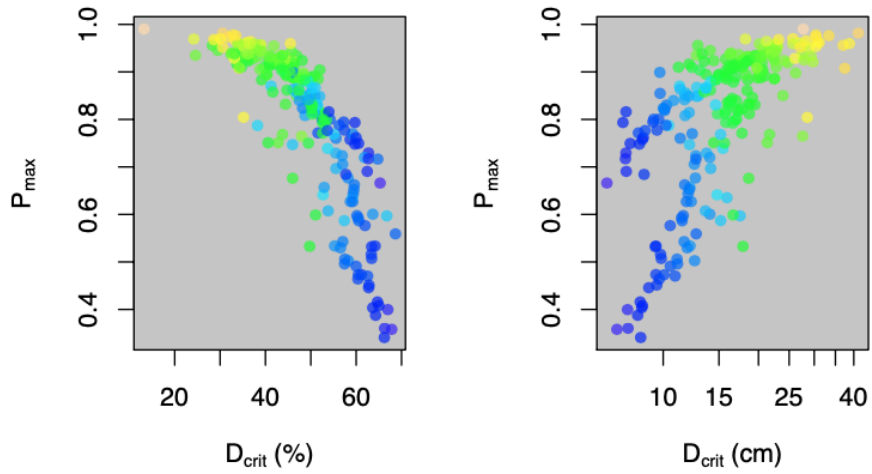


Figure 4.3: Trade-off between critical size (D_{crit}) and the maximum probability of reproduction (P_{max}). D_{crit} is shown both as a measure relative to species maximum size (D_{max}) in the left, and as an absolute measure in the right. Colors represent D_{max} and follow the legend in Fig.4.2.

for absolute D_{crit} and -0.16 ($p(\rho > 0) = 0.09$) for relative D_{crit} .

Whole-stand reproductive potential

After fitting $p \sim D$ curves for all species, we could predict the probability of reproduction of each tree in each of the four subplots used in this study. When looking at all trees, irrespective of their species, two patterns become clear: 1) the vast majority of trees are small ($D < 20$ cm); and 2) the probability of reproduction increases sharply with size, especially for trees larger than 20 cm (Fig.A.1a). Interestingly, the distribution of p across all trees is close to a uniform distribution, with a peak at very low probabilities ($p < 0.2$), one at intermediate probabilities ($p \sim 0.5$), and another one at very high probabilities ($p > 0.8$; Fig.A.1b). While the first peak can be explained by the dominance of small and immature

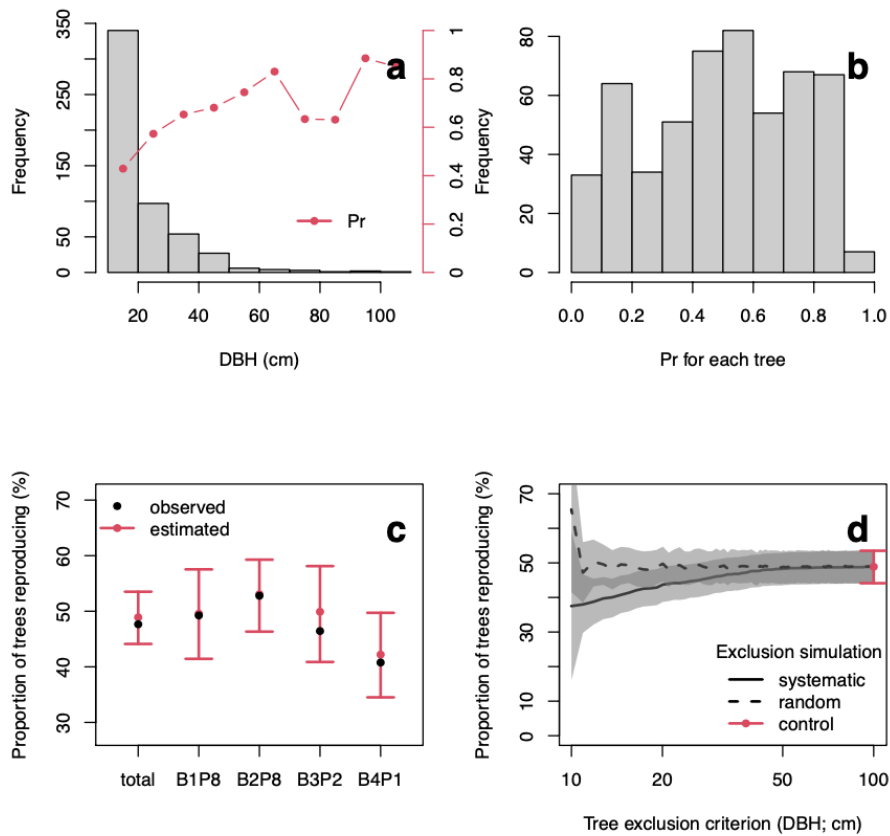


Figure 4.4: Reproductive potential of the whole forest stand depends on the distribution of tree size (D) and the probability of reproducing ($p(R = 1)$) of each size class. Because most trees are small ($D < 20$ cm) and p increases with tree size (a), the distribution of p for individual trees resembles a uniform distribution (b). From the model predictions it is possible to estimate the proportion of all trees in the forest that are already sexually mature across the subplots used in this study (c). Simulations of systematic tree exclusion based on trees' size confirm the importance of the most abundant size classes ($D = 10$ -50 cm) when compared to random exclusion simulations (d).

trees, the third peak can only be explained by the sum of the few large and many small, yet reproductive trees. Another interesting stand property that we could derive was the expected proportion of mature trees (P) in all four subplots combined and in each subplot separately (Fig.A.1c). This gives us an idea of how low P can be ($< 50\%$) and how P can vary across space. Finally, tree exclusion simulations show a somewhat surprising finding: although the largest trees are the ones most likely to reproduce, it is only after removing the smaller ($D < 30\text{ cm}$), and thus most abundant ones that P starts to decrease compared to random simulations (Fig.A.1d). In any case, it is important to remember how low the potential of reproduction of the tree community as a whole is.

4.4 Discussion

We had hypothesized that the resource allocation trade-off between growth and reproduction could contribute to the maintenance of tree species diversity in tropical forests. We then proposed two mechanisms that could make coexistence more likely, namely, a trade-off between fecundity and generation time (fitness equalizing mechanism), and species divergence into contrasting vertical niches (stabilizing mechanism). By studying a hyperdiverse forest in the Central Amazon and modeling tree reproduction as a function of their size, we could test the potential strength of these mechanisms. Indeed, we found strong evidence in favor of both of these mechanisms: 1) there was a strong correlation between the size at the onset of maturity (D_{crit}) and maximum probability of reproduction (P_{max}), as it was expected under

a fitness equalizing demographic trade-off; and 2) species maximum size (D_{max}) was closely related to their D_{crit} , meaning that the ontogenetic timing of sexual maturation may define a species D_{max} and thus its position along the forest vertical light gradient.

The physiological mechanisms that trigger the onset of maturity in plants are not well understood for plants in general, let alone for tropical trees, but our findings can shed some light on this issue. These phase shifting mechanisms vary across species and can be driven by internal cues, such as size and age, external cues, such as light quality, or a combination of both internal and external cues [191]. Because a tree's exposure to light often increases with its size and thus age, it is very difficult to disentangle these two factors in natural settings. Nevertheless, we can speculate the cost-benefit of each of these mechanisms. While exogenous regulation may give the tree the ability to exploit surges in resource availability, as when a gap opens in the forest (opportunistic strategy), it may also risk a tree's future performance if this gap closes rapidly. Conversely, endogenous regulation likely sets a more strict growth trajectory for the tree, which may allow it to grow taller and get more exposed to light as an adult, but this comes at the cost of losing opportunities along the way (bet-hedging). Of course the optimum strategies will depend on disturbance frequency [146], which is very low for the studied forest [136], and on the vertical light gradient, which can be very sharp in tropical forests [153].

In the studied forest, tree size was associated with reproductive strategies, with short-statured trees being more opportunistic and tall species adopting bet-hedging strategies. In a forest where canopy gaps are rare and ephemeral, and where the understory is deeply

shaded, short trees may experience full light only once in a lifetime, and they may take this opportunity to reproduce. Of course this precocious maturation will come at the cost of future growth, survival and even reproduction [192], which is also supported by our results (small trees had lower reproductive potential than taller ones). Canopy and emergent trees, on the other hand, may take advantage of these gaps to grow faster towards the canopy where it can have unlimited access to full light. This bet-hedging strategy, however, is quite risky, especially considering the relatively high risk of mortality of these trees, which causes most trees to die before reaching sexual maturity [193]. These ideas were confirmed by our analysis, which shows that as trees approach a size of 50 cm in stem diameter, which roughly corresponds to a tree that is as tall as the studied forest canopy (30-35 m), the reproduction potential nears 100%. This means that further growth in size will have diminishing returns for the plant, thus making further delays in reproduction disadvantageous. In fact, once trees reach the canopy they become susceptible to new threats, such as lightning, droughts, and strong winds that can cause their mortality [28, 29]. Our results also support the increased costs and risks of delaying reproduction after reaching the canopy: no species had a reproductive size threshold > 50 cm.

Perhaps the most important of our findings was the confirmation of the demographic trade-off between reproductive potential after reaching sexual maturity and how fast sexual maturation can be reached. We found that almost all adult trees from large species in the study area reproduced during the period considered, but that even the largest trees from small species were unlikely to reproduce ($p < 0.4$; Fig.D.2). This information adds to the

already known fecundity advantage of large trees that comes from full sun exposure [57, 154]. Moreover, if we assume that growth rates of immature trees in the shade are not widely different between understory and canopy species, then generation times for small species should be much shorter compared to large species. These shorter generation times may compensate for the less consistent reproduction schedule of smaller species, thus defining a size-mediated growth-reproduction trade-off. Other similar trade-offs have been proposed, such as the one between the high fecundity of large trees and the high recruitment rates of small trees [154, 194], or the one between the high light interception efficiency of large trees and the high light use efficiency of small trees [57]. Together these equalizing trade-offs may help to reduce fitness differences among large and small species, thus making their coexistence more likely [39].

Of course species do differ in their growth rates as immature trees growing in the shade, further complicating species coexistence. A great deal of these interspecific differences in growth rates can be attributed to variation in wood density, which also may confer species higher survival rates [195, 196]. Wood density, therefore, defines a demographic trade-off between growth and survival, which has been shown to be important in tropical forests, although per se they are insufficient to explain the high diversity of tropical trees [78, 197]. The consideration of another trade-off axis, however, may greatly improve our understanding of tropical tree diversity. The so-called stature-recruitment trade-off [84] describes a trade-off that seems to align to the trade-off described in this work. We argue, though, that instead of stature per se, this trade-off axis is defined by generation time, which in turn correlates with

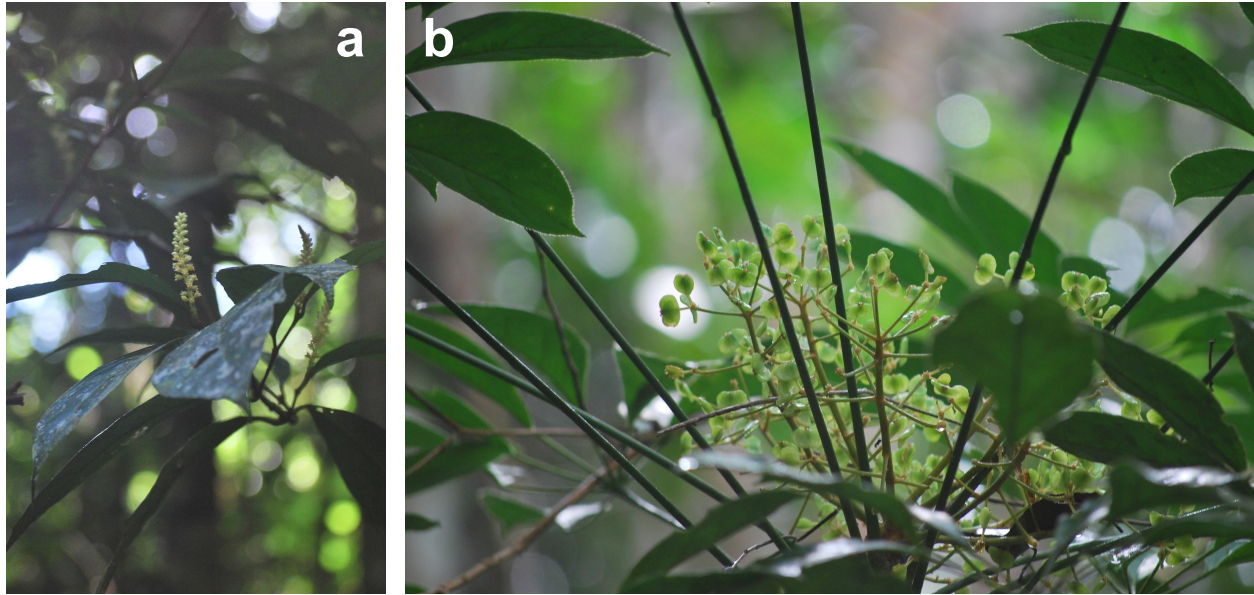


Figure 4.5: Contrasting reproductive strategies between pioneer and shade-tolerant trees. (a) Finding reproductive individuals in the shaded understory of the forest, such as this *Rinorea macrocarpa* (Violaceae), is quite a rare sighting. Understory species not only reproduce less often, but also less intensely than canopy species, as can be seen by the modest and scarce flowers in the photograph. (b) On the other hand, pioneer species, like this *Didymopanax morototoni* (Araliaceae), have enough energy to reproduce while still growing. The plant shown here still has the leaves typical of juveniles, yet it is already fully mature.

species' adult sizes, as shown here. Similar to other classification schemes [53], these two axes define four main types of tree species: short-lived pioneers, short-lived shade-tolerants, long-lived pioneers, and long-lived shade-tolerants (Fig.4.5). These two main trade-off axes may not be completely independent though, as the size at the onset of maturity can be negatively related to both wood density [198] and shade-tolerance [199]. If this is true, then long-lived pioneers should make up most of the canopy and emergent trees in a forest, and short-lived shade-tolerants should dominate the understory.

The most interesting insight deriving from this work is that allocation trade-offs between growth and reproduction may result not only in demographic trade-offs, but also in the

determination of species' vertical niches. If species with contrasting reproductive strategies have low fitness differences, but occupy contrasting niches along the vertical light gradient of the forest, as shown here, then they are more likely to coexist [39]. This coexistence mechanism could also explain the maintenance of the wide range of adult tree sizes often found in tropical forests [83]. The mechanism has also interesting consequences for the evolution of tree size: if the fitness of species with different reproductive strategies does not vary widely, then the evolution of tree size may be less restricted; if there are some optimal points along the vertical light gradient [167], then divergent selection would promote the diversification of tree adult sizes. Indeed, adult size may vary substantially within Amazonian tree genera [200], mostly due to small trees branching out of large tree lineages than vice-versa [201]. In poplars, e.g., genetic manipulation of a single gene was capable of inducing juveniles to flower [202], indicating that speciation through neoteny may just take one evolutionary step. Moreover, shorter species with shorter generation times, such as *Inga*, may undergo rapid diversification [203], thus responding to a significant amount of tree diversity in tropical forests. Therefore, the mechanism described here based on a simple allocation trade-off may be a cornerstone of both diversity maintenance and production.

As future directions we would like to offer a few suggestions. We have shown here that with the analytical framework we developed it is possible to extend this analysis not only to those other forest sites for which we have comparable phenological data, but also to sites where we only have diameter distribution data. By comparing multiple forests with varying structural complexity, gap dynamics, and tree richness, we could have a better assessment of

the ideas discussed above. An improvement to this framework that is currently underway is the inclusion of growth and mortality rates to time-calibrate our inferences about generation times. Finally, it would be helpful to incorporate allometric models that relate stem diameter to tree height in order to make the results presented here comparable to those based on tree height.

Concluding remarks

It was always difficult for me to think of cases of niche partitioning in nature that did not involve some sort of resource allocation trade-off, and the four cases analyzed here further supported my initial impression. Furthermore, the general framework used here, linking allocation trade-offs to spatial niche partitioning, allowed me to have a mechanistic understanding of the ecological processes that maintain this forest's hyperdiversity. This dissertation also further demonstrates the usefulness of trait-based approaches to simplify and understand coexistence mechanisms in communities where experimentation is often unfeasible. Finally, the patterns unveiled by my sophisticated data analyzes confirm the potential of hierarchical Bayesian models to deal with the many uncertainties of dealing with extremely rare species.

Future directions

Of course this work was only a first step in describing the mechanistic links between resource allocation and spatial niche partitioning for the trees of this forest. The most obvious next

step is to include more species and other sites to see how general these patterns are (Fig.4.6), but there are other avenues that I believe could be more fruitful. Now that the general patterns are less obscure, efforts should be concentrated in testing these eco-physiological mechanisms experimentally. The Amazon forest may not seem the best model system for this experimental approach, but we do have naturally set up experiments that we can capitalize on, such as a wide range in size of treefall gaps and a varying intensity and length of El Niño droughts. The Biological Dynamics of Forest Fragments Project also offers a tremendous opportunity for this kind of approach.

This dissertation was also only a small step towards a better integration between ecology and evolution. While it is recognized that the mechanisms described here can play an important role in adaptive radiations [117, 204], a proper general framework for trait-based eco-evolutionary processes is missing. This will perhaps depend on the advance of theory as much as on further empirical work, especially studies that explore the genetic bases of the allocational decisions made by individual plants in response to internal and external cues. Understanding the link between negative genetic correlations (trade-offs) between plant life history traits and their ecological consequences (fitness equalization in homogeneous environments, niche partitioning in heterogeneous environments) could help us identify the genetic constraints that may limit the ability of local populations to adapt to rapidly changing environments. For example, populations from a widely distributed species may adapt to local climatic conditions by adjusting their above-to-belowground biomass ratio: the longer the growing season, the taller plants can get, and thus the stronger the selective pressure for

above-ground biomass allocation. Such an allocation adjustment will necessarily involve a trade-off between above and below-ground allocation, a genetic constraint that can limit the potential of plants to respond to climate warming. Alternatively, if local genetic diversity can be maintained by divergent selection on plant allocation strategies, then local populations may stand a chance against the odds of going extinct even in the presence of such genetic constraints. Naturally, the evolution of many other performance traits that are coupled with climate, such as photosynthetic rates and the timing of reproduction, must also be restricted by similar genetic constraints. Understanding the evolutionary potential of such traits will help us predict whether species can survive global change through rapid evolution of local populations or through immigration from pre-adapted populations. Predicting the fate of natural populations should be this century's priority, as we devise ways to conserve what is left of ecosystems and their essential services.

Another promising path forward is to search for more trade-offs and integrate them into a high-dimensional framework. One of the issues of trying to understand the mechanisms driving forest diversity is precisely the dismissal of the high-dimensionality of natural communities [60]. Because the framework used here is general enough to be applied to any resource allocation trade-off, and because we know there are many more similar trade-offs already described [61], the concomitant consideration of several trade-offs could potentially explain the coexistence of many more functional groups. For example, many more niches could exist if, on top of sapling and adult illumination niches being decoupled, light and soil niches were decoupled too. By the same token, temporal niches certainly exist on top of the

spatial ones described here and would greatly increase our capacity to explain why there are so many kinds of trees in the Amazon.



Figure 4.6: Epiphytes and lianas are functional groups that make up for a great deal of plant diversity in this forest. Studying them, however, is far from trivial. Their study is a frontier we have advanced little to date.

Appendix A

Supplement for chapter 1

Determination of prior distributions

Parameter means

In order to reduce the parameter space to be explored during the MCMC simulations, and thus make them converge more efficiently, we used the ranges observed in our own data. For example, to set the priors for the means of the intercept parameters (β) we calculated the mean of the range of logged values for each leaf nutrient ($\theta_N = 2.35$, $\theta_P = -0.92$, $\theta_K = 1.45$, $\theta_{Ca} = 1.10$, $\theta_{Mg} = 0.52$, $\theta_S = 1.35$). For the habitat and fixation effect parameters (γ and ϕ), however, we chose the vaguest means possible, i.e., zero.

Ranges for species-specific parameters (β and γ)

We applied the range rule for all variances, which were then transformed into precision. By this approach, we first find reasonable ranges for each parameters and use them to estimate the largest variance in those parameters, i.e., we set the priors for variance to be as vague as possible within realistic constraints. For species-specific intercepts (β), we simply calculated the ranges (R) observed across all our samples ($R_{\beta_N} = 3.12$, $R_{\beta_P} = 3.78$, $R_{\beta_K} = 3.73$, $R_{\beta_{Ca}} = 4.20$, $R_{\beta_{Mg}} = 4.26$, $R_{\beta_S} = 4.25$). As habitat type (H) is a binary variable, the widest range of γ will be twice the range of β : the highest possible value for γ is when leaf nutrient (M) is minimal in the plateau ($H = 0$) and maximal in the gully ($H = 1$), i.e.:

$$\gamma_{max} = \frac{M_{max} - M_{min}}{1 - 0} = R_{\beta}$$

By similarity, $\gamma_{min} = -R_{\beta}$. Therefore, $R_{\gamma} = 2 \times R_{\beta}$.

Ranges for across-species parameters (θ and ϕ)

As the across-species intercepts (θ) represents the averages of β and γ , they should have the same ranges ($R_{\theta_{\beta}} = R_{\beta}$ and $R_{\theta_{\gamma}} = 2 \times R_{\beta}$). To calculate the ranges of fixation effects (ϕ) we followed the same logic from the section above to find that $R_{\phi_{\beta}} = 2 \times R_{\beta}$ and $R_{\phi_{\gamma}} = 2 \times R_{\gamma} = 4 \times R_{\beta}$.

Variations and precisions

Once we had calculated the likely ranges of each parameter, we could estimate the variance of their prior distributions. We did this using the range method, which consists in assuming that the range found in the data corresponds to four standard deviations. This means that instead of using the ranges derived from our data to curtail the parameter space (domain), we only paved the way for the MCMC sampler. In other words, parameter values were allowed to be out of the ranges used to derive the prior distributions. With that, we then calculated parameter prior variances as $var = \left(\frac{R}{4}\right)^2$. We then converted variances into precisions (τ) as var^{-1} . All precisions corresponding to covariances in the variance-covariance matrices (Σ) were set to zero.

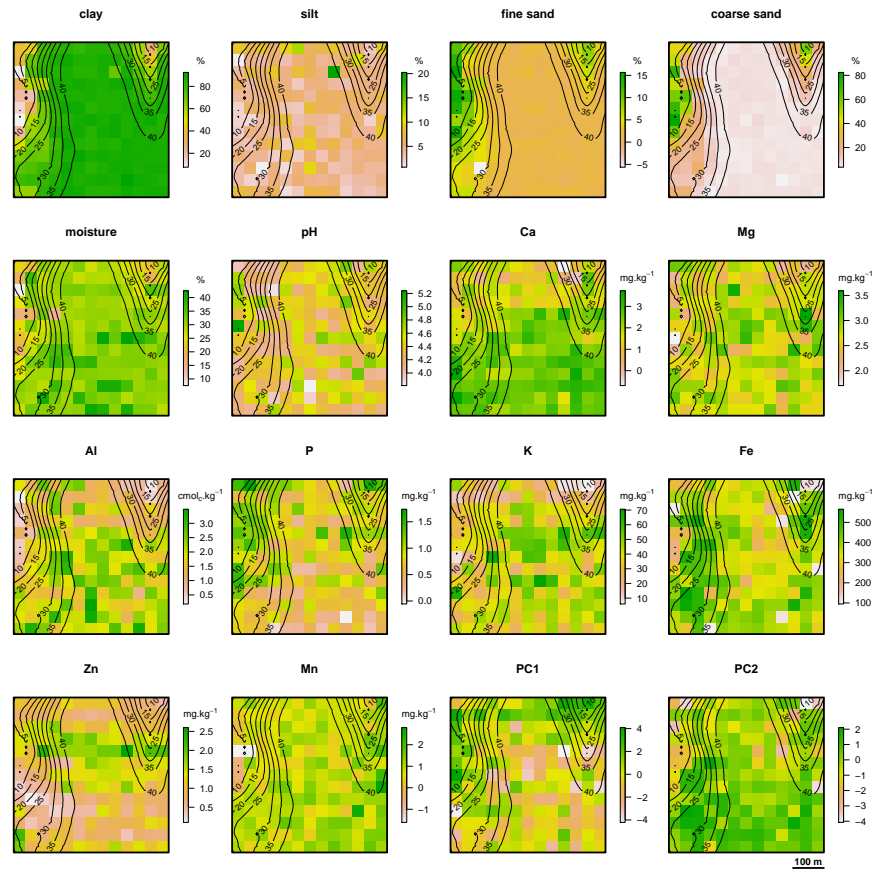


Figure A.1: The K37 permanent plot is situated on a clayey plateau cut by two sandy stream gullies. Using the lowest point within the plot as a reference, we defined the plateau as the area above 35 m of elevation (15.2 ha or 61% of the total area of the plot), the gullies as the area below 15 m (2.6 ha or 10 %), and the slope as the area in between (7 ha or 29%). The maps show soil physico-chemical properties, overlaid with elevation contours. Soil texture, represented by relative contents of clay, silt, and fine and coarse sand, were clearly associated with the topography, with gullies having much higher contents of larger soil particles. This difference results from erosion caused by rainwater runoff (podzolization). The sandy soil of the gullies cannot hold as much water as the plateau one, but the perenniality of the streams indicate that lack of water is not a problem there. Soil chemical properties, on the other hand, do not always covary with topography, like soil pH and soil contents of calcium (Ca), magnesium (Mg), potassium (K), and zinc (Zn), whereas soil aluminium (Al), phosphorus (P), iron (Fe), and manganese (Mn) were more obviously associated with elevation. Iron (Fe) was the only soil mineral that was more abundant in the slopes than anywhere else. (Contents of soil Ca, Mg, P, and Mn are shown in logarithmic scale.) Finally, we map the first two principal components that explain 50% of the variation in all soil nutrients. PC1 (34%) was negatively correlated with Al, Ca, K, Mg, Mn, and Zn, while PC2 (16%) was positively related to Fe and negatively related to P, but both PC1 and PC2 are clearly associated with elevation. In summary, the clayey soils of the plateau can retain more water and nutrients, except for P, but also contain higher, likely toxic levels of Al and Fe compared to the sandy soils of the gullies.

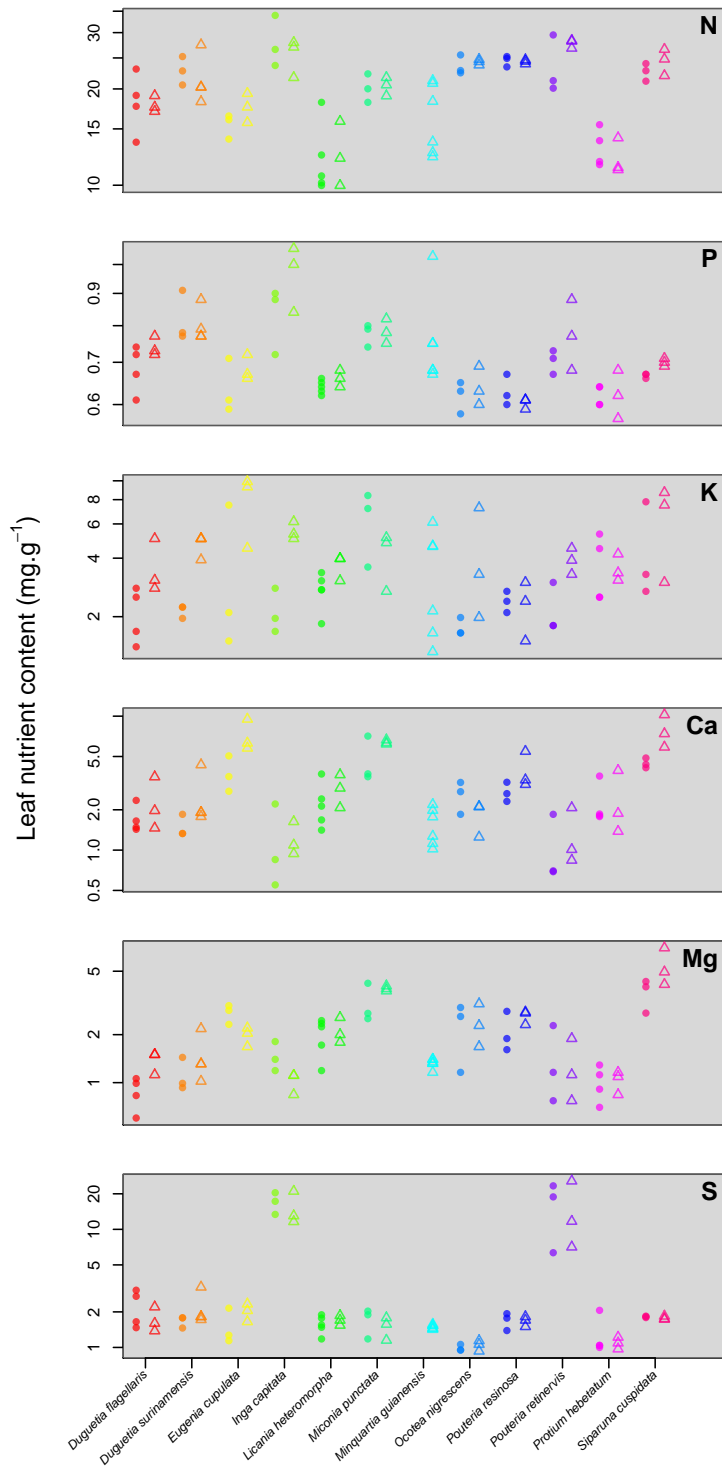


Figure A.2: Intraspecific variation in leaf nutrients for the best sampled species. Filled circles and open triangles represent plants sampled on the plateau and in the gully, respectively.

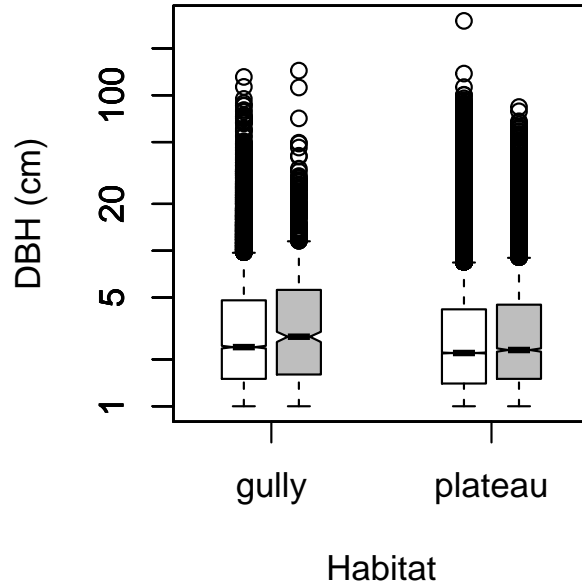


Figure A.3: Differences in tree size (stem diameter at breast height or *DBH*) between fixers and non-fixers in the plateau and in the gully.



Figure A.4: Richness, abundance, and basal area of N-fixing legumes (black), non-fixing legumes (grey), and non-legumes (white) across the three main habitats in the plot (plateau, slopes, and gullies). Values are given in relative terms to make the habitats comparable.

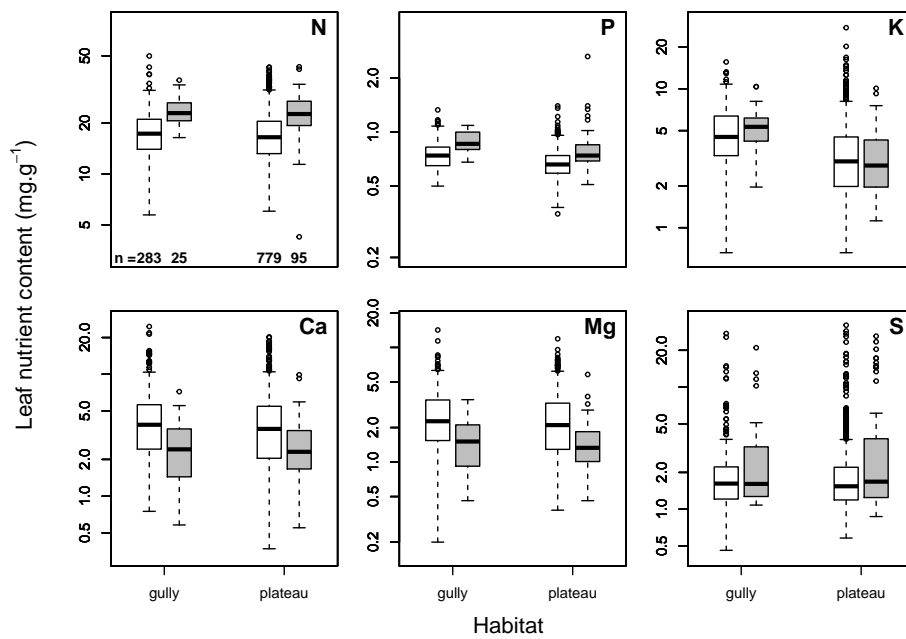


Figure A.5: Differences in leaf nutrient content between two habitats and between nitrogen-fixing legumes (gray) and non-fixing species (white). Values refer to the values that were directly quantified from the sampled leaves.

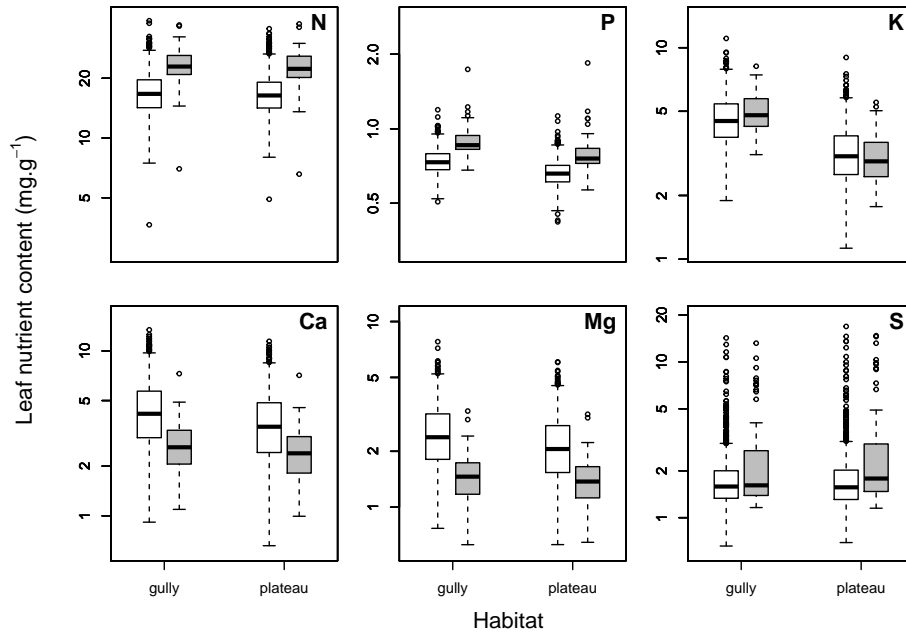


Figure A.6: Differences in foliar content of six macronutrients (N, P, K, Ca, Mg, and S) between the gully and the plateau and between nitrogen-fixing legumes (grey; 106 species) and non-fixing species (white; 872 species). Values represented by the boxplots are species-specific estimates of leaf nutrients for each habitat. The overlaid error bars represent the 95% credible intervals of across-species estimates of leaf nutrients.

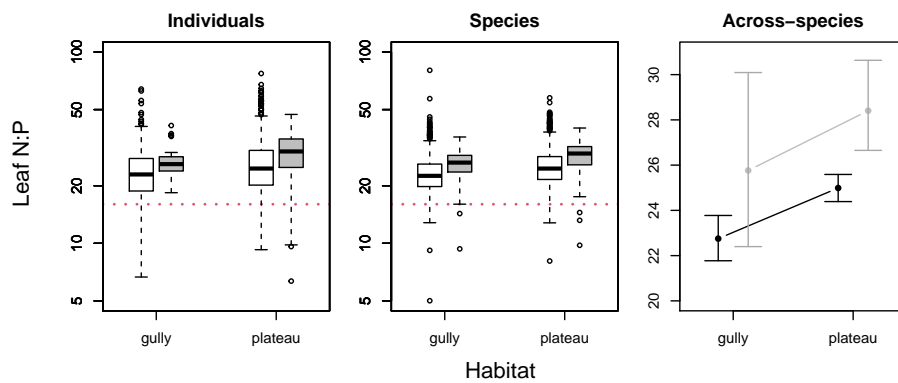


Figure A.7: Differences in foliar nitrogen to phosphorus ratio ($N : P$) between two habitats and between nitrogen-fixing legumes (gray) and non-fixing species (white). Observed values (a), species-specific estimates (b), and across-species estimates (c) of $N : P$ are contrasted with the Redfield ratio for terrestrial habitats ($N : P = 16$; dotted red line).

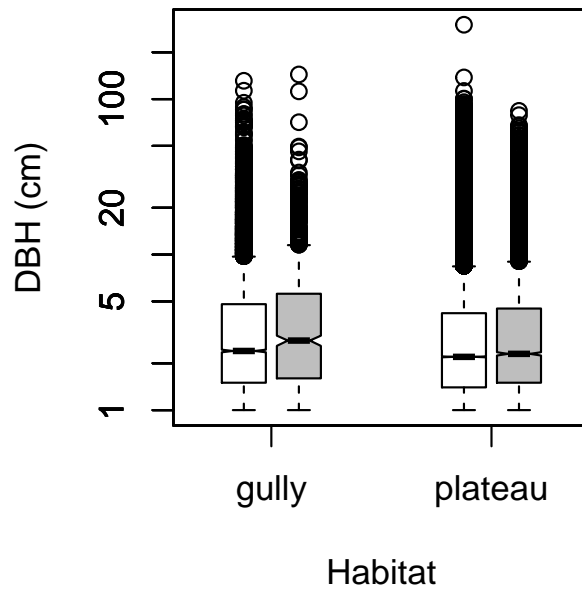


Figure A.8: Differences in tree size (stem diameter at breast height or *DBH*) between fixers and non-fixers in the plateau and in the gully.

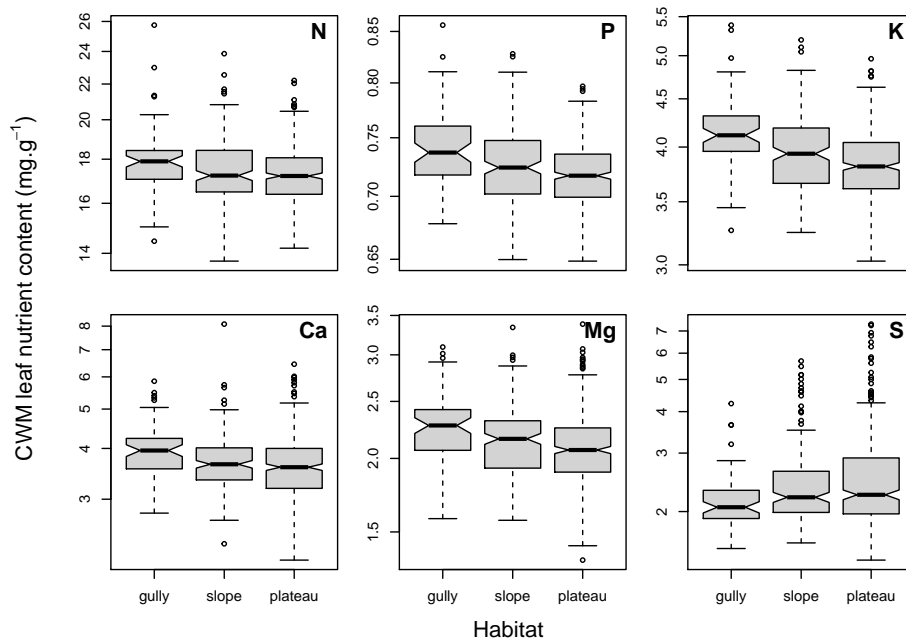


Figure A.9: Mean leaf nutrient content weighted by trees' basal area in each quadrat of each major habitat type. Values refer to community weighted means based on the point-estimates of species' leaf nutrient contents averaged across habitats.

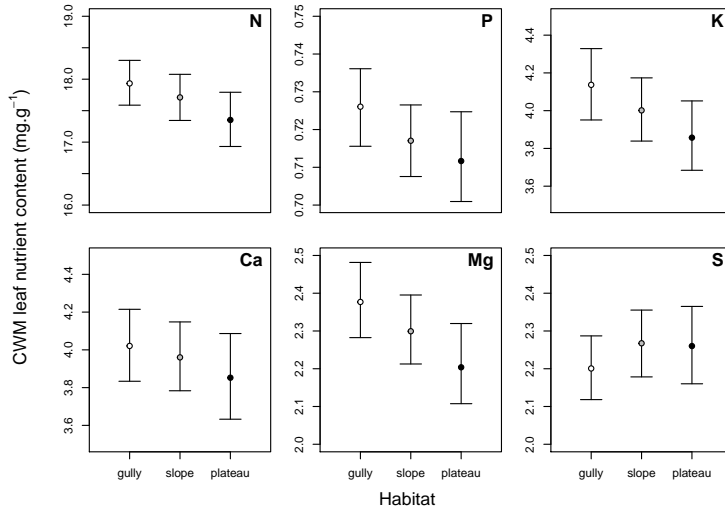


Figure A.10: Mean leaf nutrient content weighted by species' abundance in each major habitat type. Points and bars refer, respectively, to the median and 95% credible interval of the estimates of community weighted mean (*CWM*) of leaf nutrient content.

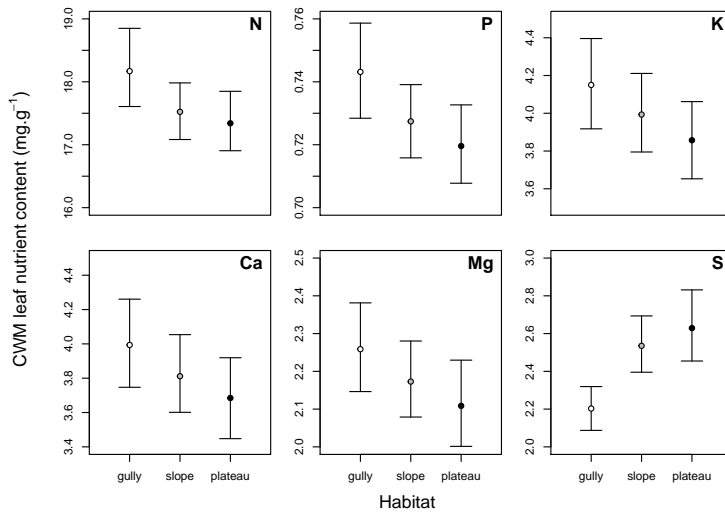


Figure A.11: Mean leaf nutrient content weighted by trees' basal area in each major habitat type. Basal area is a measure of a tree's size and a proxy of its biomass. Points and bars refer, respectively, to the median and 95% credible interval of the estimates of community weighted mean (*CWM*) of leaf nutrient content.

Appendix B

Supplement for chapter 2

Determination of prior distributions

Total leaf number model

Parameter means

The means of the prior distributions were all set to zero. This was done to avoid biasing the species-specific effect parameters ($\eta_D, \eta_L, \eta_M, \eta_S$). Because the observed leaf number was logged and then centered prior to data analysis, the prior mean for the intercept (η_0) should also be zero.

Ranges for species-specific parameters (η)

Ranges for species-specific *etas* were taken from the ranges of our own observed data. For the intercept (η_0), range was defined as the observed range of the logarithm of leaf number ($R_N = 5.88$). For the effect parameters, ranges were defined as $2 \times \frac{R_N}{R_x}$, where x is each predictor variable (D , L , M , and SLA). In this way, ranges for the remaining η s were calculated as follows: $R_{\eta_D} = 6.27$, $R_{\eta_L} = 4.70$, $R_{\eta_M} = 2.05$, and $R_{\eta_S} = 5.63$.

Variances and precisions

Variances for prior distributions were derived by the range method, i.e., $var(z) = \left(\frac{range(z)}{4}\right)^2$, where z is an observed variable or a parameter. Variances were then transformed into precisions ($\tau = var(z)^{-1}$), which resulted in the following values: $\tau_{\eta_0} = 0.46$, $\tau_{\eta_D} = 0.41$, $\tau_{\eta_L} = 0.72$, $\tau_{\eta_M} = 3.80$, and $\tau_{\eta_S} = 0.51$.

Relative growth rate model

Parameter means

Uncertainty around stem diameter measurements (D)

We assumed that there cannot be negative growth, and that all negative diametric increment is due to measurement error. Because D increment ranged roughly from -2 to 2 cm, we assumed measurement error must be ≤ 2 cm. The true value of the smallest measured D (0.624 cm) should thus be < 2.624 , but it cannot be < 0 so we assumed it to be 0.1, which is

already an unlikely low size for a plant to have been included in the plot census. (The plot census only included ≥ 1 cm plants, but due to breakage and resprout of the main stem there can be plants with a stem diameter below 1 cm.) Now the largest recorded diameter in this study was 4.073 cm, and its true value must be between 2.073 and 6.073 cm. After logging and centering D , the error variances for both the smallest and largest D , as estimated by the range method, were 0.67 and 0.07, respectively. This shows that error variance is sensitive to scale, but also that it cannot be larger than 0.67 among the sampled plants. Assuming the inverse Gamma distribution that describes error variance has a mean of 0.33, i.e., exactly in the middle of the possible range for error variance (0-0.67), then we can estimate the shape of the Gamma distribution that represents the prior for measurement precision (τ_D , the inverse of error variance). τ_D should thus have a minimum value of 1.5 (minimum precision) and a mean of 3.0. By applying the range method we have that the variance of τ_D should be:

$$var(\tau_D) = \left(\frac{mean(\tau_D) - min(\tau_D)}{2} \right)^2 = 0.56$$

with which we could then estimate the shape (α) and rate (β) parameters of the Gamma distribution, as follows:

$$\alpha = \frac{mean(\tau_D)^2}{var(\tau_D)} = 16$$

$$\beta = \frac{mean(\tau_D)}{var(\tau_D)} = 5.34$$

Uncertainty around relative growth rates (R)

Again, we assumed that R could never be negative, and thus modeled it as a random variable with a lognormal distribution, which in turn should be limited by the maximum R possible. The maximum R reported for tropical saplings ($D = 1-5$ cm) by Condit et. al [78] was $0.157 \text{ cm.cm}^{-1}\text{y}^{-1}$ at the Mudumalai plot (1992-1996). That is equivalent to a diametric increase of 4 cm over a period of 10 years for a sapling with $D = 1$ cm ($R = \frac{\log_e 5 - \log_e 1}{10} = 0.16$). Taking the same steps described in the previous section, we found that if $0 \leq R \leq 0.16$, $\text{var}(R) = 0.21$ and precision has mean 2.9 and must be ≥ 1.5 . With that we found that $\text{var}(\tau_R) = 5.45$ and, therefore, that $\alpha = 16$ and $\beta = 1.71$.

Means and ranges for species-specific parameters (δ)

We set the means for δ parameters as zero, except for the intercept (δ_0), for which we used the mean of the logarithm of R_{max} and R_{min} (-0.93). We then set the ranges for δ , as before, using the range method: $\delta_0 = 0.21$, $\delta_D = 0.43$, $\delta_L = 0.14$, and $\delta_A = 0.03$

Means and precisions for across-species parameters (ν)

We set all ν parameters to have prior means of zero, except for ν_{δ_0} , which was -0.93. From the ranges in δ and in leaf average traits and their interaction (m , sla , and $m \times sla$) we derived the ranges and variances for ν via the range method. We obtained the following precision values: $\nu_{\delta_0} = 4.67$, $\nu_{\delta_D} = 2.32$, $\nu_{\delta_L} = 7.29$, $\nu_{\delta_T} = 32.93$, $\nu_{M_{\delta_0}} = 38.32$, $\nu_{M_{\delta_D}} =$

Table B.1: Summary of the species-specific parameters fitted in this study when modeling total leaf number and relative growth rate as a function of sapling size, illumination, leaf dry mass and specific leaf area. Also shown are the 2.5% and 97.5% quantiles, and the proportion of species whose point-estimates were larger than zero.

| | Parameter | symbol | median | $Q_{2.5;97.5\%}$ | $P(x > 0)$ |
|-----------------------------|-----------------|------------|--------|------------------|------------|
| Total leaf number | intercept | η_0 | 105 | [91;123] | 0.17 |
| | size | η_D | 1.45 | [1.35;1.53] | 1 |
| | light | η_L | 0.08 | [-0.02;0.15] | 0.95 |
| | M | η_M | -0.81 | [-1.1;-0.48] | 0 |
| | <i>SLA</i> | η_S | -0.72 | [-0.84;-0.6] | 0 |
| Relative growth rate | intercept | δ_0 | 0.01 | [0.01;0.01] | 0 |
| | size | δ_D | -1.92 | [-2.02;-1.86] | 0 |
| | light | δ_L | 0.07 | [-0.1;0.27] | 0.87 |
| | total leaf area | δ_T | 0.58 | [0.2;0.95] | 0.99 |

19.07, $\nu_{M\delta_L} = 59.88$, $\nu_{M\delta_T} = 270.35$, $\nu_{S\delta_0} = 3.40$, $\nu_{S\delta_D} = 1.69$, $\nu_{S\delta_L} = 5.31$, $\nu_{S\delta_T} = 23.99$,
 $\nu_{MS\delta_0} = 0.51$, $\nu_{MS\delta_D} = 0.25$, $\nu_{MS\delta_L} = 0.80$, and $\nu_{MS\delta_T} = 3.61$.

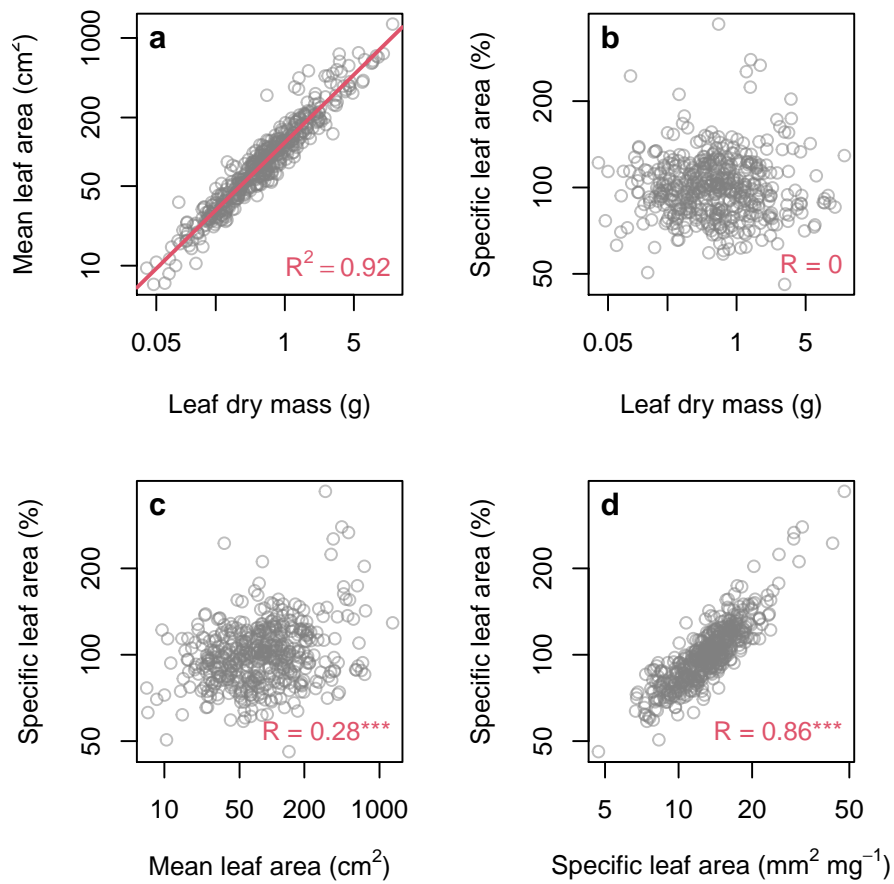


Figure B.1: Relationship among leaf area, leaf dry mass and two forms of calculating specific leaf area.

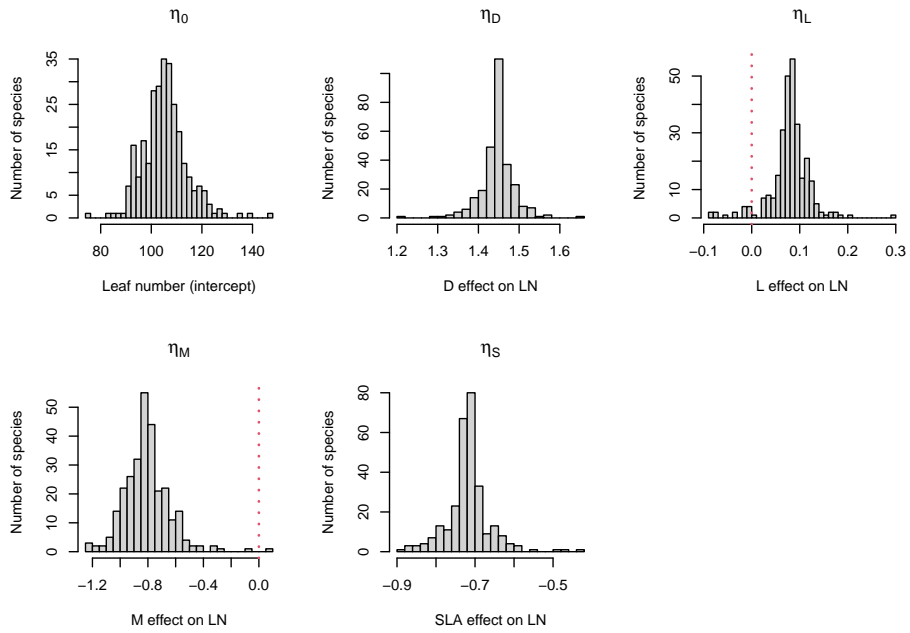


Figure B.2: Across-species distribution of the point estimates of the species-specific parameters η_0 , η_D , η_L , η_M , and η_S from eq.2.3.

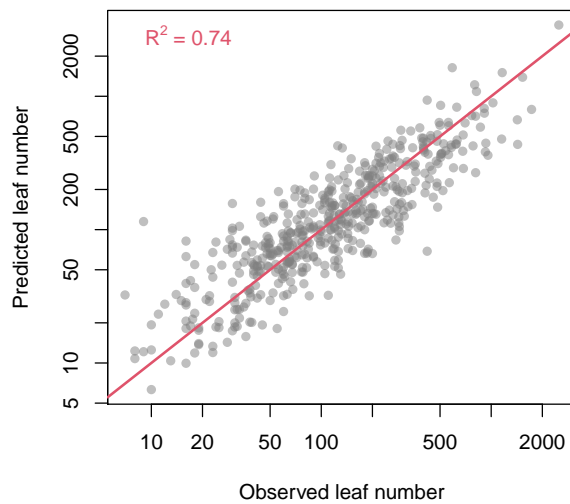


Figure B.3: Goodness of fit of the model describing total leaf number per sapling (N_{ij}). Points represent each individual sapling in our sample and the red line represents a perfect fit, i.e., if the observed N was equal to the N predicted by eq.2.3.

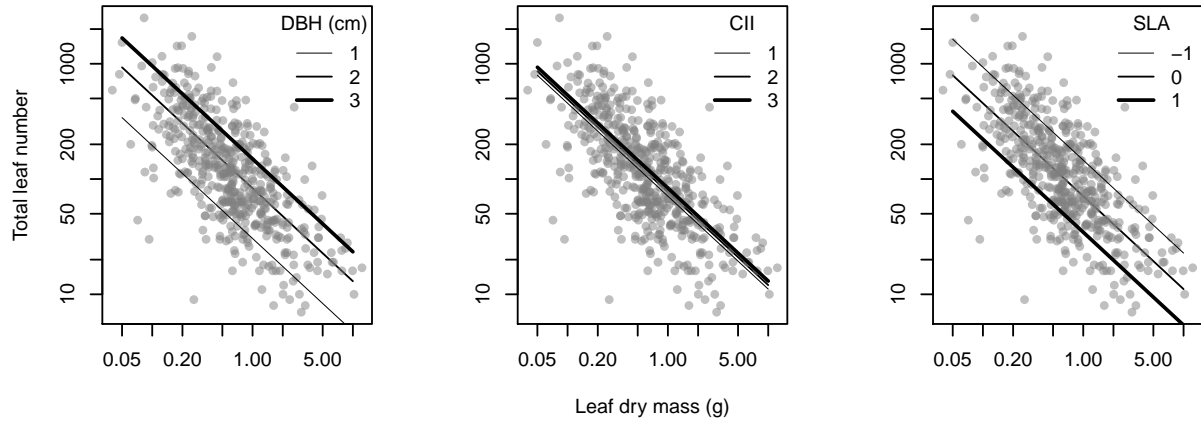


Figure B.4: General tradeoff model contrasted against observed sapling data. As expected, sapling size (*DBH*) and *SLA* had an important influence on *N*, while crown illumination (*CII*) not so much.

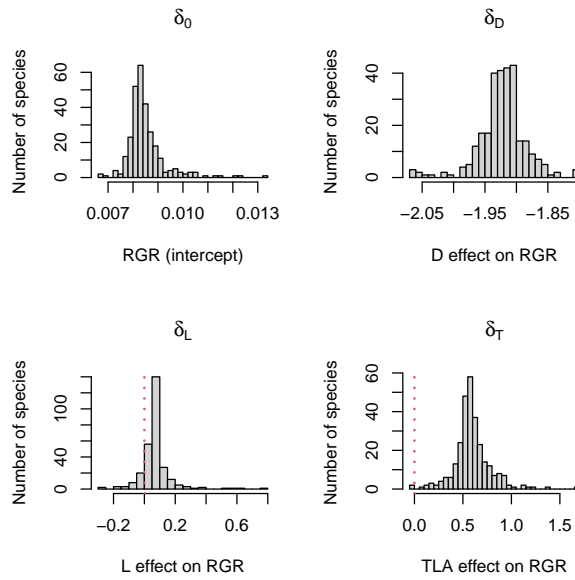


Figure B.5: Across-species distribution of the point estimates of the species-specific parameters δ_0 , δ_D , δ_L , and δ_T from eq.2.3.

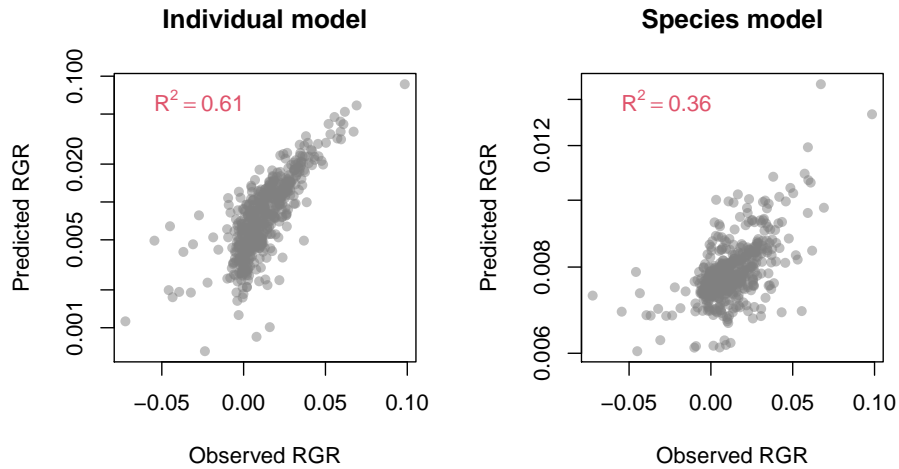


Figure B.6: Goodness of fit of the model describing relative growth rate (R_{ij}). Points represent each individual sapling in our sample and the expected R is derived by the individual-specific and species-specific models (eq. 2.6 and 2.7, respectively).

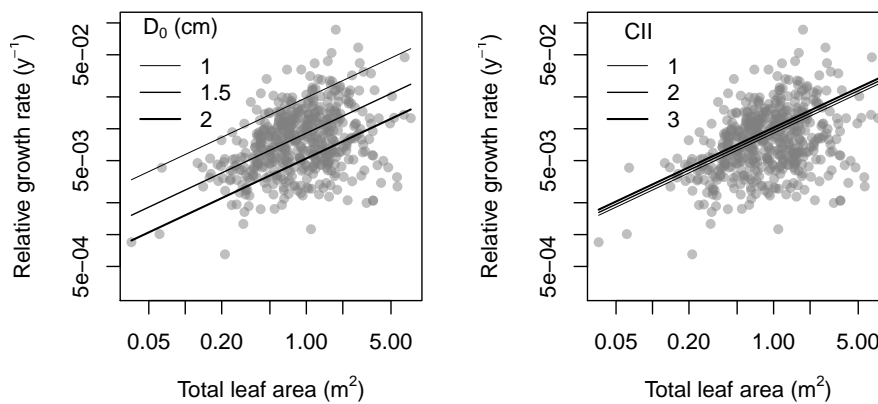


Figure B.7: General relative growth rate (RGR) model contrasted against observed sapling total leaf area and predicted RGR by the individual model (eq.2.6).

Appendix C

Supplement for chapter 3

Determination of prior distributions

Ranges for species-specific parameters (β , α , and ϕ)

After all response variables (H , W , and T) and the response variable D were transformed and then centered, we used the ranges for each of these variables to set realistic boundaries (domains) for the prior distributions. We found the following ranges: $R_H = 1.46$, $R_W = 4.35$, $R_T = 5.67$, $R_D = 1.92$, and $R_L = 2.5$. We used these observed ranges to estimate the possible ranges for effect parameters α , and ϕ ; the intercepts β were assumed to have the same ranges as the response variables. Because we assumed it would be impossible for a plant to reduce in height or crown size as it grows, we forced size effects on H and W to be positive; because T was relative to height, we did not constrain α_T . We thus found the following ranges:

$R_{\beta_H} = 1.46$, $R_{\beta_W} = 4.35$, $R_{\beta_T} = 5.67$, $R_{\alpha_H} = 0.76$, $R_{\alpha_W} = 2.27$, $R_{\alpha_T} = 5.90$, $R_{\phi_H} = 1.17$,
 $R_{\phi_W} = 3.48$, and $R_{\phi_T} = 4.53$. H_{max} in turn ranged from 4 to 47 ($R_{H_{max}} = 43$).

Ranges for across-species parameters (κ and θ)

Based on the ranges shown above we could derive the ranges for the hyperparameters κ and θ . We found the following ranges: $R_{\kappa_{\beta_H}} = -1.73$, $R_{\kappa_{\beta_W}} = -5.16$, $R_{\kappa_{\beta_T}} = -6.72$,
 $R_{\kappa_{\alpha_H}} = -0.90$, $R_{\kappa_{\alpha_W}} = -2.69$, $R_{\kappa_{\alpha_T}} = -7.00$, $R_{\kappa_{\phi_H}} = -1.38$, $R_{\kappa_{\phi_W}} = -4.13$, $R_{\kappa_{\phi_T}} =$
 -5.38 , $R_{\theta_{\beta_H}} = 0.07$, $R_{\theta_{\beta_W}} = 0.20$, $R_{\theta_{\beta_T}} = 0.26$, $R_{\theta_{\alpha_H}} = 0.04$, $R_{\theta_{\alpha_W}} = 0.11$, $R_{\theta_{\alpha_T}} = 0.27$,
 $R_{\theta_{\phi_H}} = 0.05$, $R_{\theta_{\phi_W}} = 0.16$, and $R_{\theta_{\phi_T}} = 0.21$.

Parameter means

For the sake of simplicity, we set the means of the prior distributions to be the middle point in the range of possible values for the parameters.

Variations and precisions

Finally, through the range method, we set the precision for the prior distributions of the hyperparameters based on their possible ranges. Precisions are as follows: $\tau_{\kappa_{\beta_H}} = 0.19$,
 $\tau_{\kappa_{\beta_W}} = 1.66$, $\tau_{\kappa_{\beta_T}} = 2.82$, $\tau_{\kappa_{\alpha_H}} = 0.05$, $\tau_{\kappa_{\alpha_W}} = 0.45$, $\tau_{\kappa_{\alpha_T}} = 3.06$, $\tau_{\kappa_{\phi_H}} = 0.12$, $\tau_{\kappa_{\phi_W}} = 1.07$,
 $\tau_{\kappa_{\phi_T}} = 1.81$, $\tau_{\theta_{\beta_H}} = 0.0003$, $\tau_{\theta_{\beta_W}} = 0.003$, $\tau_{\theta_{\beta_T}} = 0.004$, $\tau_{\theta_{\alpha_H}} = 0.0001$, $\tau_{\theta_{\alpha_W}} = 0.001$,
 $\tau_{\theta_{\alpha_T}} = 0.005$, $\tau_{\theta_{\phi_H}} = 0.0002$, $\tau_{\theta_{\phi_W}} = 0.002$, and $\tau_{\theta_{\phi_T}} = 0.003$.

Table C.1: Number of species, abundance, and sample size for each stratum using three different H_{max} estimates (H_{lit} , H_{herb} , and $H_{D_{max}}$). Relative numbers in % are shown in parentheses.

| Metric | Stratum | $H_{max}(m)$ | Richness | Abundance | Sampled |
|---------------|--------------|--------------|----------|-------------|----------------|
| $H_{D_{max}}$ | Shrubby | 1-10 | 298 (21) | 17,752 (12) | 32 |
| | Understory | 11-20 | 541 (38) | 73,682 (49) | 192 |
| | Subcanopy | 21-30 | 358 (25) | 44,875 (30) | 136 |
| | Canopy | 31-40 | 165 (12) | 11,578 (8) | 55 |
| | Emergent | >40 | 50 (4) | 2,500 (2) | 14 |
| | Total | | | 1412 | 150,387 |
| H_{lit} | Shrubby | 1-10 | 155 (20) | 30,510 (26) | 56 |
| | Understory | 11-20 | 225 (28) | 29,751 (25) | 102 |
| | Subcanopy | 21-30 | 249 (31) | 41,922 (36) | 104 |
| | Canopy | 31-40 | 124 (16) | 13,981 (12) | 55 |
| | Emergent | >40 | 38 (5) | 1,320 (1) | 7 |
| | Total | | | 791 | 117,484 |
| H_{herb} | Shrubby | 1-10 | 35 (12) | 24,224 (26) | 35 |
| | Understory | 11-20 | 94 (32) | 24,837 (27) | 94 |
| | Subcanopy | 21-30 | 108 (37) | 34,037 (36) | 108 |
| | Canopy | 31-40 | 45 (16) | 9,194 (10) | 45 |
| | Emergent | >40 | 8 (3) | 1,171 (1) | 8 |
| | Total | | | 290 | 93,463 |
| H_{cons} | Shrubby | 1-10 | 76 (18) | 13,728 (17) | 50 |
| | Understory | 11-20 | 159 (37) | 35,524 (43) | 160 |
| | Subcanopy | 21-30 | 125 (29) | 26,997 (33) | 151 |
| | Canopy | 31-40 | 61 (14) | 5,869 (7) | 61 |
| | Emergent | >40 | 10 (2) | 736 (1) | 7 |
| | Total | | | 431 | 82,854 |

Table C.2: Well-sampled and outlier species, their families, architectural models (sensu Halle1978), maximum adult size (H_{max} ; m), and sample size (n). The architecture of a median-sized sapling ($D = 1.77\text{ cm}$) growing in the shade ($L = 1$) is described by the optimism index (Θ) and the following architecture parameters: height (β_H ; m), crown projected area (β_W ; m^2), and relative crown thickness (β_T ; unitless). Values for the reference sapling refer to the hyperparameters estimated across all species. Also shown are the range of estimated β s.

| Family | Species | Model | H_{max} | n | Θ | β_H | β_W | β_T |
|--------------------------|----------------------------------|-------------|-----------|-----------|------------|-------------|-------------|-------------|
| Annonaceae | <i>Duguetia flagellaris</i> | Roux | 9 | 17 | 2.2* | 3.20* | 0.33 | 0.50* |
| Apocynaceae | <i>Tabernaemontana muricata</i> | Leeuwenberg | 10 | 10 | 3.1* | 3.38 | 0.26* | 0.25* |
| Burseraceae | <i>Protium decandrum</i> | Attim | 25 | 10 | 3.3* | 3.41 | 0.26 | 0.21* |
| | <i>Protium hebetatum</i> | Attim | 25 | 22 | 3.0* | 3.70 | 0.28 | 0.27 |
| | <i>Protium trifoliolatum</i> | Roux | 16 | 10 | 2.0 | 4.14* | 0.44 | 0.48 |
| Chrysobalanaceae | <i>Hirtella myrmecophila</i> | Troll | 9 | 7 | 2.1 | 4.19 | 0.48 | 0.38 |
| | <i>Licania heteromorpha</i> | Troll | 25 | 13 | 2.6* | 3.97 | 0.44* | 0.26* |
| Dichapetalaceae | <i>Tapura guianensis</i> | Roux | 14 | 8 | 2.5 | 3.24 | 0.30 | 0.44 |
| Euphorbiaceae | <i>Hevea guianensis</i> | Corner | 33 | 6 | 3.9* | 4.85 | 0.26* | 0.12* |
| | <i>Micrandropsis scleroxylon</i> | Troll | 30 | 9 | 2.2* | 4.09* | 0.51 | 0.33* |
| | <i>Pausandra macropetala</i> | Corner | 10 | 19 | 3.7* | 3.99 | 0.23* | 0.17 |
| Fabaceae | <i>Tachigali myrmecophila</i> | Corner | 41 | 2 | 4.0 | 4.41 | 0.20* | 0.14 |
| | <i>Zygia juruana</i> | Attim | 13 | 10 | 2.5* | 4.50* | 0.36* | 0.34* |
| | <i>Zygia racemosa</i> | Attim | 28 | 5 | 2.2* | 3.63 | 0.43* | 0.38 |
| Lecythidaceae | <i>Eschweilera coriacea</i> | Troll | 35 | 11 | 2.2 | 4.01 | 0.42 | 0.38 |
| | <i>Eschweilera grandiflora</i> | Troll | 20 | 15 | 2.7* | 3.42* | 0.28* | 0.36 |
| | <i>Eschweilera pedicellata</i> | Troll | 22 | 10 | 2.4 | 3.63 | 0.37 | 0.38 |
| | <i>Eschweilera wachenheimii</i> | Troll | 26 | 10 | 2.1* | 3.93 | 0.43 | 0.45* |
| | <i>Gustavia elliptica</i> | Fagerlind | 23 | 12 | 2.9 | 4.27 | 0.27 | 0.31 |
| Malvaceae | <i>Scleronema micranthum</i> | Aubreville | 37 | 12 | 2.9* | 3.56 | 0.25 | 0.34* |
| | <i>Theobroma sylvestre</i> | Nozeran | 16 | 10 | 3.9 | 4.12 | 0.27 | 0.11 |
| Melastomataceae | <i>Henriettea caudata</i> | Rauh | 8 | 6 | 1.4 | 3.82* | 0.71 | 0.52 |
| Moraceae | <i>Naucleopsis caloneura</i> | Cook | 18 | 9 | 2.2 | 3.30 | 0.48 | 0.36 |
| | <i>Sorocea muriculata</i> | Roux | 9 | 13 | 2.4* | 3.61 | 0.32 | 0.43* |
| Myristicaceae | <i>Virola guggenheimii</i> | Massart | 28 | 5 | 3.8 | 3.45* | 0.29* | 0.12 |
| Ochnaceae | <i>Ouratea discophora</i> | Roux | 22 | 11 | 2.5* | 4.12 | 0.37* | 0.34 |
| Olacaceae | <i>Minquartia guianensis</i> | Nozeran | 30 | 9 | 2.6 | 3.93 | 0.35* | 0.33 |
| Rubiaceae | <i>Duroia macrophylla</i> | Corner | 19 | 2 | 4.6 | 3.67 | 0.16 | 0.09 |
| | <i>Psychotria pacimonica</i> | Leeuwenberg | 6 | 4 | 3.5* | 2.73 | 0.19* | 0.24* |
| Sapotaceae | <i>Manilkara huberi</i> | Aubreville | 46 | 13 | 2.1* | 3.47 | 0.41 | 0.46* |
| | <i>Pouteria resinosa</i> | Attim | 28 | 4 | 2.8 | 3.73* | 0.31 | 0.31 |
| | <i>Pouteria retinervis</i> | Attim | 29 | 5 | 3.9* | 4.67 | 0.23 | 0.14* |
| | <i>Pouteria</i> sp.1 | Attim | 34 | 1 | 3.3 | 4.87* | 0.25 | 0.22* |
| Siparunaceae | <i>Siparuna cuspidata</i> | Mangenot | 12 | 10 | 2.0* | 3.51 | 0.54 | 0.39* |
| Violaceae | <i>Rinorea amapensis</i> | Fagerlind | 11 | 11 | 2.3* | 3.80 | 0.49 | 0.32* |
| | <i>Rinorea guianensis</i> | Fagerlind | 23 | 10 | 2.4 | 3.88 | 0.42 | 0.33 |
| Vochysiaceae | <i>Erisma bicolor</i> | Massart | 40 | 6 | 3.7* | 3.66 | 0.22* | 0.17 |
| Minimum | | | 4 | 1 | 1.4 | 2.73 | 0.16 | 0.09 |
| Median | | | 21 | 1 | 2.9 | 3.96 | 0.30 | 0.29 |
| Maximum | | | 47 | 22 | 4.6 | 4.87 | 0.71 | 0.52 |
| Reference sapling | | | | | 2.9 | 3.95 | 0.30 | 0.28 |

* Parameter values whose 95% credible interval does not overlap with that of the reference sapling.

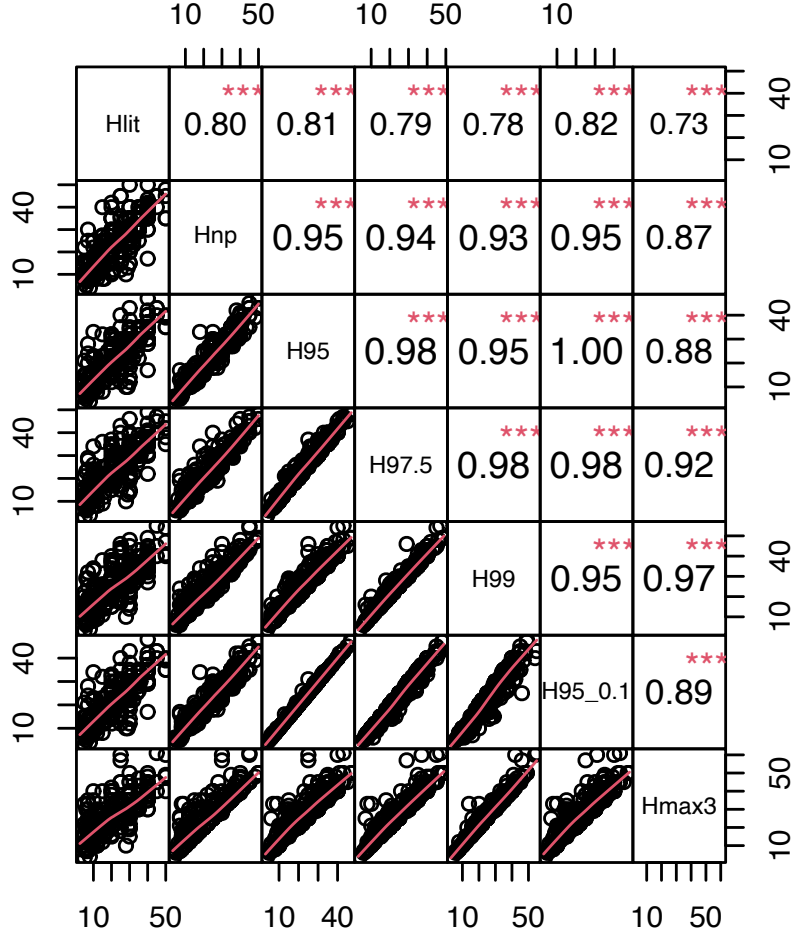


Figure C.1: Correlation between several H_{herb} metrics and H_{lit} .

Table C.3: Sapling trait combinations that maximize the correlation between D_{Hmax} and $D_{sapling}$. The results of Mantel correlations after 999 simulations are also shown.

| Trait combination | Mantel correlation | p |
|-----------------------------|--------------------|-------|
| α_T, ϕ_T | 0.52 | 0.001 |
| $\beta_H, \alpha_T, \phi_T$ | 0.49 | 0.001 |
| α_T, ϕ_H, ϕ_T | 0.48 | 0.001 |
| α_T | 0.47 | 0.001 |
| α_T, ϕ_W, ϕ_T | 0.47 | 0.001 |

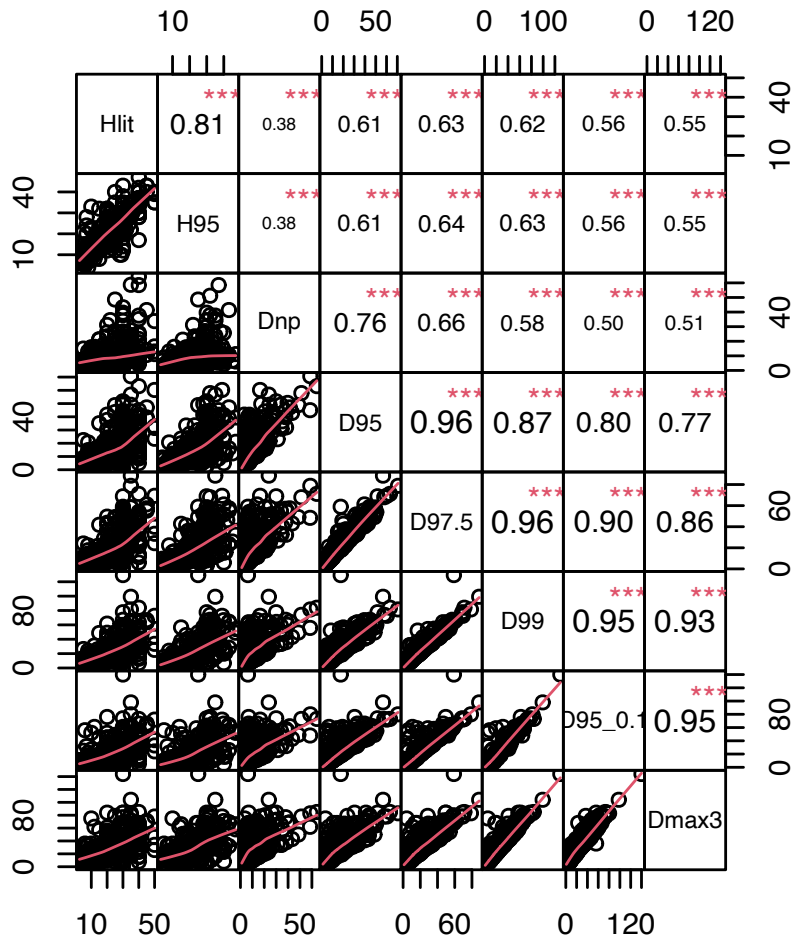


Figure C.2: Correlation between several D_{max} metrics and H_{herb} and H_{lit} .

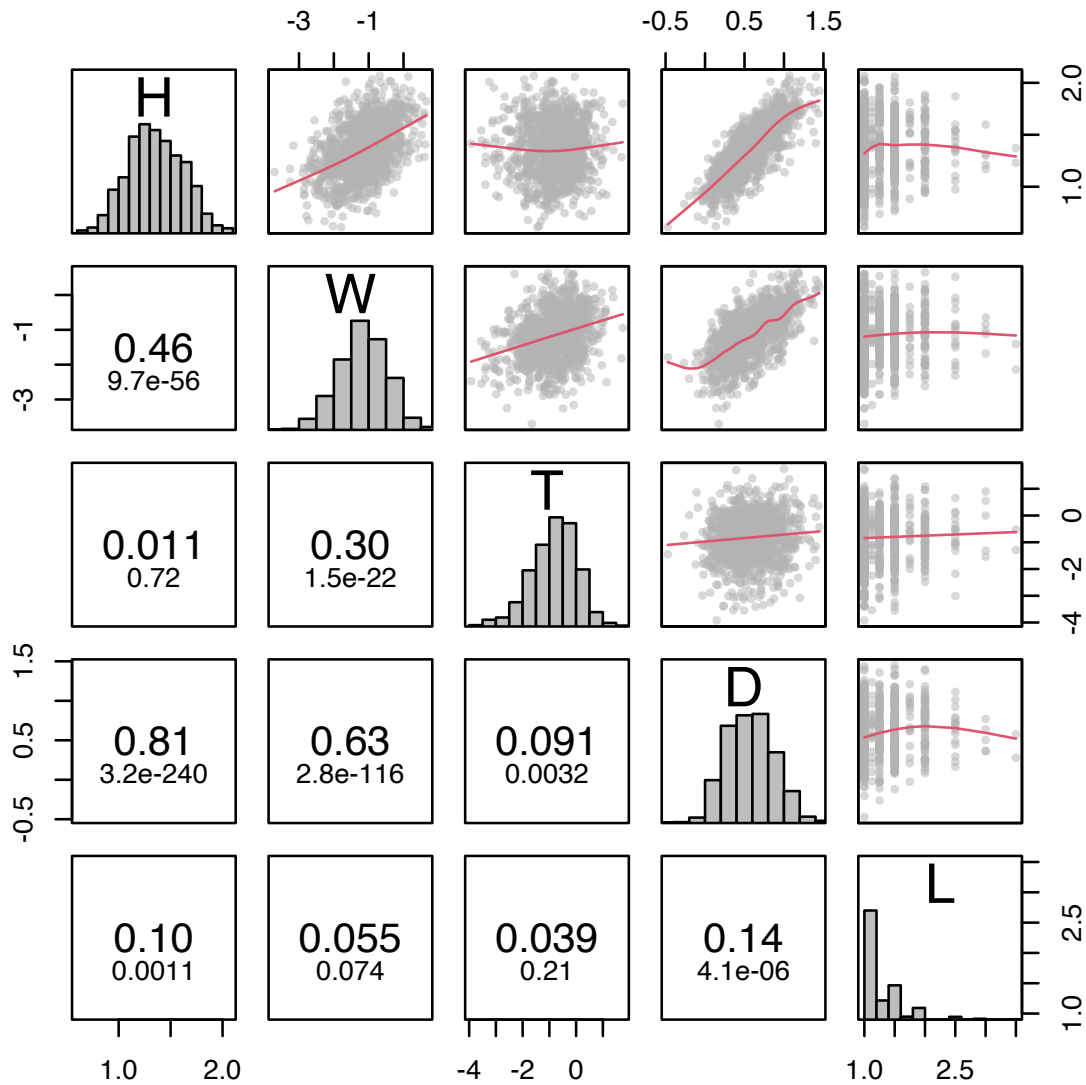


Figure C.3: Sapling architectural traits: height (cm , H), crown projected area (m^2 , W), crown relative thickness (unitless, T), stem diameter at breast height (cm , D), and crown illumination index (unitless, L). Diagonal panel histograms shows values distributions for each measured variable, while upper panel shows raw data plotted against each other (fitted smoothing spline in red), and lower panel shows the results of Pearson correlation (R statistic above and probability below). H , W and D were log-transformed, T was logit-transformed.

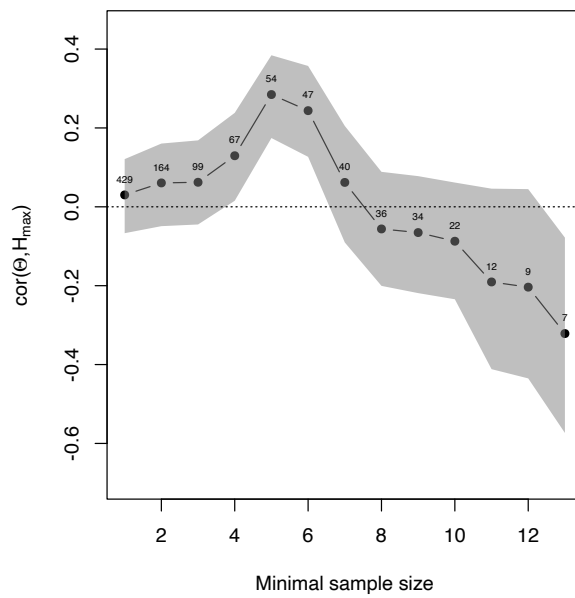


Figure C.4: Effects of sample size on the correlation between sapling optimism index (Θ) and adult size (H_{max}). The numbers above each point indicate the number of species used to calculate the correlation.

Table C.4: Spatial autocorrelation of sapling traits in each of 25 1-ha subplots. The number of saplings considered in the analysis (N) varied across subplots. Also shown is the sample representativeness (R), i.e., N in relation to all saplings present in each subplot. The traits tested were: adult size (H_{max}); sapling architecture predicted from the species-specific allometric models fitted in this study (\hat{H} , \hat{W} , \hat{T}); sapling stem diameter at breast size (D); and the nine species-specific parameters from these allometric models (β s, α s, and ϕ s). Values are Moran's I metric of spatial autocorrelation.

| Subplot | N | $R(\%)$ | H_{max} | \hat{H} | \hat{W} | \hat{T} | D | β_H | β_W | β_T | α_H | α_W | α_T | ϕ_H | ϕ_W | ϕ_T |
|---------|------|---------|-----------|-----------|-----------|-----------|----------|-----------|-----------|-----------|------------|------------|------------|----------|----------|----------|
| 1 | 2689 | 61 | 0.005*** | 0.001 | 0.001 | 0.009*** | 0 | 0.005*** | 0 | 0.008*** | 0.001 | 0.003*** | 0.001** | 0.009*** | 0.003*** | 0.009*** |
| 2 | 2424 | 61 | 0.006*** | -0.001 | 0.001 | 0.009*** | -0.001 | 0.007*** | 0.003*** | 0.008*** | 0 | 0.006*** | 0.001* | 0.005*** | 0.004*** | 0.011*** |
| 3 | 1870 | 52 | 0.009*** | 0.001* | 0 | 0.016*** | 0 | 0.013*** | 0.001* | 0.015*** | 0.009*** | 0 | 0.004*** | 0.013*** | 0.007*** | 0.018*** |
| 4 | 2641 | 57 | 0.001** | 0 | 0.001 | 0.005*** | 0 | 0.003*** | 0.003*** | 0.005*** | 0.001** | 0.003*** | 0.002*** | 0.001** | 0.002** | 0.007*** |
| 5 | 2493 | 59 | 0.001 | -0.001 | -0.001 | 0.002*** | -0.001 | 0.002*** | 0.001** | 0.002** | 0.001 | 0.001** | 0.002** | 0 | 0.002** | 0.001* |
| 6 | 3502 | 66 | 0.009*** | 0 | 0.001* | 0.011*** | 0 | 0.006*** | 0.001** | 0.011*** | 0.006*** | 0.005*** | 0.007*** | 0.004*** | 0.004*** | 0.014*** |
| 7 | 3210 | 69 | 0.004*** | 0.001** | 0 | 0.010*** | 0 | 0.006*** | 0.003*** | 0.012*** | 0.003*** | 0.007*** | 0.011*** | 0.004*** | 0.001** | 0.007*** |
| 8 | 3166 | 68 | 0.008*** | 0.002*** | 0.002*** | 0.006*** | 0.002*** | 0.004*** | 0.006*** | 0.008*** | 0.004*** | 0.009*** | 0.014*** | 0.002*** | 0.001** | 0.007*** |
| 9 | 3365 | 69 | 0.003*** | 0 | 0 | 0.007*** | 0 | 0.003*** | 0.001** | 0.006*** | 0.002*** | 0.001** | 0.002*** | 0.003*** | 0.002*** | 0.007*** |
| 10 | 2822 | 70 | 0.002*** | 0.002*** | 0.003*** | 0.002*** | 0.002*** | 0.002*** | 0.002*** | 0.002*** | 0.001 | 0.001** | 0.005*** | 0.002*** | 0 | 0.003*** |
| 11 | 3496 | 78 | 0.003*** | 0 | 0.001* | 0.008*** | 0 | 0.005*** | 0.003*** | 0.008*** | 0.006*** | 0.004*** | 0.007*** | 0.003*** | 0.001*** | 0.007*** |
| 12 | 3658 | 79 | 0.005*** | 0.004*** | 0 | 0.007*** | 0.002*** | 0.005*** | 0.006*** | 0.008*** | 0.009*** | 0.013*** | 0.011*** | 0.002*** | 0.001*** | 0.005*** |
| 13 | 3593 | 72 | 0.003*** | 0.003*** | 0.002*** | 0.003*** | 0.002*** | 0.003*** | 0.001*** | 0.003*** | 0.002*** | 0.003*** | 0.001** | 0.002*** | 0.002*** | 0.007*** |
| 14 | 3445 | 74 | 0.003*** | 0.001*** | 0.002*** | 0.002*** | 0.001 | 0.003*** | 0.003*** | 0.002*** | 0.001** | 0.001* | 0.002*** | 0.003*** | 0.002*** | 0.005*** |
| 15 | 3081 | 74 | 0.006*** | 0.002*** | 0.001** | 0.011*** | 0.001** | 0.006*** | 0.006*** | 0.012*** | 0.007*** | 0.006*** | 0.011*** | 0.002*** | 0.003*** | 0.007*** |
| 16 | 3684 | 76 | 0.002*** | 0.003*** | 0.001** | 0.008*** | 0.001*** | 0.004*** | 0.006*** | 0.008*** | 0.007*** | 0.005*** | 0.006*** | 0.007*** | 0.005*** | 0.005*** |
| 17 | 3888 | 77 | 0.006*** | 0.002*** | 0 | 0.013*** | 0 | 0.006*** | 0.006*** | 0.014*** | 0.008*** | 0.007*** | 0.014*** | 0.007*** | 0.009*** | 0.010*** |
| 18 | 3766 | 78 | 0.003*** | 0.002*** | 0.001* | 0.003*** | 0.001** | 0.007*** | 0.001** | 0.003*** | 0 | 0.001*** | 0.001 | 0.004*** | 0.001* | 0.007*** |
| 19 | 4165 | 79 | 0.004*** | 0 | 0 | 0.007*** | 0 | 0.002*** | 0.001*** | 0.007*** | 0.001*** | 0.001* | 0.003*** | 0.005*** | 0.002*** | 0.009*** |
| 20 | 4158 | 78 | 0.004*** | 0.001** | 0.001*** | 0.001*** | 0 | 0.002*** | 0.001*** | 0.001** | 0.001*** | 0.007*** | 0.002*** | 0.005*** | 0.003*** | 0.006*** |
| 21 | 3283 | 74 | 0.002*** | 0 | 0 | 0.005*** | 0 | 0.002*** | 0.003*** | 0.005*** | 0.002*** | 0.001** | 0.005*** | 0.002*** | 0.004*** | 0.003*** |
| 22 | 3954 | 76 | 0.004*** | 0 | 0 | 0.005*** | 0 | 0.002*** | 0.002*** | 0.006*** | 0.003*** | 0.004*** | 0.011*** | 0.001*** | 0.003*** | 0.004*** |
| 23 | 3456 | 75 | 0.006*** | 0 | 0 | 0.008*** | 0 | 0.003*** | 0.002*** | 0.008*** | 0.002*** | 0.003*** | 0.005*** | 0.005*** | 0.003*** | 0.010*** |
| 24 | 3198 | 71 | 0.006*** | 0.001** | 0 | 0.006*** | 0 | 0.004*** | 0.001*** | 0.006*** | 0.006*** | 0.007*** | 0.008*** | 0.005*** | 0.009*** | 0.007*** |
| 25 | 2787 | 65 | 0.009*** | 0.002*** | 0 | 0.01*** | 0.001* | 0.010*** | 0.002*** | 0.010*** | 0.002*** | 0.004*** | 0.003*** | 0.01*** | 0.006*** | 0.021*** |
| Median | 3365 | 72 | 0.004 | 0.001 | 0.001 | 0.007 | 0 | 0.004 | 0.002 | 0.008 | 0.002 | 0.004 | 0.005 | 0.004 | 0.003 | 0.007 |

* $p < 0.05$; ** $p < 0.01$; *** $p < 0.001$; where p is the probability that the observed metric does not differ from the expected one under the null model.

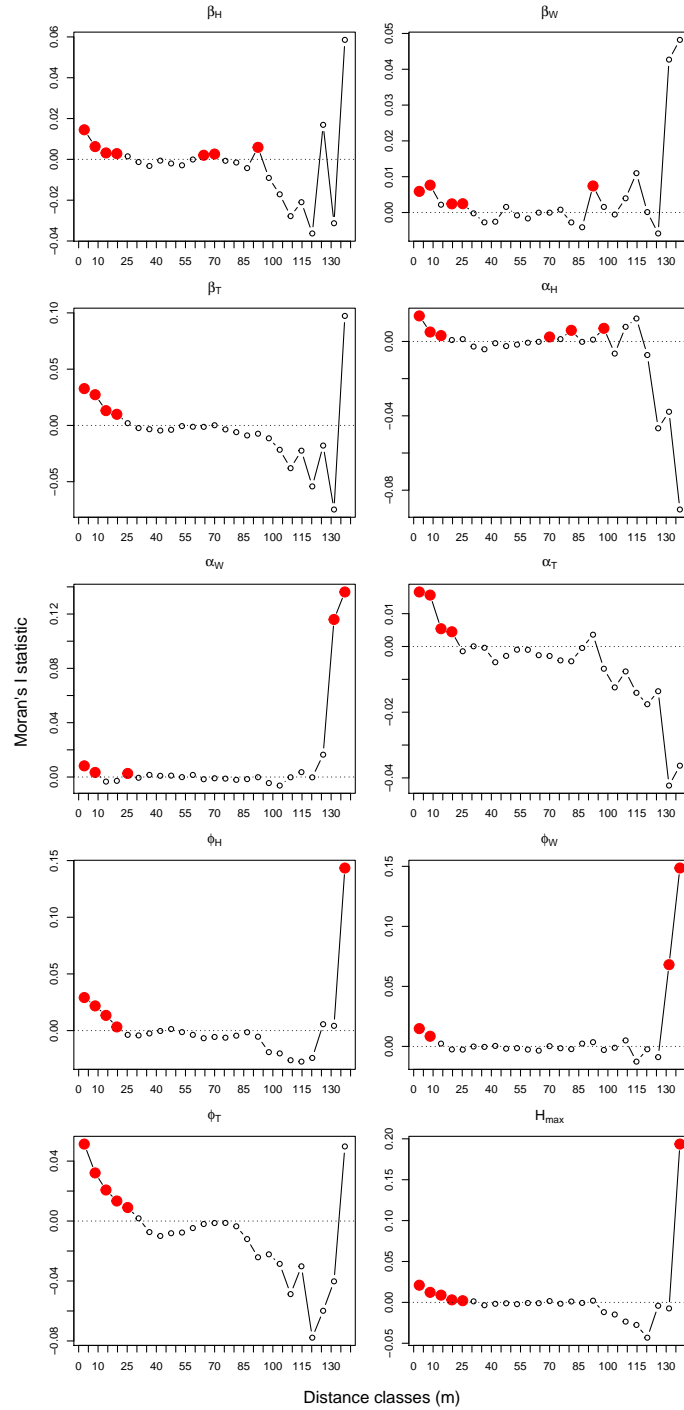


Figure C.5: Spatial autocorrelation (SAC) of species-specific traits for the subplot with the highest sampling coverages (82% of all trees). β , α , and ϕ are the estimated sapling architecture traits and H_{max} is the species maximum adult height. The SAC metric used was Moran's I, which was estimated through normal approximations.

Appendix D

Supplement for chapter 4

Determination of D_{crit}

There is an analytic solution to find the diameter (D_{crit}) at which a tree reaches half of its maximum reproductive potential ($\kappa/2$), i.e., the inflexion point of the following equation:

$$P_R = \frac{\kappa}{1 + e^{-y}}$$

where κ is the maximum reproduction probability ($P_{R_{max}}$) and the function y represents how P_R changes as a function of tree size (D), as follows:

$$y = \beta + \alpha * D$$

The first derivative shows the distribution of a species' critical size (D_{crit}):

$$P'_R = \frac{\kappa * e^{-y}}{(e^{-y} + 1)^2} = \frac{\kappa * e^y}{(e^y + 1)^2}$$

Setting the second derivative to zero gives us the species' D_{crit} as follows:

$$P''_R = -\frac{\kappa * e^y * (e^y - 1)}{(e^y + 1)^3} = 0$$

because neither $(e^y + 1)^3$ can be infinite or e^y can be zero, the only "real" solution is $e^y - 1 = 0$, which means $y = 0$. Therefore:

$$y = \beta + \alpha * D_{crit} = 0$$

then solving for D_{crit} :

$$D_{crit} = \frac{-\beta}{\alpha}$$

Determination of prior distributions

Parameter means

The vaguest mean for a probability is 50%, so we set the mean for both θ_π and θ_κ to be zero, as in the model we first logit-transformed P_{repr} . All the other hyperparameters are slopes (θ_α , ϕ_β , ϕ_α , and ϕ_κ), so we set all their means at zero.

Ranges for species-specific parameters (θ)

We applied the range rule for all variances, which were then transformed into precision. This approach assumes that P_{repr} ranges from 1 to 9% and then uses the observed ranges in D and D_{max} to produce minimally informed priors (vague, but still acknowledging the limits

of the data). Because $P_{repr} = [0.01, 0.99]$, we have that both κ and π should have this exact range. α in turn should have a range as follows:

$$\alpha_{max} = \frac{range(logit(P_{repr}))}{range(D/D_{max} - D_{ref})} \approx \frac{4.6 - (-4.6)}{0.5 - (-0.4)} \approx \frac{9.2}{0.9} \approx 10.3$$

where P_{repr} has been previously logit-transformed and D has been relativized in relation to D_{max} and centered around the median (D_{ref}). Because α is a $P \sim D$ slope it could theoretically be just as negative as well, although quite biologically unrealistic. We thus set α_{min} to be the exact opposite of α_{max} , i.e., -10.3 , thus making the range of possible α s be ~ 20.6 .

Ranges for D_{max} effects (ϕ)

Now the ranges for the D_{max} effects (ϕ s) were solely based on the ranges of the species-specific parameters (β s, α s, and κ s). We used the same method we had used to derive the possible range of α , as follows: $\phi_{\beta_{max}} = \phi_{\kappa_{max}} \approx \frac{range(logit(P_{repr}))}{range(log(D_{max}) - D_{max_{ref}})}$

$$\approx \frac{4.6 - (-4.6)}{1.84 - (-1.18)} \approx \frac{9.2}{3.02} \approx 3.05 \text{ which means that the } range(\phi_{\beta}) = range(\phi_{\kappa}) \approx [-3.05, 3.05].$$

Then, finally, the range for ϕ_{α} was set as follows: $\phi_{\alpha_{max}} \approx \frac{range(\alpha)}{range(log(D_{max}) - D_{max_{ref}})}$

$$\approx \frac{10.3 - (-10.3)}{1.84 - (-1.18)} \approx \frac{20.6}{3.02} \approx 6.83 \text{ meaning that } range(\phi_{\alpha}) \approx [-6.83, 6.83].$$

Variations and precisions for θ and ϕ

To estimate prior variances, and then precisions, we used the range rule, which assumes $range(x) \approx 4\sigma_x^2$ to estimate variance as follows:

$$var(x) \approx \left(\frac{range(x)}{4} \right)^2$$

Precision (τ) was then simply estimated as $var(x)^{-1}$ and are as follows:

$$\tau_{\theta_\beta} = \tau_{\theta_\kappa} \approx 0.19$$

$$\tau_{\theta_\alpha} \approx 0.04$$

$$\tau_{\phi_\beta} = \tau_{\phi_\kappa} \approx 0.43$$

$$\tau_{\phi_\alpha} \approx 0.09$$

Variations and precisions for variance parameters (σ^2)

Variations are the most complicated parameters to set priors. In order to provide realistic values to these parameters (σ_β^2 , σ_α^2 , σ_κ^2 , and σ_ζ^2) we also used the observed and estimated ranges shown above. We then converted these variance values into precisions ($\tau(x) = 1/var(x)$), which were then used to model gamma distributions whose mean is a/b and variance is a/b^2 , where a and b are the shape and rate parameters, respectively. The reasoning was that the variance based on the maximum possible ranges should also be the maximum possible variance (σ_{max}^2). With that we can roughly estimate the mean of the random distribution of variations (inverse gamma) as a midpoint between 0 and σ_{max}^2 , i.e., $mean(var(x)) = \sigma_{max}^2/2$.

We thus have that the bulk of the gamma distribution representing the distribution of precisions should be constrained between $1/\sigma_{max}^2$ (τ_{min}) and infinite, but with mean around $2/\sigma_{max}^2$. If we can assume that the distance between τ_{min} and $mean(\tau)$ roughly approximates two standard deviations, as it would be the case for the normal distribution, then we have that the gamma distribution has a standard deviation of $1/(2\sigma_{max}^2)$ and thus a variance of $1/(2\sigma_{max}^2)^2$. Replacing $sigma_{max}^2$ by τ_{min} and using the gamma distribution formulas for mean gives us:

$$mean(x) = \frac{2}{\sigma_{max}^2} = 2\tau_{min} = \frac{a}{b}$$

so isolating a we have:

$$a = b2\tau_{min}$$

which we then can use into the formula for the gamma distribution variance as follows:

$$var(x) = \frac{1}{4(\sigma_{max}^2)^2} = \frac{\tau_{min}^2}{4} = \frac{a}{b^2} = \frac{b2\tau_{min}}{b^2} = \frac{2\tau_{min}}{b}$$

isolating b yields:

$$b = \frac{4 * 2\tau_{min}}{\tau_{min}^2} = \frac{8}{\tau_{min}}$$

thus:

$$a = \frac{8 * 2\tau_{min}}{\tau_{min}} = 16$$

meaning that a should be a constant while b should be a function of τ_{min} . Applying these formulas to the precision values derived above for θ s, we had that:

$$b_{\beta} = b_{\kappa} = b_{\zeta} \approx \frac{8}{0.19} \approx 42.2$$

$$b_\alpha \approx \frac{8}{0.04} \approx 212$$

Note that the prior of σ_ζ^2 followed that of the σ_β^2 and σ_κ^2 .

Table D.1: Summary of the species-specific parameters (β , α , and κ) for all the 233 species used in this study. P refers to the proportion of species whose parameter x is larger than zero (α) or 0.5 (β and κ).

| | Median | 95% quantiles | P($x_i > 0$) |
|------------|--------|---------------|----------------|
| β | 0.55 | [0.16;0.92] | 0.57 |
| α | 11.56 | [9.71;13.54] | 1 |
| κ | 0.85 | [0.41;0.97] | 0.93 |
| D_{crit} | 0.48 | [0.29;0.66] | 1 |

Table D.2: D_{max} effects on species-specific parameters (β , α , and κ).

| | Median | $CI_{95\%}$ | $p(x > 0)$ |
|------------|--------|--------------|------------|
| θ_b | 0.33 | [-1.39;1.93] | 0.66 |
| θ_a | 11.54 | [7.43;16.43] | 1 |
| θ_k | 1.72 | [0.96;3.49] | 1 |
| ϕ_b | 1.87 | [0.52;3.07] | 1 |
| ϕ_a | 1.29 | [-3.71;5.5] | 0.7 |
| ϕ_k | 1.58 | [-0.03;2.84] | 0.97 |

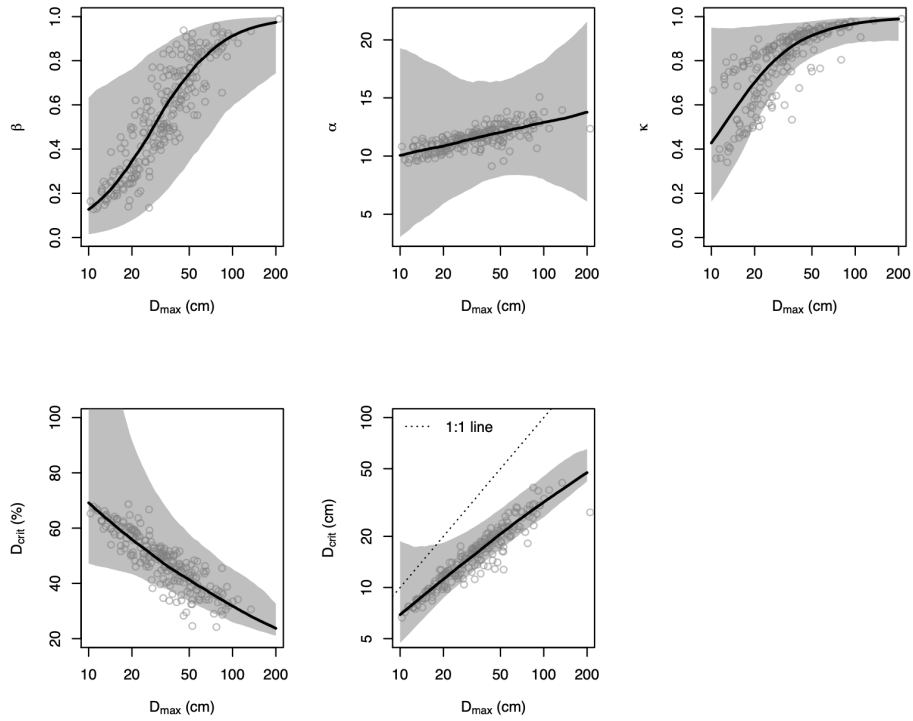


Figure D.1: Effect of species' adult maximum size (D_{max}) on each of the species-specific parameters: β , α , and κ . Also shown is the effect of D_{max} on D_{crit} . The 95% credible envelope for each curve is represented by the shaded area and each point correspond to the parameters fit for each of the sampled species.

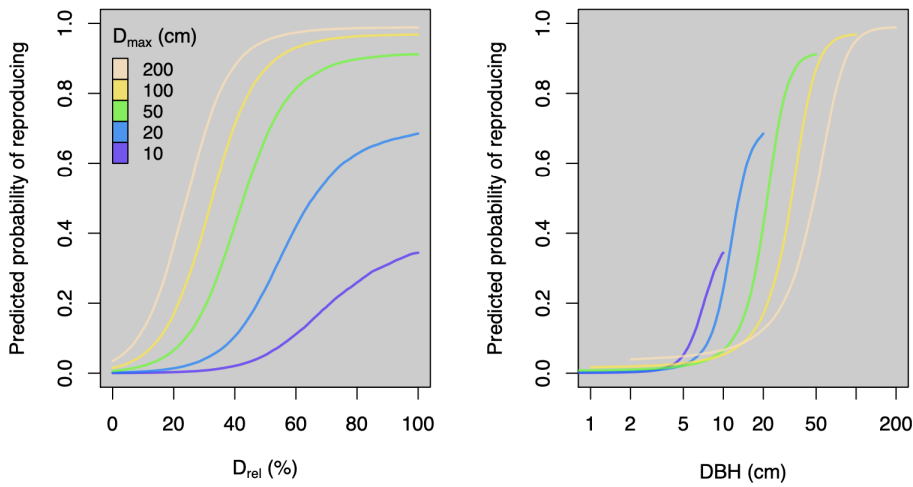


Figure D.2: Predicted P_R for hypothetical species with contrasting D_{max} .

Bibliography

1. Piperno, D. R. & Becker, P. Vegetational history of a site in the central Amazon basin derived from phytolith and charcoal records from natural soils. *Quaternary research* **45**, 202–209 (1996).
2. De Oliveira, A. A. & Mori, S. A. A central Amazonian terra firme forest. I. High tree species richness on poor soils. *Biodiversity & Conservation* **8**, 1219–1244 (1999).
3. Humboldt, A. v., Bonpland, A., Cuvier, G. & Valenciennes, M. *Recueil d'observations de zoologie et d'anatomie compar* (Paris, 1805).
4. Darwin, C., Wallace, A. R., Lyell, S. C. & Hooker, J. D. On the tendency of species to form varieties: and on the perpetuation of varieties and species by natural means of selection. *Proceedings of the Linnean Society of London* **3**, 45–50 (1858).
5. Warming, E. *Plantesaemfund: Grundtræk Af Den Økologiske Plantegeografi* (Philipsen Publishers, Copenhagen, 1895).
6. Schimper, A. F. W. *Pflanzen-geographie auf physiologischer Grundlage* (G. Fischer, 1898).

7. Galtung, J. Scientific colonialism. *Transition*, 11–15 (1967).
8. Trisos, C. H., Auerbach, J. & Katti, M. Decoloniality and anti-oppressive practices for a more ethical ecology. *Nature Ecology & Evolution*, 1–8 (2021).
9. Connell, J. H. Diversity in tropical rain forests and coral reefs. *Science* **199**, 1302–1310 (1978).
10. Richards, P. W., Frankham, R. & Walsh, R. *The tropical rain forest: an ecological study* (Cambridge University Press, 1996).
11. Wallace, A. R. *Tropical nature, and other essays* (Macmillan and Co., London, 1878).
12. Kraft, N. J. *et al.* Disentangling the drivers of β diversity along latitudinal and elevational gradients. *Science* **333**, 1755–1758 (2011).
13. Jablonski, D., Roy, K. & Valentine, J. W. Out of the tropics: evolutionary dynamics of the latitudinal diversity gradient. *Science* **314**, 102–106 (2006).
14. Donoghue, M. J. A phylogenetic perspective on the distribution of plant diversity. *Proceedings of the National Academy of Sciences* **105**, 11549–11555 (2008).
15. Wiens, J. J. & Graham, C. H. Niche conservatism: integrating evolution, ecology, and conservation biology. *Annual Review of Ecology, Evolution, and Systematics* **36**, 519–539 (2005).
16. Zanne, A. E. *et al.* Three keys to the radiation of angiosperms into freezing environments. *Nature* **506**, 89–92 (2014).

17. Lambers, H., Brundrett, M. C., Raven, J. A. & Hopper, S. D. Plant mineral nutrition in ancient landscapes: high plant species diversity on infertile soils is linked to functional diversity for nutritional strategies. *Plant and Soil* **348**, 7–27 (2011).
18. Ter Steege, H. *et al.* Biased-corrected richness estimates for the Amazonian tree flora. *Scientific reports* **10**, 1–13 (2020).
19. Ter Steege, H. *et al.* Towards a dynamic list of Amazonian tree species. *Scientific reports* **9**, 1–5 (2019).
20. Bebbler, D. P. *et al.* Herbaria are a major frontier for species discovery. *Proceedings of the National Academy of Sciences* **107**, 22169–22171 (2010).
21. Davies, S. J. *et al.* ForestGEO: Understanding forest diversity and dynamics through a global observatory network. *Biological Conservation* **253**, 108907 (2021).
22. Quesada, C. A. *et al.* Basin-wide variations in Amazon forest structure and function are mediated by both soils and climate. *Biogeosciences* **9**, 2203–2246 (2012).
23. Feng, X. *et al.* How deregulation, drought and increasing fire impact Amazonian biodiversity. *Nature*, 1–6 (2021).
24. Hubbell, S. P. *et al.* How many tree species are there in the Amazon and how many of them will go extinct? *Proceedings of the National Academy of Sciences* **105**, 11498–11504 (2008).

25. Pimm, S. L. *et al.* The biodiversity of species and their rates of extinction, distribution, and protection. *Science* **344** (2014).
26. Williamson, G. B. *et al.* Amazonian tree mortality during the 1997 El Nino drought. *Conservation Biology* **14**, 1538–1542 (2000).
27. Leitold, V. *et al.* El Niño drought increased canopy turnover in Amazon forests. *New Phytologist* **219**, 959–971 (2018).
28. Rowland, L. *et al.* Death from drought in tropical forests is triggered by hydraulics not carbon starvation. *Nature* **528**, 119–122 (2015).
29. Price, M. Tallying the Tropical Toll on Trees From Lightning. *Science* **356**, 1222 (2017).
30. Aleixo, I. *et al.* Amazonian rainforest tree mortality driven by climate and functional traits. *Nature Climate Change* **9**, 384–388 (2019).
31. Staver, A. C., Archibald, S. & Levin, S. A. The global extent and determinants of savanna and forest as alternative biome states. *Science* **334**, 230–232 (2011).
32. Lovejoy, T. E. & Nobre, C. Amazon tipping point. *Science Advances* **4**, eaat2340 (2018).
33. Lovejoy, T. E. & Nobre, C. Amazon tipping point: Last chance for action. *Science Advances* **5**, eaba2949 (2019).

34. Barber, C. P., Cochrane, M. A., Souza Jr, C. M. & Laurance, W. F. Roads, deforestation, and the mitigating effect of protected areas in the Amazon. *Biological Conservation* **177**, 203–209 (2014).
35. Hutchinson, G. E. Homage to Santa Rosalia or why are there so many kinds of animals? *The American Naturalist* **93**, 145–159 (1959).
36. Hutchinson, G. E. The paradox of the plankton. *The American Naturalist* **95**, 137–145 (1961).
37. Hardin, G. The competitive exclusion principle. *Science* **131**, 1292–1297 (1960).
38. MacArthur, R. H. Population ecology of some warblers of northeastern coniferous forests. *Ecology* **39**, 599–619 (1958).
39. Chesson, P. Mechanisms of Maintenance of Species Diversity. *Annual Review of Ecology and Systematics* **31**, 343–366 (2000).
40. Amarasekare, P. Competitive coexistence in spatially structured environments: a synthesis. *Ecology Letters* **6**, 1109–1122 (2003).
41. Hastings, A. Disturbance, coexistence, history, and competition for space. *Theoretical Population Biology* **18**, 363–373 (1980).
42. Wright, J. S. Plant diversity in tropical forests: a review of mechanisms of species coexistence. *Oecologia* **130**, 1–14 (2002).

43. Murrell, D. J. & Law, R. Heteromyopia and the spatial coexistence of similar competitors. *Ecology Letters* **6**, 48–59 (2003).
44. Janzen, D. H. Herbivores and the number of tree species in tropical forests. *The American Naturalist* **104**, 501–528 (1970).
45. LaManna, J. A., Mangan, S. A. & Myers, J. A. Conspecific negative density dependence and why its study should not be abandoned. *Ecosphere* **12**, e03322 (2021).
46. MacArthur, R. H. & Wilson, E. O. *The theory of island biogeography* (Princeton University Press, 1967).
47. Hubbell, S. P. *The Unified Neutral Theory of Biodiversity and Biogeography* (Princeton University Press, 2001).
48. Hérault, B. Reconciling niche and neutrality through the Emergent Group approach. *Perspectives in Plant Ecology, Evolution and Systematics* **9**, 71–78 (2007).
49. Kraft, N. J. & Ackerly, D. D. Functional trait and phylogenetic tests of community assembly across spatial scales in an Amazonian forest. *Ecological monographs* **80**, 401–422 (2010).
50. Cornelissen, J. *et al.* A handbook of protocols for standardised and easy measurement of plant functional traits worldwide. *Australian journal of Botany* **51**, 335–380 (2003).
51. Cohen, J. E. Mathematics is biology’s next microscope, only better; biology is mathematics’ next physics, only better. *PLoS biology* **2**, e439 (2004).

52. Clark, J. S. Why environmental scientists are becoming Bayesians. *Ecology Letters* **8**, 2–14 (2005).
53. Turner, I. M. *The ecology of trees in the tropical rain forest* (Cambridge University Press, 2001).
54. Comita, L. S. & Hubbell, S. P. Local neighborhood and species' shade tolerance influence survival in a diverse seedling bank. *Ecology* **90**, 328–334 (2009).
55. McFadden, I. R. *et al.* Disentangling the functional trait correlates of spatial aggregation in tropical forest trees. *Ecology* **100**, e02591 (2019).
56. Agrawal, A. A., Conner, J. K. & Rasmann, S. in *Evolution since Darwin: the first 150 years* (eds Bell, M. A., Futuyma, D. J., Eanes, W. F. & Levinton, J. S.) 243–268 (Sinauer Associates, Sunderland, 2010).
57. Onoda, Y. *et al.* Trade-off between light interception efficiency and light use efficiency: implications for species coexistence in one-sided light competition. *Journal of Ecology* **102**, 167–175 (2014).
58. Kneitel, J. M. & Chase, J. M. Trade-offs in community ecology: linking spatial scales and species coexistence. *Ecology Letters* **7**, 69–80 (2004).
59. Baraloto, C., Goldberg, D. E. & Bonal, D. Performance trade-offs among tropical tree seedlings in contrasting microhabitats. *Ecology* **86**, 2461–2472 (2005).

60. Clark, J. S. *et al.* Resolving the biodiversity paradox. *Ecology Letters* **10**, 647–659 (2007).
61. Grubb, P. J. Trade-offs in interspecific comparisons in plant ecology and how plants overcome proposed constraints. *Plant Ecology and Diversity* **9**, 3–33 (2016).
62. Van Noordwijk, A. J. & de Jong, G. Acquisition and Allocation of Resources: Their Influence on Variation in Life History Tactics. *The American Naturalist* **128**. Trade-off vs. performance differences, 137–142 (1986).
63. Grubb, P. J. The maintenance of species-richness in plant communities: the importance of the regeneration niche. *Biological Reviews* **52**, 107–145 (1977).
64. Silvertown, J. Plant coexistence and the niche. *Trends in Ecology Evolution* **19**, 605–611 (2004).
65. Tuomisto, H., Ruokolainen, K. & Yli-Halla, M. Dispersal, environment, and floristic variation of western Amazonian forests. *Science* **299**, 241–244 (2003).
66. Valencia, R. *et al.* Tree species distributions and local habitat variation in the Amazon: large forest plot in eastern Ecuador. *Journal of Ecology* **92**, 214–229 (2004).
67. Fine, P. V. *et al.* The growth–defense trade-off and habitat specialization by plants in Amazonian forests. *Ecology* **87**, S150–S162 (2006).

68. Russo, S. E., Brown, P., Tan, S. & Davies, S. J. Interspecific demographic trade-offs and soil-related habitat associations of tree species along resource gradients. *Journal of Ecology* **96**, 192–203 (2008).
69. Quesada, C. *et al.* Variations in chemical and physical properties of Amazon forest soils in relation to their genesis. *Biogeosciences* **7**, 1515–1541 (2010).
70. Laurance, S. G. W. *et al.* Influence of soils and topography on Amazonian tree diversity: a landscape-scale study. *Journal of Vegetation Science* **21**, 96–106 (2010).
71. John, R. *et al.* Soil nutrients influence spatial distributions of tropical tree species. *Proceedings of the National Academy of Sciences* **104**, 864–869 (2007).
72. McFadden, I. R. *et al.* Temperature shapes opposing latitudinal gradients of plant taxonomic and phylogenetic β diversity. *Ecology Letters* **22**, 1126–1135 (2019).
73. McLaughlin, B. C. *et al.* Hydrologic refugia, plants, and climate change. *Global change biology* **23**, 2941–2961 (2017).
74. Kraft, N. J. B., Valencia, R. & Ackerly, D. D. Functional Traits and Niche-Based Tree Community Assembly in an Amazonian Forest. *Science* **322**, 580–582 (2008).
75. Fyllas, N. M. *et al.* Basin-wide variations in foliar properties of Amazonian forest: phylogeny, soils and climate. *Biogeosciences* **6**, 2677–2708 (2009).

76. Hansen, S. R. & Hubbell, S. P. Single-nutrient microbial competition: qualitative agreement between experimental and theoretically forecast outcomes. *Science* **207**, 1491–1493 (1980).
77. Tilman, D. *Resource Competition and Community Structure* (Princeton University Press, 1982).
78. Condit, R. *et al.* The importance of demographic niches to tree diversity. *science* **313**, 98–101 (2006).
79. Nasto, M. K. *et al.* Interactions among nitrogen fixation and soil phosphorus acquisition strategies in lowland tropical rain forests. *Ecology Letters* **17**, 1282–1289 (2014).
80. Hayes, P., Turner, B. L., Lambers, H. & Laliberté, E. Foliar nutrient concentrations and resorption efficiency in plants of contrasting nutrient-acquisition strategies along a 2-million-year dune chronosequence. *Journal of Ecology* **102**, 396–410 (2014).
81. Poole, P., Ramachandran, V. & Terpolilli, J. Rhizobia: from saprophytes to endosymbionts. *Nature Reviews Microbiology* **16**, 291–303 (2018).
82. Wright, I. J. *et al.* The worldwide leaf economics spectrum. *Nature* **428**, 821–827 (2004).
83. Falster, D. S. & Westoby, M. Plant height and evolutionary games. *Trends in Ecology Evolution* **18**, 337–343 (2003).

84. Rüger, N. *et al.* Demographic trade-offs predict tropical forest dynamics. *Science* **368**, 165–168 (2020).
85. Hedin, L. O., Brookshire, E. J., Menge, D. N. & Barron, A. R. The nitrogen paradox in tropical forest ecosystems. *Annual Review of Ecology, Evolution, and Systematics* **40**, 613–635 (2009).
86. Fernside, P. M. & Leal-Filho, N. in *Lessons from Amazonia: The ecology and conservation of a fragmented forest* (eds Bierregard, R. O., Gascon, C., Lovejoy, T. E. & Mesquita, R.) 291–312 (Yale University Press, 2001).
87. Laurance, W. F. *et al.* Relationship between soils and Amazon forest biomass: a landscape-scale study. *Forest Ecology and Management* **118**, 127–138 (1999).
88. De Castilho, C. V. *et al.* Variation in aboveground tree live biomass in a central Amazonian Forest: Effects of soil and topography. *Forest Ecology and Management* **234**, 85–96 (2006).
89. Siefert, A. *et al.* A global meta-analysis of the relative extent of intraspecific trait variation in plant communities. *Ecology Letters* **18**, 1406–1419 (2015).
90. Baraloto, C. *et al.* Functional trait variation and sampling strategies in species-rich plant communities. *Functional Ecology* **24**, 208–216 (2010).
91. Tedersoo, L. *et al.* Global database of plants with root-symbiotic nitrogen fixation: Nod DB. *Journal of Vegetation Science* **29**, 560–568 (2018).

92. R Core Team. *R: A Language and Environment for Statistical Computing* R Foundation for Statistical Computing (Vienna, Austria, 2019).
93. Plummer, M. *JAGS: A program for analysis of Bayesian graphical models using Gibbs sampling* (2003).
94. Plummer, M., Best, N., Cowles, K. & Vines, K. CODA: Convergence Diagnosis and Output Analysis for MCMC. *R News* **6**, 7–11 (2006).
95. Chapin III, F. S. The mineral nutrition of wild plants. *Annual review of ecology and systematics* **11**, 233–260 (1980).
96. Houlton, B. Z., Wang, Y.-P., Vitousek, P. M. & Field, C. B. A unifying framework for dinitrogen fixation in the terrestrial biosphere. *Nature* **454**, 327–330 (2008).
97. Cuevas, E. & Medina, E. Nutrient dynamics within Amazonian forests. *Oecologia* **76**, 222–235 (1988).
98. Turner, B. L. Resource partitioning for soil phosphorus: a hypothesis. *Journal of Ecology* **96**, 698–702 (2008).
99. Laliberté, E., Lambers, H., Burgess, T. I. & Wright, S. J. Phosphorus limitation, soil-borne pathogens and the coexistence of plant species in hyperdiverse forests and shrublands. *New Phytologist* **206**, 507–521 (2015).
100. Wilhelm Scherer, H. Sulfur in soils. *Journal of Plant Nutrition and Soil Science* **172**, 326–335 (2009).

101. Anjum, N. A. *et al.* ATP-sulfurylase, sulfur-compounds, and plant stress tolerance. *Frontiers in Plant Science* **6**, 210 (2015).
102. Baribault, T. W., Kobe, R. K. & Finley, A. O. Tropical tree growth is correlated with soil phosphorus, potassium, and calcium, though not for legumes. *Ecological Monographs* **82**, 189–203 (2012).
103. Batterman, S. A. *et al.* Phosphatase activity and nitrogen fixation reflect species differences, not nutrient trading or nutrient balance, across tropical rainforest trees. *Ecology Letters* **21**, 1486–1495 (2018).
104. Miller, R. W. & Sirois, J. C. Calcium and magnesium effects on symbiotic nitrogen fixation in the alfalfa (*M. sativa*)–*Rhizobium meliloti* system. *Physiologia Plantarum* **58**, 464–470 (1983).
105. Kinzel, H. Calcium in the vacuoles and cell walls of plant tissue. *Flora* **182**, 99–125 (1989).
106. Franceschi, V. R. & Nakata, P. A. Calcium oxalate in plants: formation and function. *Annual Review of Plant Biology* **56**, 41–71 (2005).
107. Taylor, B. N. & Ostrowsky, L. R. Nitrogen-fixing and non-fixing trees differ in leaf chemistry and defence but not herbivory in a lowland Costa Rican rain forest. *Journal of Tropical Ecology* **35**, 270–279 (2019).
108. Lev-Yadun, S. Avoiding rather than resisting herbivore attacks is often the first line of plant defence. *Biological Journal of the Linnean Society* (2021).

109. Marazzi, B. *et al.* Extrafloral nectaries in Leguminosae: phylogenetic distribution, morphological diversity and evolution. *Australian Systematic Botany* **32**, 409–458 (2019).
110. Niinemets, Ü. A review of light interception in plant stands from leaf to canopy in different plant functional types and in species with varying shade tolerance. *Ecological Research* **25**, 693–714 (2010).
111. Menge, D. N. & Chazdon, R. L. Higher survival drives the success of nitrogen-fixing trees through succession in Costa Rican rainforests. *New Phytologist* **209**, 965–977 (2016).
112. Menge, D. N. & Levin, S. A. Spatial heterogeneity can resolve the nitrogen paradox of tropical forests. *Ecology* **98**, 1049–1061 (2017).
113. Carvalho, M. R. *et al.* Extinction at the end-Cretaceous and the origin of modern Neotropical rainforests. *Science* **372**, 63–68 (2021).
114. Kandlikar, G. S., Johnson, C. A., Yan, X., Kraft, N. J. & Levine, J. M. Winning and losing with microbes: how microbially mediated fitness differences influence plant diversity. *Ecology Letters* **22**, 1178–1191 (2019).
115. Lotka, A. J. Analytical note on certain rhythmic relations in organic systems. *Proceedings of the National Academy of Sciences* **6**, 410–415 (1920).
116. Leibold, M. A., Urban, M. C., De Meester, L., Klausmeier, C. A. & Vanoverbeke, J. Regional neutrality evolves through local adaptive niche evolution. *Proceedings of the National Academy of Sciences* **116**, 2612–2617 (2019).

117. Wainwright, P. C. Functional versus morphological diversity in macroevolution. *Annual Review of Ecology, Evolution, and Systematics* **38**, 381–401 (2007).
118. Hubbell, S. P. Neutral theory and the evolution of ecological equivalence. *Ecology* **87**, 1387–1398 (2006).
119. Thomas, S. C. & Bazzaz, F. A. Asymptotic height as a predictor of photosynthetic characteristics in Malaysian rain forest trees. *Ecology* **80**, 1607–1622 (1999).
120. Muller-Landau, H. C. The tolerance–fecundity trade-off and the maintenance of diversity in seed size. *Proceedings of the National Academy of Sciences* **107**, 4242–4247 (2010).
121. Fine, P. V., Mesones, I. & Coley, P. D. Herbivores promote habitat specialization by trees in Amazonian forests. *Science* **305**, 663–665 (2004).
122. Thomas, S. C. Relative Size at Onset of Maturity in Rain Forest Trees: A Comparative Analysis of 37 Malaysian Species. *Oikos* **76**, 145–154 (1996).
123. Kohyama, T. Significance of Architecture and Allometry in Saplings. *Functional Ecology* **1**, 399–404 (1987).
124. Smith, C. C. & Fretwell, S. D. The Optimal Balance between Size and Number of Offspring. *The American Naturalist* **108**, 499–506 (1974).
125. Foster, S. & Janson, C. H. The relationship between seed size and establishment conditions in tropical woody plants. *Ecology* **66**, 773–780 (1985).

126. Westoby, M., Jurado, E. & Leishman, M. Comparative evolutionary ecology of seed size. *Trends in Ecology & Evolution* **7**, 368–372 (1992).
127. Van Der Sande, M. T., Poorter, L., Schnitzer, S. A., Engelbrecht, B. M. & Markesteijn, L. The hydraulic efficiency–safety trade-off differs between lianas and trees. *Ecology* **100**, e02666 (2019).
128. Patiño, S. *et al.* Coordination of physiological and structural traits in Amazon forest trees. *Biogeosciences* **9**, 775–801 (2012).
129. Givnish, T. J. Comparative studies of leaf form: assessing the relative roles of selective pressures and phylogenetic constraints. *New phytologist* **106**, 131–160 (1987).
130. Malhado, A. C. M. *et al.* Spatial trends in leaf size of Amazonian rainforest trees. *Biogeosciences* **6**, 1563–1576 (2009).
131. Sack, L. & Grubb, P. Why do species of woody seedlings change rank in relative growth rate between low and high irradiance? *Functional Ecology* **15**, 145–154 (2001).
132. Kleiman, D. & Aarssen, L. W. The leaf size/number trade-off in trees. *Journal of Ecology* **95**, 376–382 (2007).
133. Pickup, M., Westoby, M. & Basden, A. Dry mass costs of deploying leaf area in relation to leaf size. *Functional Ecology* **19**, 88–97 (2005).
134. Westoby, M. & Wright, I. J. The leaf size–twig size spectrum and its relationship to other important spectra of variation among species. *Oecologia* **135**, 621–628 (2003).

135. Yates, M. J., Anthony Verboom, G., Rebelo, A. G. & Cramer, M. D. Ecophysiological significance of leaf size variation in Proteaceae from the Cape Floristic Region. *Functional Ecology* **24**, 485–492 (2010).
136. Laurance, W. F. in *Lessons from Amazonia: The ecology and conservation of a fragmented forest* (eds Bierregard, R. O., Gascon, C., Lovejoy, T. E. & Mesquita, R.) 47–53 (Yale University Press, 2001).
137. Clark, D. A. & Clark, D. B. Life History Diversity of Canopy and Emergent Trees in a Neotropical Rain Forest. *Ecological Monographs* **62**, 315–344 (1992).
138. Schneider, C. A., Rasband, W. S. & Eliceiri, K. W. NIH Image to ImageJ: 25 years of image analysis. *Nature methods* **9**, 671–675 (2012).
139. Plummer, M. *rjags: Bayesian Graphical Models using MCMC* R package version 4-8 (2018).
140. King, D. A. Influence of leaf size on tree architecture: first branch height and crown dimensions in tropical rain forest trees. *Trees* **12**, 438–445 (1998).
141. Poorter, L. & Rozendaal, D. M. Leaf size and leaf display of thirty-eight tropical tree species. *Oecologia* **158**, 35–46 (2008).
142. King, D. A. Correlations Between Biomass Allocation, Relative Growth Rate and Light Environment in Tropical Forest Saplings. *Functional Ecology* **5**, 485–492 (1991).

143. Veneklaas, E. J. & Poorter, L. in *Inherent variation in plant growth: physiological mechanisms and ecological consequences* (eds Lambers, H., Poorter, H. & VanVuuren, M.) 337–362 (Backhuys Publishers, Leiden, The Netherlands, 1998).
144. Coley, P. D. Herbivory and defensive characteristics of tree species in a lowland tropical forest. *Ecological monographs* **53**, 209–234 (1983).
145. Poorter, H. & Remkes, C. Leaf area ratio and net assimilation rate of 24 wild species differing in relative growth rate. *Oecologia* **83**, 553–559 (1990).
146. Clark, D. B. & Clark, D. A. The Impact of Physical Damage on Canopy Tree Regeneration in Tropical Rain Forest. *Journal of Ecology* **79**, 447–457 (1991).
147. Parkhurst, D. F. & Loucks, O. Optimal leaf size in relation to environment. *The Journal of Ecology*, 505–537 (1972).
148. Berenguer, E. *et al.* Tracking the impacts of El Niño drought and fire in human-modified Amazonian forests. *Proceedings of the National Academy of Sciences* **118** (2021).
149. Jensen, K. H. & Zwieniecki, M. A. Physical limits to leaf size in tall trees. *Physical review letters* **110**, 018104 (2013).
150. Diaz, S. *et al.* The global spectrum of plant form and function. *Nature* **529**, 167–171 (2016).

151. Kitajima, K. Relative importance of photosynthetic traits and allocation patterns as correlates of seedling shade tolerance of 13 tropical trees. *Oecologia* **98**, 419–428 (1994).
152. Clark, J. S. Why species tell more about traits than traits about species: predictive analysis. *Ecology* **97**, 1979–1993 (2016).
153. Yoda, K. Three-dimensional distribution of light intensity in a tropical rain forest of West Malaysia. *Japanese Journal of Ecology* **24**, 247–254 (1974).
154. Terborgh, J., Zhu, K., Álvarez-Loayza, P. & Cornejo Valverde, F. How many seeds does it take to make a sapling? *Ecology* **95**, 991–999 (2014).
155. Kohyama, T. Size-Structured Tree Populations in Gap-Dynamic Forest—The Forest Architecture Hypothesis for the Stable Coexistence of Species. *Journal of Ecology* **81**, 131–143 (1993).
156. D’Andrea, R. *et al.* Counting niches: Abundance-by-trait patterns reveal niche partitioning in a Neotropical forest. *Ecology* **101**, e03019 (2020).
157. Spicer, M. E., Mellor, H. & Carson, W. P. Seeing beyond the trees: a comparison of tropical and temperate plant growth forms and their vertical distribution. *Ecology* **101**, e02974 (2020).
158. MacArthur, R. & Levins, R. The limiting similarity, convergence, and divergence of coexisting species. *The American Naturalist* **101**, 377–385 (1967).

159. Scheffer, M. & van Nes, E. H. Self-organized similarity, the evolutionary emergence of groups of similar species. *Proceedings of the National Academy of Sciences* **103**, 6230–6235 (2006).
160. Barabás, G., D’Andrea, R., Rael, R., Meszéna, G. & Ostling, A. Emergent neutrality or hidden niches? *Oikos* **122**, 1565–1572 (2013).
161. Chazdon, R. L. & Fetcher, N. Photosynthetic Light Environments in a Lowland Tropical Rain Forest in Costa Rica. *Journal of Ecology* **72**, 553–564 (1984).
162. Bever, J. D., Mangan, S. A. & Alexander, H. M. Maintenance of plant species diversity by pathogens. *Annual review of ecology, evolution, and systematics* **46**, 305–325 (2015).
163. Tilman, D. Competition and biodiversity in spatially structured habitats. *Ecology* **75**, 2–16 (1994).
164. Condit, R., Hubbell, S. P. & Foster, R. B. Identifying fast-growing native trees from the Neotropics using data from a large, permanent census plot. *Forest Ecology and Management* **62**, 123–143 (1993).
165. Hallé, F., Oldeman, R. A. & Tomlinson, P. B. *Tropical trees and forests: an architectural analysis* (Springer-Verlag, Berlin, 1978).
166. Henry, H. A. & Aarssen, L. W. On the relationship between shade tolerance and shade avoidance strategies in woodland plants. *Oikos*, 575–582 (1997).

167. Terborgh, J. The Vertical Component of Plant Species Diversity in Temperate and Tropical Forests. *The American Naturalist* **126**, 760–776 (1985).
168. Valladares, F., Skillman, J. B. & Pearcy, R. W. Convergence in light capture efficiencies among tropical forest understory plants with contrasting crown architectures: a case of morphological compensation. *American Journal of Botany* **89**, 1275–1284 (2002).
169. Küppers, M. Canopy gaps: competitive light interception and economic space filling—a matter of whole-plant allocation. *Exploitation of environmental heterogeneity by plants. Ecophysiological processes above-and belowground*, 111–144 (1994).
170. SpeciesLink. *Rede speciesLink* <http://www.splink.org.br/> (2019).
171. Dietze, M. C., Wolosin, M. S. & Clark, J. S. Capturing diversity and interspecific variability in allometries: A hierarchical approach. *Forest Ecology and Management* **256**, 1939–1948 (2008).
172. Giraudoux, P. *pgirmess: Spatial Analysis and Data Mining for Field Ecologists* R package version 1.7.0 (2021).
173. Poorter, L., Bongers, F., Sterck, F. J. & Wöll, H. Beyond the regeneration phase: differentiation of height–light trajectories among tropical tree species. *Journal of Ecology* **93**, 256–267 (2005).
174. Poorter, L., Bongers, F., Sterck, F. J. & Wöll, H. Architecture of 53 rain forest tree species differing in adult stature and shade tolerance. *Ecology* **84**, 602–608 (2003).

175. Sterck, F. J., Bongers, F. & Newbery, D. M. Tree architecture in a Bornean lowland rain forest: intraspecific and interspecific patterns. *Plant Ecology* **153**, 279–292 (2001).
176. Valladares, F. & Niinemets, Ü. Shade tolerance, a key plant feature of complex nature and consequences. *Annual Review of Ecology, Evolution, and Systematics* **39**, 237–257 (2008).
177. Sterck, F. J. & Bongers, F. Crown development in tropical rain forest trees: patterns with tree height and light availability. *Journal of Ecology* **89**, 1–13 (2001).
178. Lüttge, U. *Physiological ecology of tropical plants* (Springer Science & Business Media, 2007).
179. Sakai, S. Evolutionarily stable growth of a sapling which waits for future gap formation under closed canopy. *Evolutionary Ecology* **9**, 444–452 (1995).
180. Poorter, L. Are Species Adapted to Their Regeneration Niche, Adult Niche, or Both? *The American Naturalist* **169**, 433–442 (2007).
181. Nunes, M. H. *et al.* Recovery of logged forest fragments in a human-modified tropical landscape during the 2015-16 El Niño. *Nature communications* **12**, 1–11 (2021).
182. Falster, D. S. *et al.* BAAD: a Biomass And Allometry Database for woody plants. *Ecology* **96**, 1445–1445 (2015).
183. Loehle, C. Tree life history strategies: the role of defenses. *Canadian Journal of Forest Research* **18**, 209–222 (1988).

184. Alvarez-Buylla, E. R. & Martinez-Ramos, M. Demography and Allometry of *Cecropia Obtusifolia*, a Neotropical Pioneer Tree - An Evaluation of the Climax-Pioneer Paradigm for Tropical Rain Forests. *Journal of Ecology* **80**, 275–290 (1992).
185. Chambers, J. Q., Higuchi, N. & Schimel, J. P. Ancient trees in Amazonia. *Nature* **391**, 135–136 (1998).
186. Levins, R. *Evolution in changing environments* (Princeton University Press, 1968).
187. Bazzaz, F. A. & Grace, J. *Plant resource allocation* (Academic Press, San Diego, 1997).
188. Bierregaard Jr, R. O., Lovejoy, T. E., Kapos, V., dos Santos, A. A. & Hutchings, R. W. The biological dynamics of tropical rainforest fragments. *BioScience*, 859–866 (1992).
189. De Oliveira, A. A. & Mori, S. A. A central Amazonian terra firme forest. I. High tree species richness on poor soils. *Biodiversity & Conservation* **8**, 1219–1244 (Sept. 1999).
190. Chauvel, A., Lucas, Y. & Boulet, R. On the genesis of the soil mantle of the region of Manaus, Central Amazonia, Brazil. *Experientia* **43**, 234–241 (1987).
191. Taiz, L. & Zeiger, E. *Plant physiology and development*. **Ed. 4** (Sinauer Associates Incorporated, 2006).
192. Thomas, S. C. in *Size-and age-related changes in tree structure and function* 33–64 (Springer, 2011).

193. Snyder, R. E. & Ellner, S. P. We happy few: using structured population models to identify the decisive events in the lives of exceptional individuals. *The American Naturalist* **188**, E28–E45 (2016).
194. Kohyama, T., Suzuki, E., Partomihardjo, T., Yamada, T. & Kubo, T. Tree species differentiation in growth, recruitment and allometry in relation to maximum height in a Bornean mixed dipterocarp forest. *Journal of Ecology* **91**, 797–806 (2003).
195. Chave, J. *et al.* Towards a worldwide wood economics spectrum. *Ecology Letters* **12**, 351–366 (2009).
196. Kraft, N. J., Metz, M. R., Condit, R. S. & Chave, J. The relationship between wood density and mortality in a global tropical forest data set. *New Phytologist* **188**, 1124–1136 (2010).
197. Russo, S. E. *et al.* The interspecific growth–mortality trade-off is not a general framework for tropical forest community structure. *Nature Ecology & Evolution*, 1–10 (2020).
198. Thomas, S. C., Martin, A. R. & Mycroft, E. E. Tropical trees in a wind-exposed island ecosystem: Height-diameter allometry and size at onset of maturity. *Journal of Ecology* **103**, 594–605 (2015).
199. Davies, S. J. & Ashton, P. S. Phenology and fecundity in 11 sympatric pioneer species of *Macaranga* (Euphorbiaceae) in Borneo. *American Journal of Botany* **86**, 1786–1795 (1999).

200. Coelho de Souza, F. *et al.* Evolutionary heritage influences Amazon tree ecology. *Proceedings of the Royal Society B: Biological Sciences* **283**, 20161587 (2016).
201. Petit, R. J. & Hampe, A. Some Evolutionary Consequences of Being a Tree. *Annual Review of Ecology, Evolution, and Systematics* **37**, 187–214 (2006).
202. Martin-Trillo, M. & Martinez-Zapater, J. M. Growing up fast: manipulating the generation time of trees. *Current opinion in biotechnology* **13**, 151–155 (2002).
203. Richardson, J. E., Pennington, R. T., Pennington, T. D. & Hollingsworth, P. M. Rapid diversification of a species-rich genus of neotropical rain forest trees. *Science* **293**, 2242–2245 (2001).
204. Losos, J. B., Mahler, D. L., *et al.* in *Evolution since Darwin: the first 150 years* (eds Bell, M. A., Futuyma, D. J., Eanes, W. F. & Levinton, J. S.) 381–420 (Sinauer Associates, Sunderland, 2010).